

# Efficient Solvers Based on Manycore computers and adaptive techniques for Cardiac Modeling

FISIOCOMP - Laboratory of Computational Physiology

*Graduate Program in Computational Modeling  
Universidade Federal de Juiz de Fora (UFJF)  
Juiz de Fora - MG - Brazil*

Prof. Dr. Rodrigo Weber dos Santos

# Efficient Solvers Based on Manycore computers and adaptive techniques for Cardiac Modeling

## Part I

### Who, When, Where and Motivation

## **PTB-Berlin (2002-2004)**

### **Group (2005 - )**

Prof. Rodrigo Weber dos Santos, Dr. Math.

Prof. Marcelo Lobosco, Dr. Comp. Sci.

Prof. Ciro Barros Barbosa, Dr. Comp. Sci.

Prof. Luis Paulo Barra, Dr. Eng.

Prof. Elson Toledo, Dr. Eng.

#### **PhD Students**

Rafael Sachetto (Cardiac Modeling)

Ricardo Campos (Cardiac Modeling)

Bernardo Rocha (Cardiac Modeling)

Barbara Quintela (Models of Immune System)

Alexandre Pigozzo (Models of Immune System)

#### **Master Students**

Bruno Gouvêa de Barros

Daniel Mendes Caldas

Micael Peters Xavier

Pedro Augusto Ferreira Rocha

#### **Former Master Students**

Caroline Costa (PhD in Graz)

Bernardo Lino Oliveira (PhD in Simula Lab)

Gustavo Miranda

Fernando Otaviano Campos (PhD in Graz)

Daves Martins

Carolina Xavier

Ronan M. Amorim (PhD in Calgary)

Elisa Portes dos Santos (PhD in Calgary)

[Página Inicial](#)[Curso](#)[Disciplinas](#)[Grade Curricular](#)[Normas e Regulamentos](#)[Corpo Docente](#)[Corpo Discente](#)[Produção Científica](#)[Dissertações Defendidas](#)[Processo Seletivo](#)[Calendário Acadêmico](#)[Horários](#)[Notícias](#)[Palestras](#)[Eventos](#)[Acervo Bibliográfico](#)[Contato](#)[Ramais](#)[Localização](#)[Galeria de Fotos](#)[Links](#)

## Corpo Docente

O Corpo Docente que atua no Programa de Mestrado em Modelagem Computacional é composto pelos seguintes Professores:

### Permanentes:

Afonso Celso de Castro Lemonge, Departamento de Mecânica Aplicada e Computacional [Lattes](#)

Carlos Cristiano Hasenclever Borges, Departamento de Ciência da Computação [Lattes](#)

Elson Magalhães Toledo, Departamento de Mecânica Aplicada e Computacional [Lattes](#)

Flávio de Souza Barbosa, Departamento de Mecânica Aplicada e Computacional [Lattes](#) [www](#)

Hélio José Corrêa Barbosa, Departamento de Ciência da Computação [Lattes](#) [www](#)

Henrique Steinherz Hipper, Departamento de Estatística [Lattes](#)

Luis Paulo da Silva Barra, Departamento de Mecânica Aplicada e Computacional [Lattes](#) [www](#)

Maicon Ribeiro Corrêa, Departamento de Ciência da Computação [Lattes](#)

Marcelo Lobosco, Departamento de Ciência da Computação [Lattes](#)

Michèle Cristina Resende Farage, Departamento de Mecânica Aplicada e Computacional [Lattes](#)

Rodrigo Weber dos Santos, Departamento de Ciência da Computação [Lattes](#)

Saul de Castro Leite, Departamento de Ciência da Computação [Lattes](#)

### Colaboradores:

Ana Paula Couto da Silva, Departamento de Ciência da Computação [Lattes](#)

Ciro de Barros Barbosa, Departamento de Ciência da Computação [Lattes](#) [www](#)

Raul Fonseca Neto, Departamento de Ciência da Computação [Lattes](#)

Sócrates Dantas de Oliveira, Departamento de Física [Lattes](#)

Wilhelm Passarella Freire, Departamento de Matemática [Lattes](#)





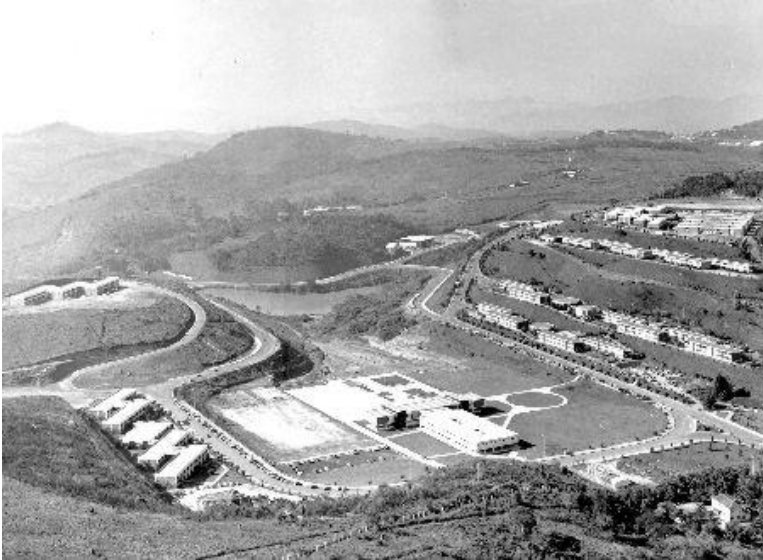
Graduate Program in Computational Modeling – 2006  
Building - 2008





Graduate Program in Computational Modeling – 2009

UFJF Campus started to be constructed in 1969



Today it offers over 100 of  
undergraduate and  
graduate courses

700 Professors  
2000 Staff  
20000 Students





Juiz de Fora city  
Around 600.000 inhabitants  
Max altitude of 1000m



# Models of Cardiac Electro-Mechanics

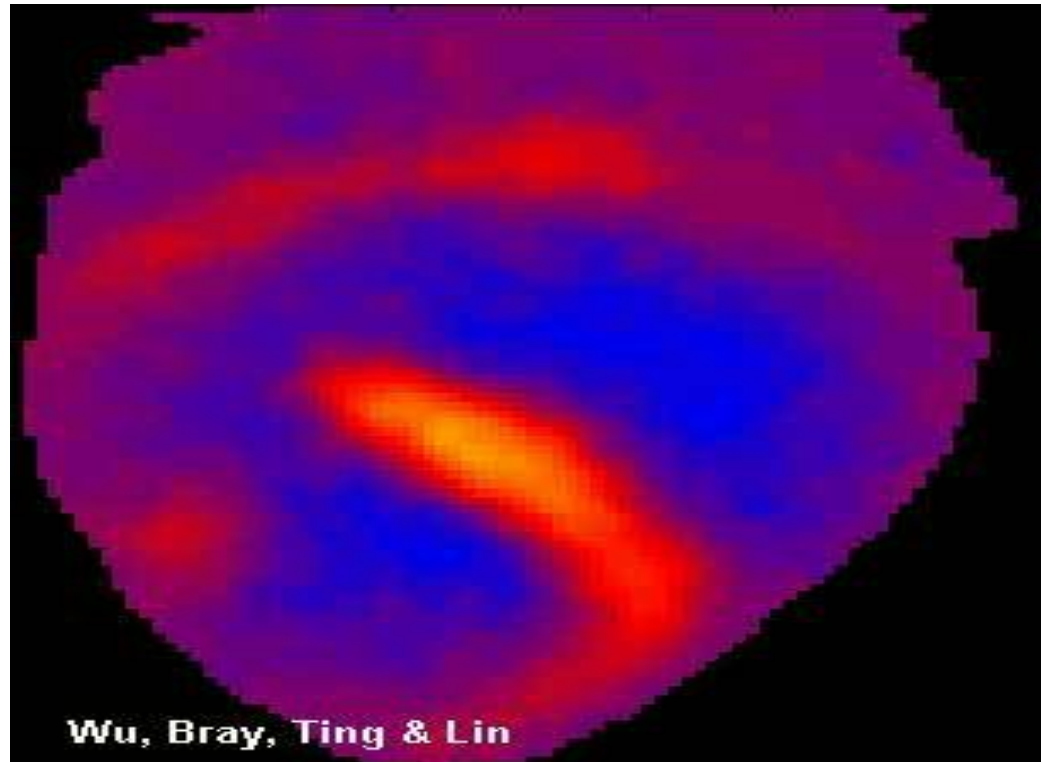
- Cardiac disease is the #1 cause of death around the world
- Today, computational models of the heart provide a better understanding of the complex phenomenon and support the development of new drugs, therapies, biomedical equipments and clinical diagnostic methods

- Heart stops - Defibrillator
- Complications during labor - Demand cesarean
- Migraine – Drugs



- Heart stops - Defibrillator
  - Complications during labor - Demand cesarean
  - Migraine – Drugs
- 
- Acute Conditions
  - Different procedures
  - Short-term

- Heart stops - Defibrillator
- Complications during labor - Demand cesarean
- Migraine – Drugs
- Acute Conditions
- **Same Phenomena**
- **Nonlinear Waves**
- **Excitable Media**
- **Spiral Waves**





- Heart stops - Defibrillator
- Complications during labor - Demand cesarean
- Migraine – Drugs
  
- Acute Conditions
- **Same Phenomena**
- **Nonlinear Waves**
- **Excitable Media**
- **Long Term**





No, no, no.  
Shout "Clear"  
**BEFORE** zapping him.



© Original Artist  
Reproduction rights obtainable from  
[www.CartoonStock.com](http://www.CartoonStock.com)

# Efficient Solvers Based on Manycore computers and adaptive techniques for Cardiac Modeling

## PART II

Crash introduction to the challenges of cardiac  
modeling?

# Mathematical and Computational Physiology

- Integrative Computational Physiology:

using models to bridge the gap between  
genes and function or  
malfunction( clinical pathology)



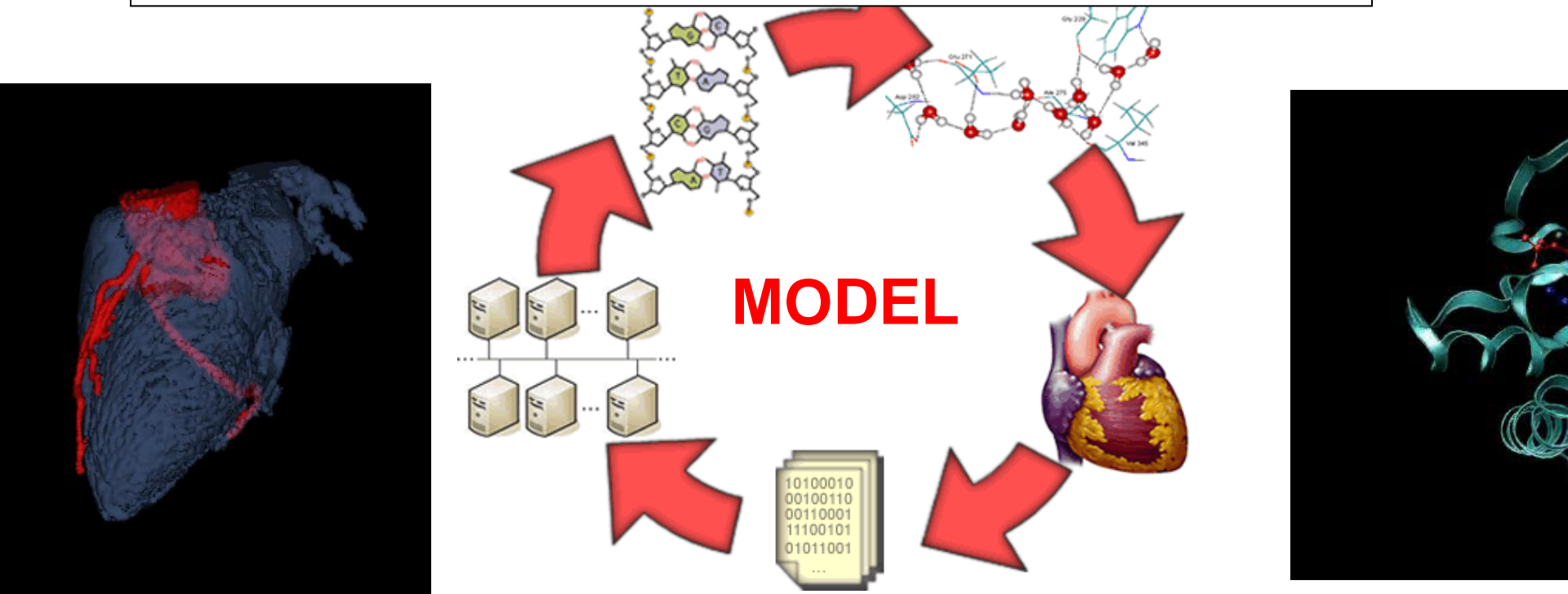
# Mathematical and Computational Physiology

- The bad news:

It is a wide gap connecting multiple scales,  
genes, proteins, cells, tissues, organs...;  
multiple physics: quantum, molecular  
dynamics, chemistry, electro-mechanics...;

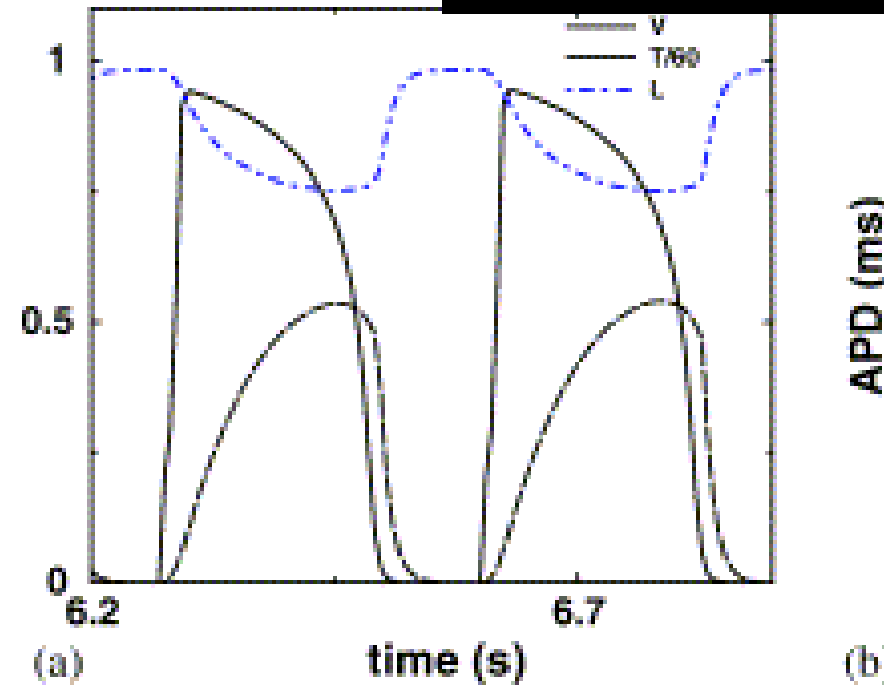
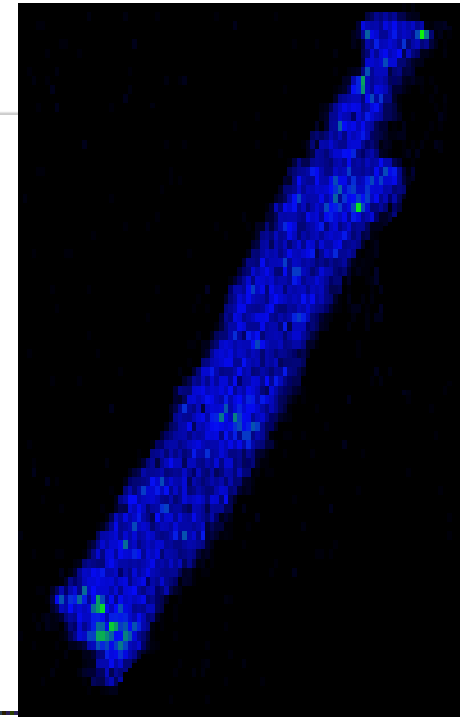
# Models of cardiac physiology

The models represent, are based and depend on multiple and diverse data



# Cardiac Cell

- **Cellular contraction:**  
An electric potential difference develops across the cell membrane and triggers a chain of electrochemical reactions that results in cellular contraction (intracellular Calcium spike, ATP, etc)

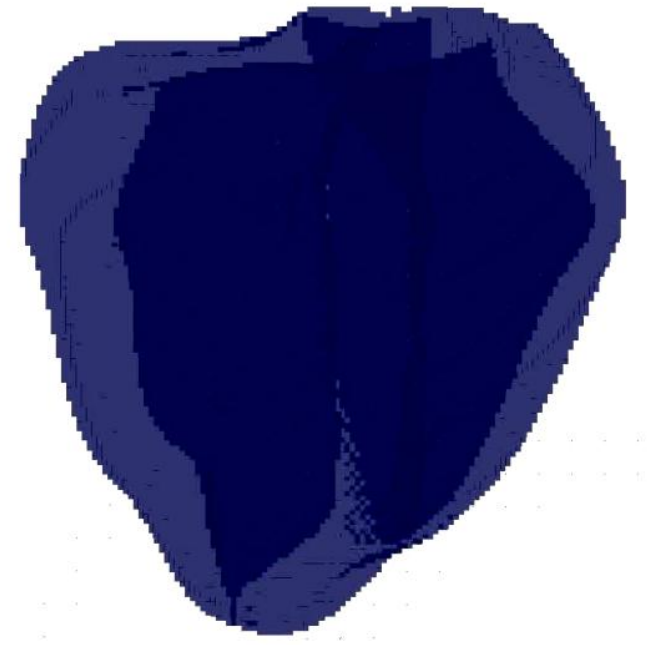




# The heart

- **How do cardiac cells synchronize and contract at the same time?**

The interior of the cells are connected by special proteins that allow the electric potential to propagate. A fast electric wave propagates and triggers heart contraction.



# The heart

- **The blood pump**

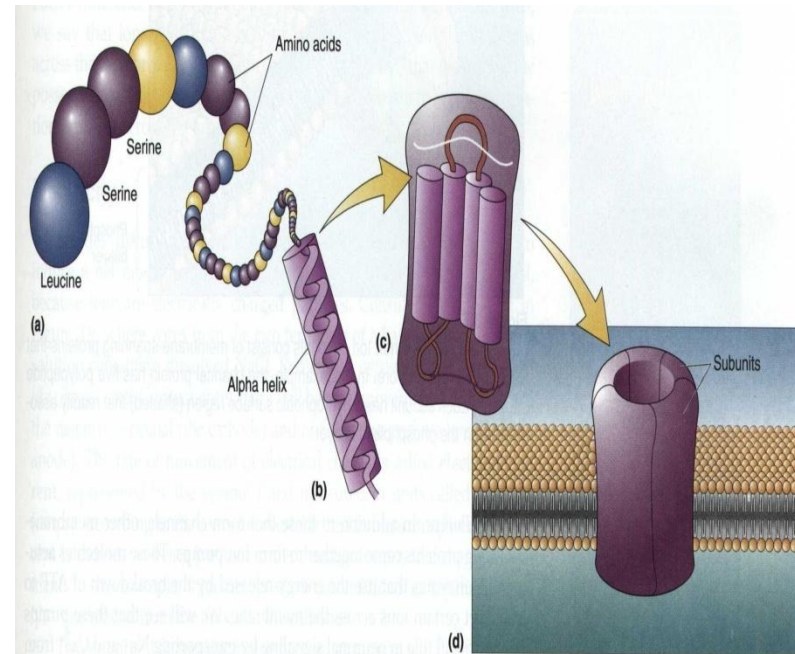
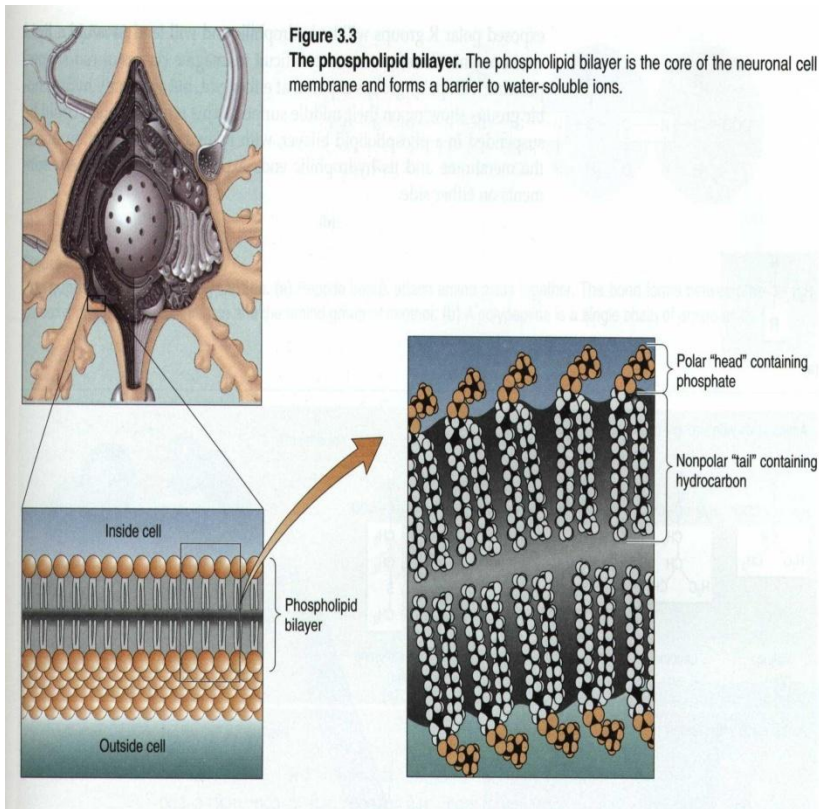
Cells contract changing the organ geometry and the blood is expelled



# Models of Cardiac Electro-Mechanics

- Bottom-up design

## Sub-cellular and cellular mathematical models



# Cell model

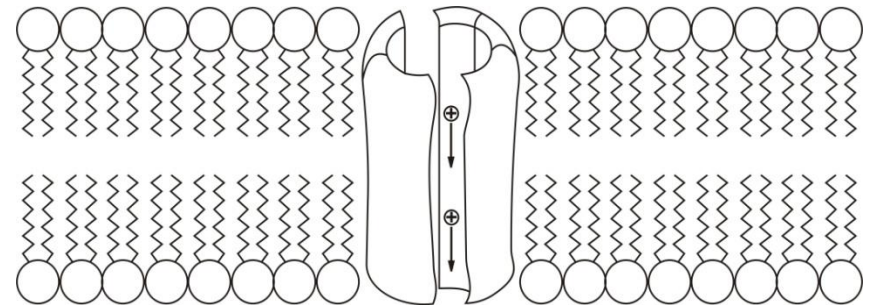
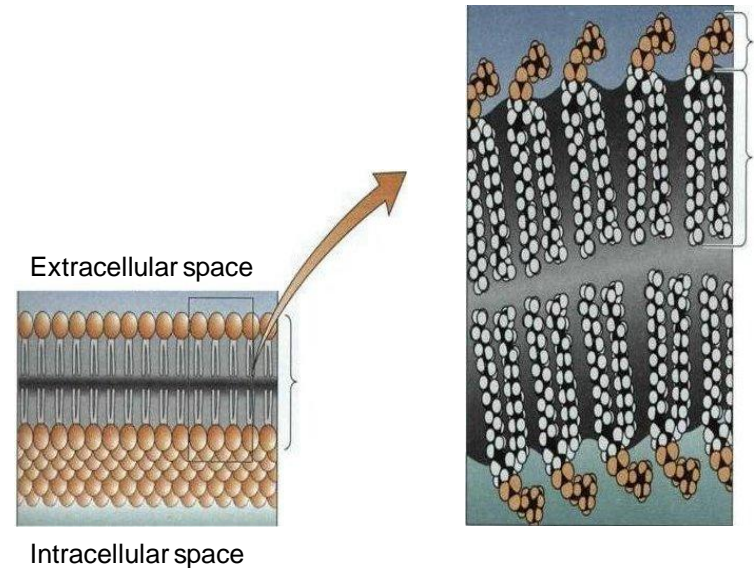
- Bi-lipid layer:

$$C_m = \frac{q}{\phi}$$

$$C_m \phi = q$$

$$C_m \frac{d\phi}{dt} = \frac{dq}{dt} = I_c$$

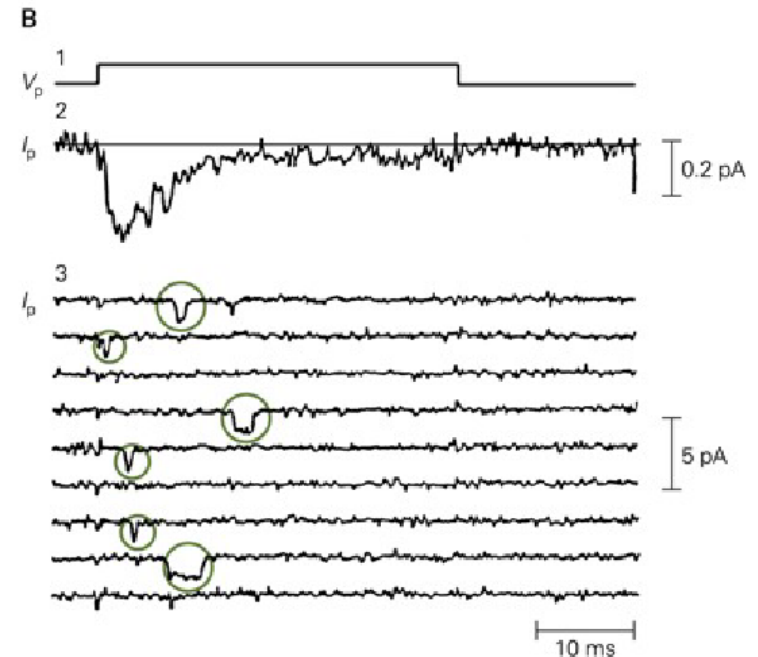
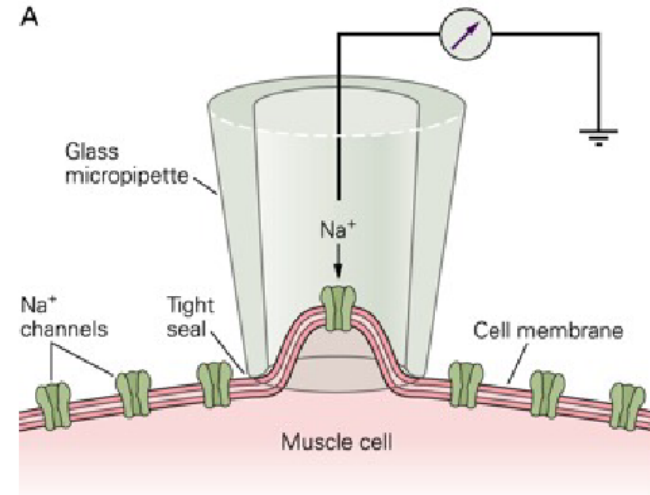
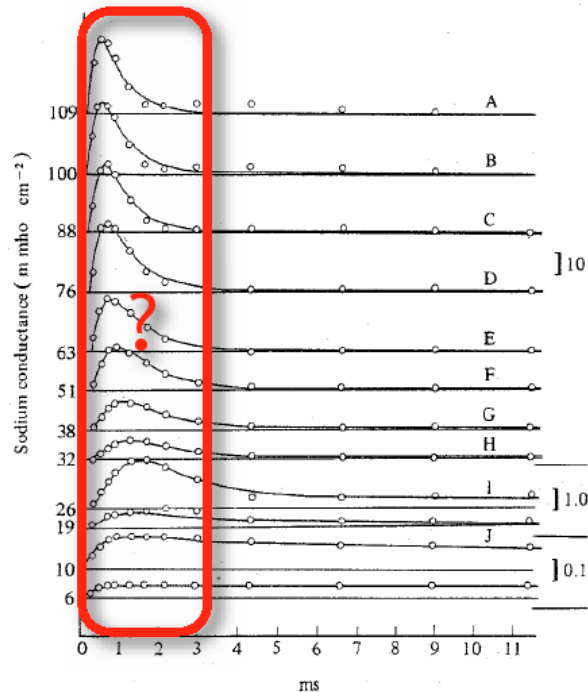
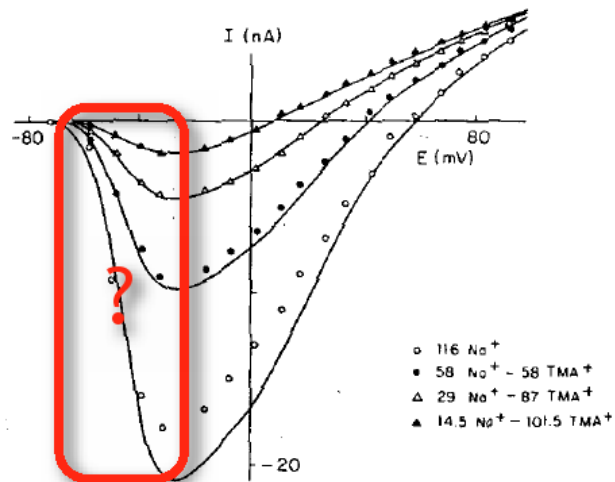
- Ionic channels: Special arrangement of proteins cut thru the membrane and allow the flow of specific ions, such as Sodium, Potassium and Calcium. Ionic currents  $I_{ion}$



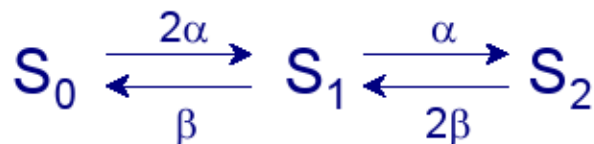
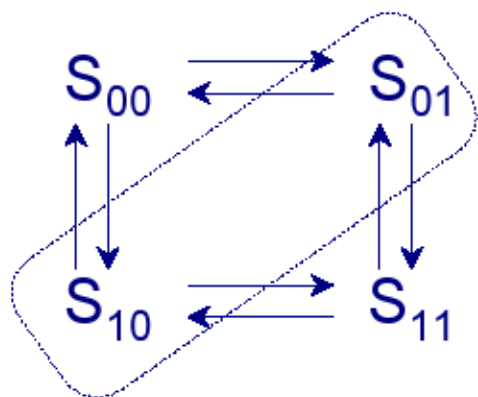
Ionic channel



# CHANNEL CURRENTS REVISITED



# K<sup>+</sup> channel gating

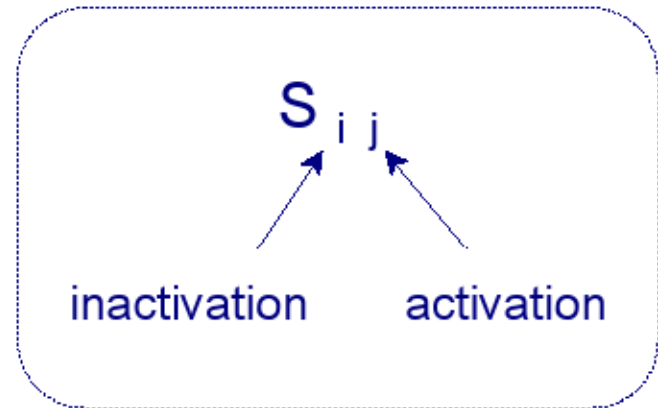
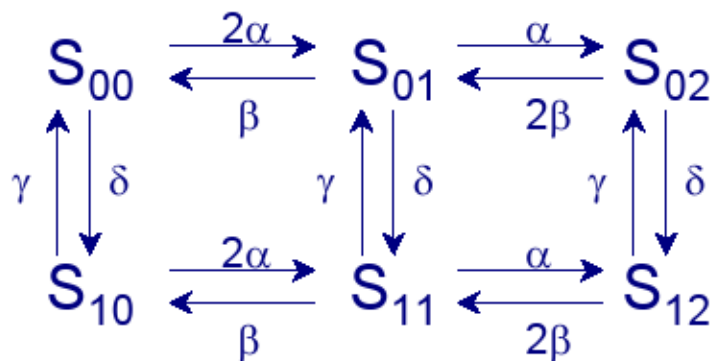


$$\left. \begin{aligned} \frac{dx_0}{dt} &= \beta x_1 - 2\alpha x_0 \\ \frac{dx_2}{dt} &= \alpha x_1 - 2\beta x_2 \\ x_0 + x_1 + x_2 &= 1 \end{aligned} \right\}$$



$$\begin{aligned} x_0 &= (1-n)^2 \\ x_1 &= 2n(1-n) \\ x_2 &= n^2 \\ \frac{dn}{dt} &= \alpha(1-n) - \beta n \end{aligned}$$

# Na<sup>+</sup> channel gating



$$x_{21} = m^2 h$$

$$\frac{dm}{dt} = \alpha(1 - m) - \beta m$$

activation

$$\frac{dh}{dt} = \gamma(1 - h) - \delta h$$

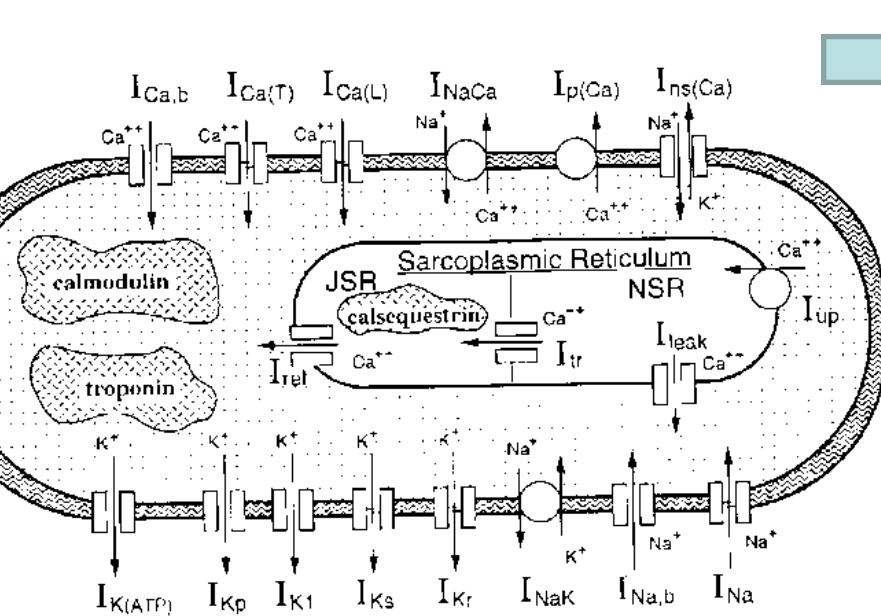
inactivation

# Models of Cardiac Electrophysiology

- Bottom-up design

## Sub-cellular and cellular mathematical models

Nonlinear System of ODEs



$$\frac{d[Ca^{2+}]_{NSR}}{dt} = \{J_{up} - J_{leak}\} \frac{V_{myo}}{V_{NSR}} - J_{up} \frac{V_{JSR}}{V_{NSR}}$$

$$B_i = \left\{ 1 + \frac{CMDN_{tot} K_m^{CMDN}}{(K_m^{CMDN} + [Ca^{2+}])^2} \right\}^{-1}$$

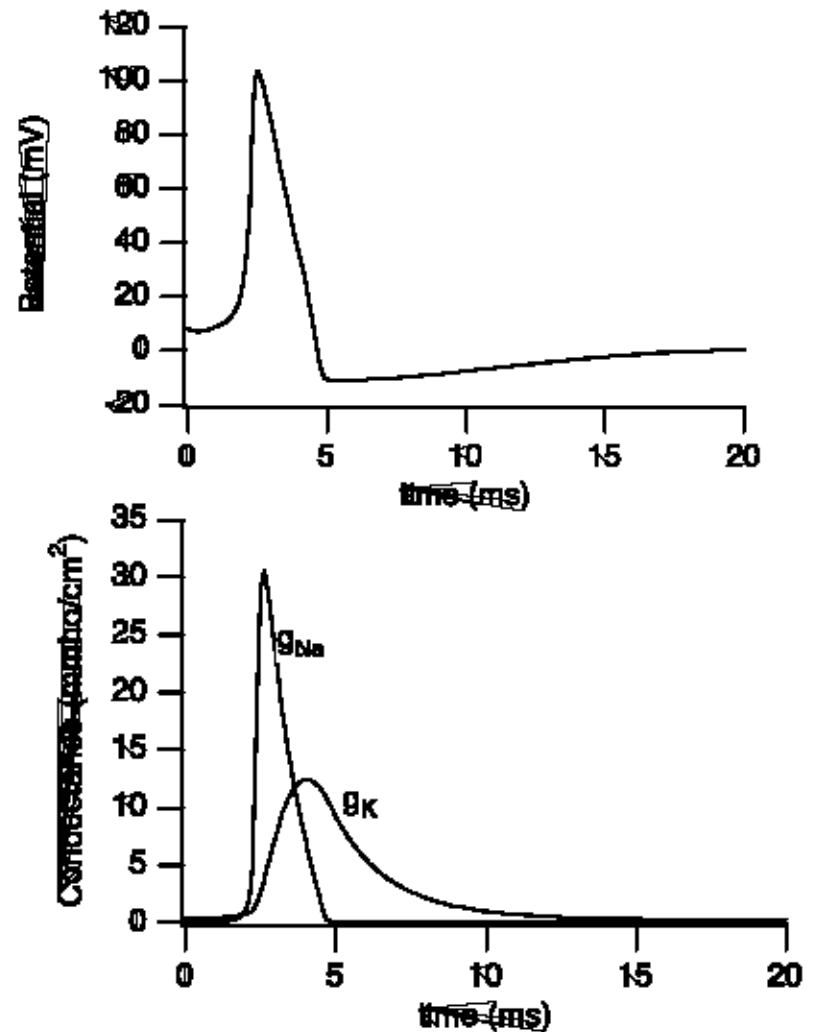
$$B_{ss} = \left\{ 1 + \frac{CMDN_{tot} K_m^{CMDN}}{(K_m^{CMDN} + [Ca^{2+}]_{ss})^2} \right\}^{-1}$$

$$B_{JSR} = \left\{ 1 + \frac{CMDN_{tot} K_m^{CMDN}}{(K_m^{CMDN} + [Ca^{2+}]_{JSR})^2} \right\}^{-1}$$



# An action potential

- $g_{Na}$  increases quickly, but then inactivation kicks in and it decreases again.
- $g_K$  increases more slowly, and only decreases once the voltage has decreased.
- The  $Na^+$  current is autocatalytic. An increase in  $V$  increases  $m$ , which increases the  $Na^+$  current, which increases  $V$ , etc.
- Hence, the threshold for action potential initiation is where the inward  $Na^+$  current exactly balances the outward  $K^+$  current.



# Intra-cellular Connection

## Electrical Synapses

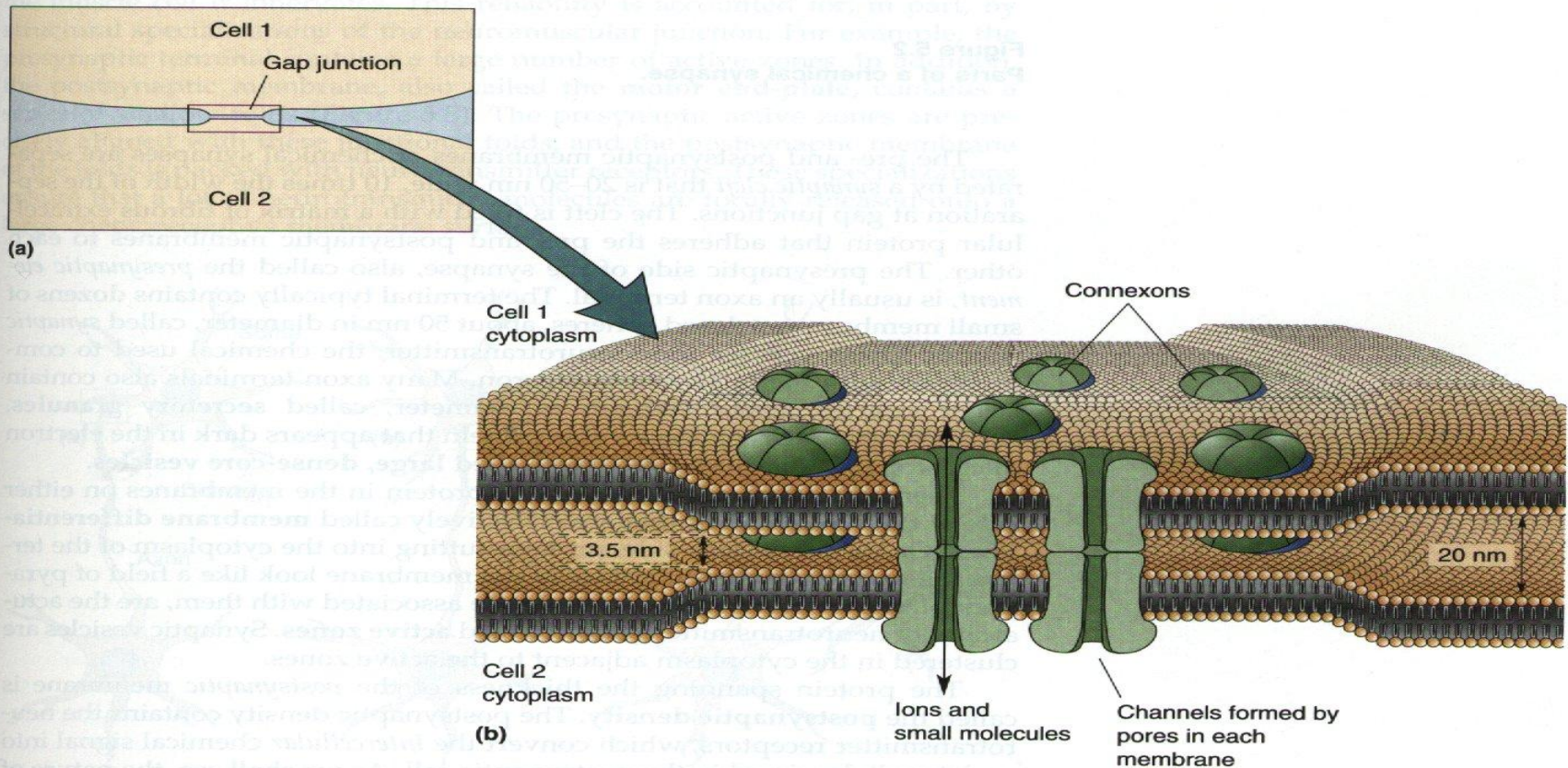
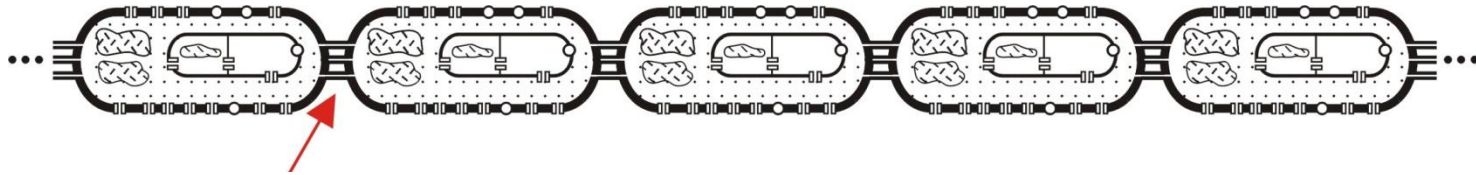


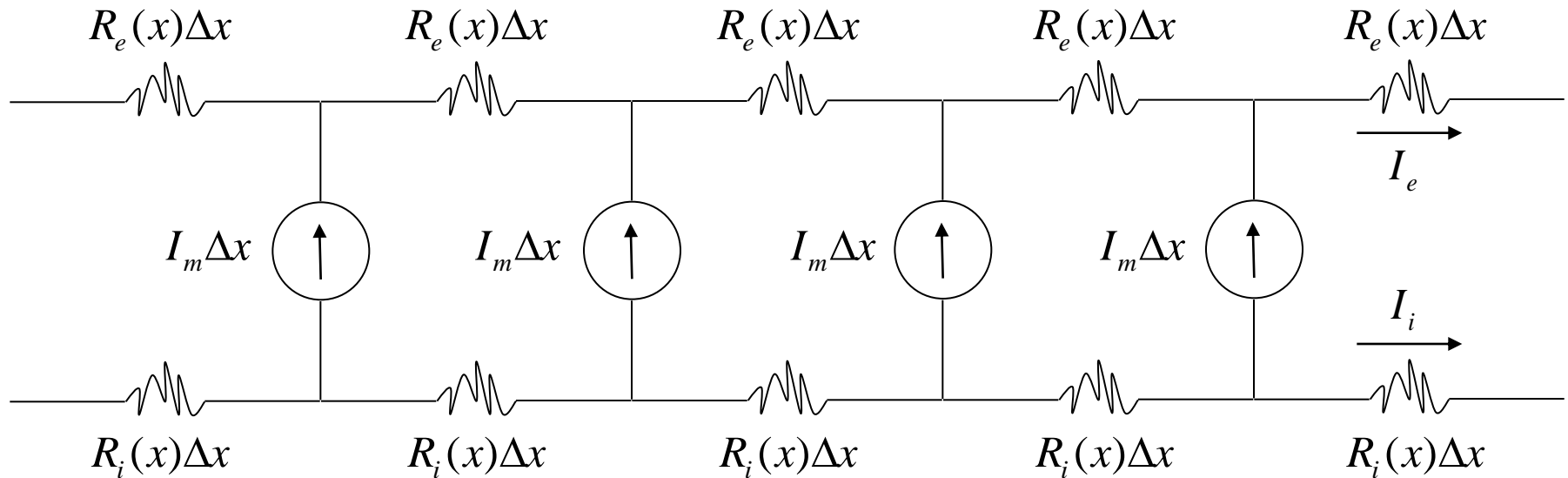
**Figure 5.1**

**A gap junction.** (a) Neurites of two cells connected by a gap junction. (b) An enlargement showing connexons, the channel proteins that bridge the cytoplasm of the two cells. Ions and small molecules can pass in both directions through these channels.

# Bidomain model



Gap junction



# Cardiac Bidomain Model

$$\begin{aligned}\nabla \cdot (\boldsymbol{\sigma}_i \nabla \phi_i) &= \chi \left( C_m \frac{\partial \phi}{\partial t} + \frac{1}{R_m} f(\phi, \vec{n}) \right), \\ -\nabla \cdot (\boldsymbol{\sigma}_e \nabla \phi_e) &= \chi \left( C_m \frac{\partial \phi}{\partial t} + \frac{1}{R_m} f(\phi, \vec{n}) \right), \\ \frac{\partial \vec{n}}{\partial t} &= g(\phi, \vec{n}), \\ \phi &= \phi_i - \phi_e, \mathbf{x} \in \Omega \text{ e } t \in [0, t_f].\end{aligned}$$

- $\sigma_{i,e}$  are the conductivity tensors
- Tissue anisotropy (fibers orientation) or orthotropy (fiber-laminar).
- $\sigma_i(x,y)$  and  $\sigma_e(x,y)$  : spatial variation of fibers/sheets orientation, different extracellular and intracellular (gap junctions) conductivity values.



# Cardiac Bidomain Model

- Tissue Model for cardiac electrophysiology
- Intracellular and extracellular spaces (domains) modeled from an electrostatic point of view
- The coupling of the two domains is via non-linear cell modeling. Total cell membrane current spreads to both intracellular and extracellular spaces

# Action Potential Propagation Reaction-Diffusion

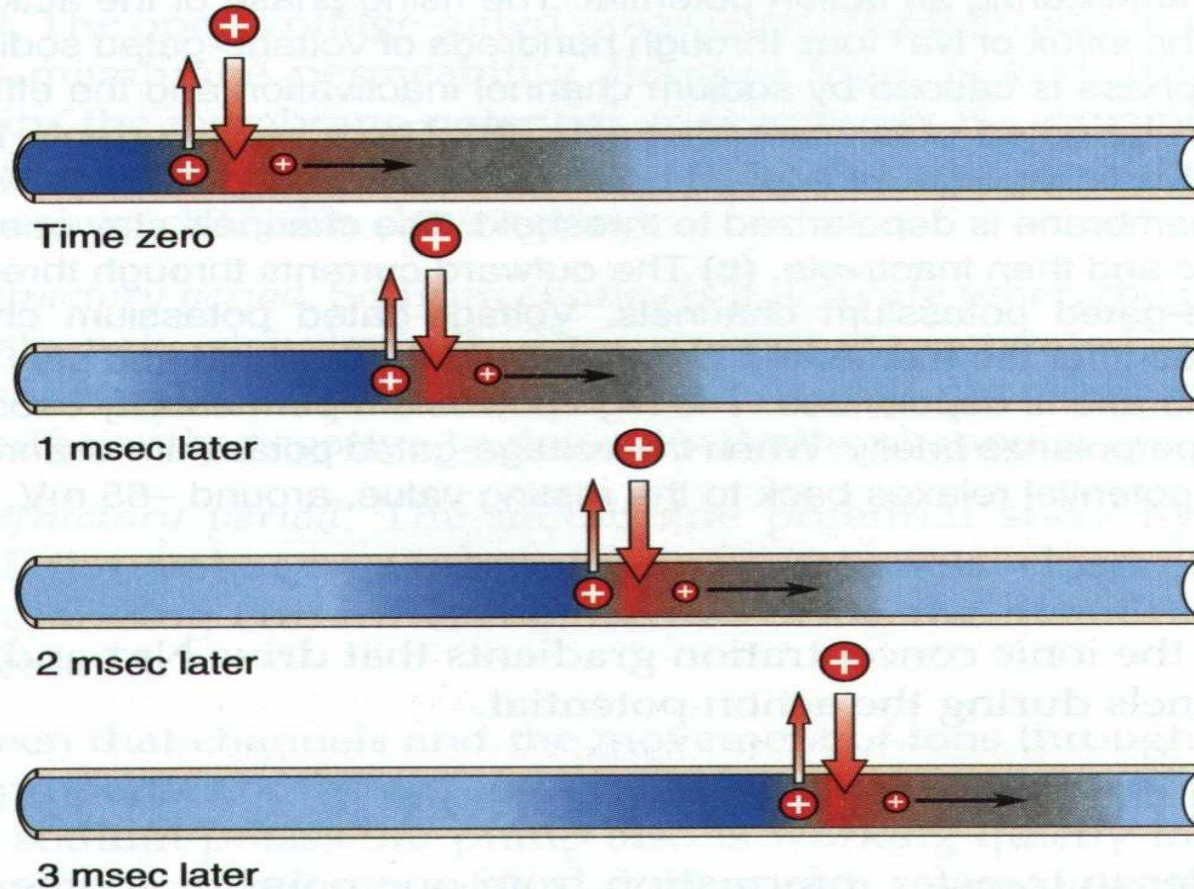


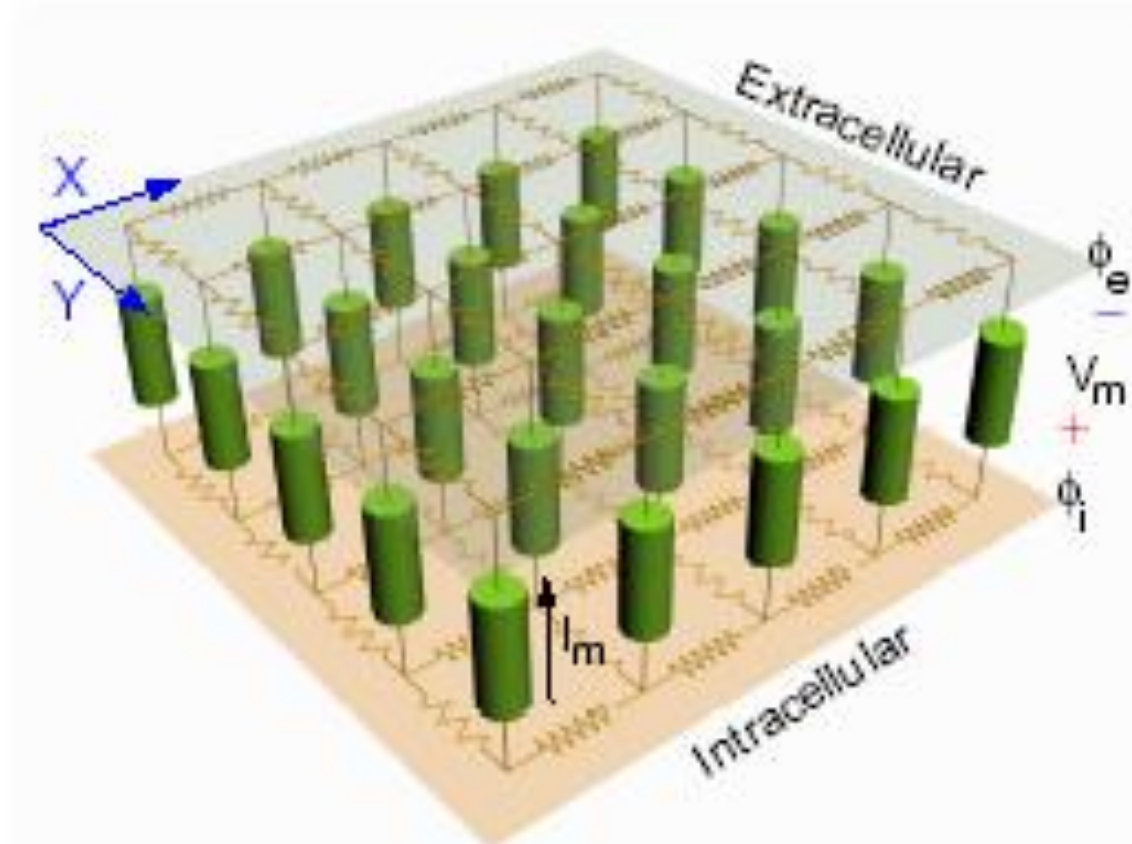
**Figure 4.10**

**Action potential conduction.** The entry of positive charge during the action potential causes the membrane just ahead to depolarize to threshold.

# Models of Cardiac Electro-Mechanics

- Bottom-up design

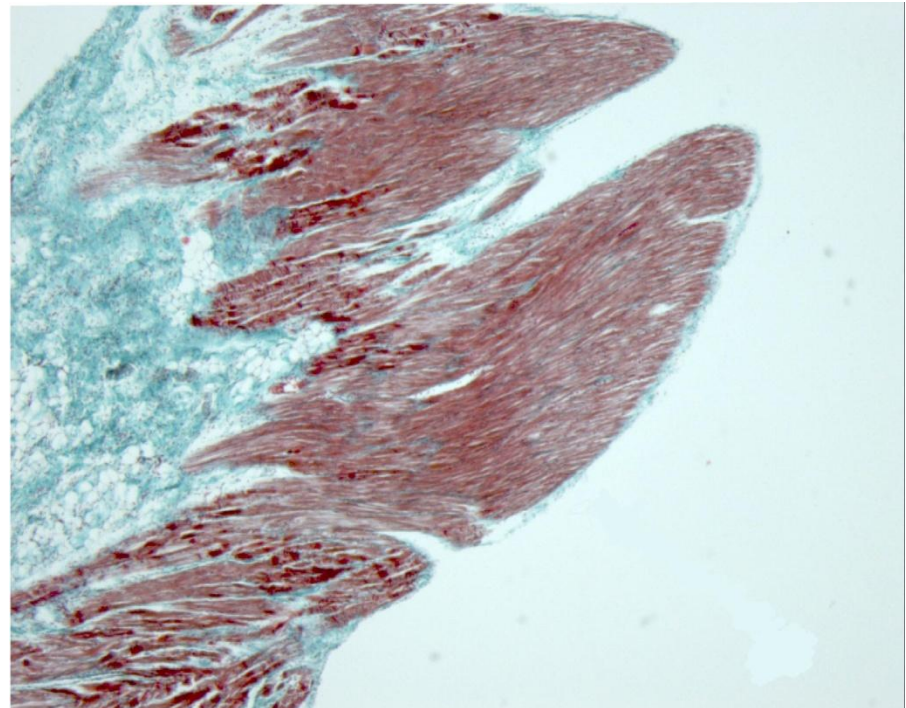
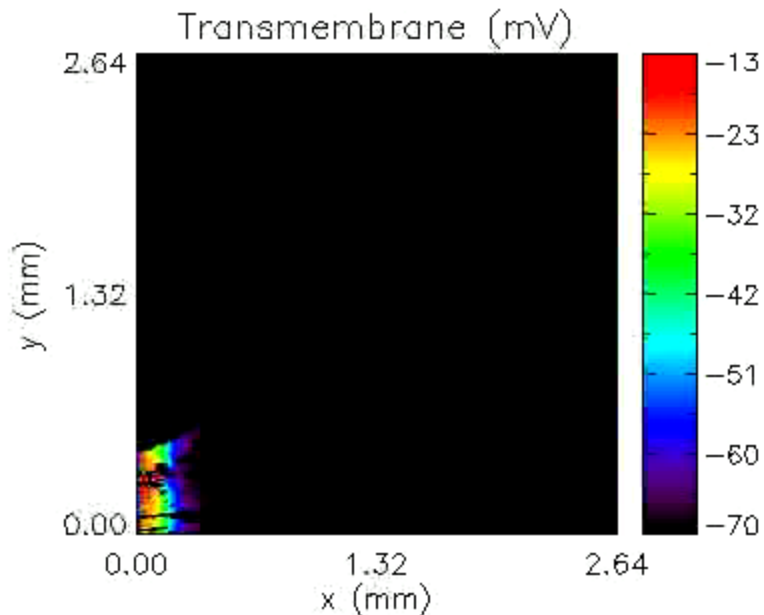
**Tissue mathematical and computational model**



# Models of Cardiac Electro-Mechanics

- Bottom-up design

**Tissue mathematical models:** electric activity

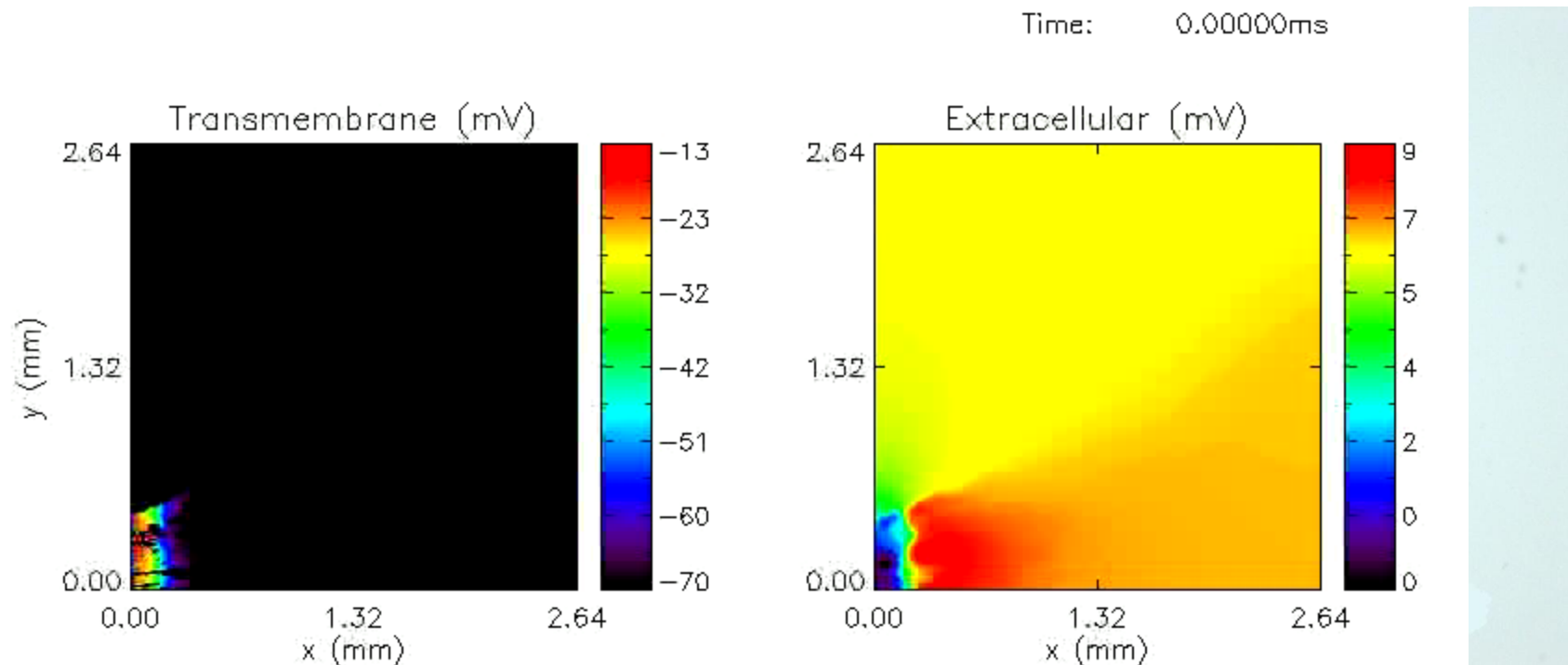




# Models of Cardiac Electro-Mechanics

- Bottom-up design

**Tissue mathematical models: electric activity**



# Models of Cardiac Electro-Mechanics

- Bottom-up design

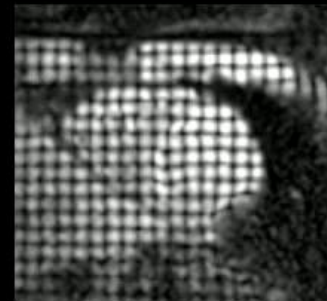
## Tissue mathematical models: mechanical coupling

$$\delta W = \int_{V_0} \mathbf{S} : \delta \dot{\mathbf{E}} dV_0 - \int_{V_0} \mathbf{f}_0 \cdot \delta \mathbf{v} dV_0 - \int_{\partial V_0} \mathbf{t}_0 \cdot \delta \mathbf{v} dA_0 = 0$$

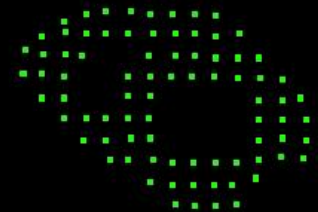
$$S_{ij} = \frac{1}{2} \left( \frac{\partial W}{\partial E_{ij}} + \frac{\partial W}{\partial E_{ji}} \right) + S_a$$

Theory of Large Deformations  
Nonlinear Hyper-elastic Materials

Tagged MRI raw data



Identify control points



Generate displacement matrices



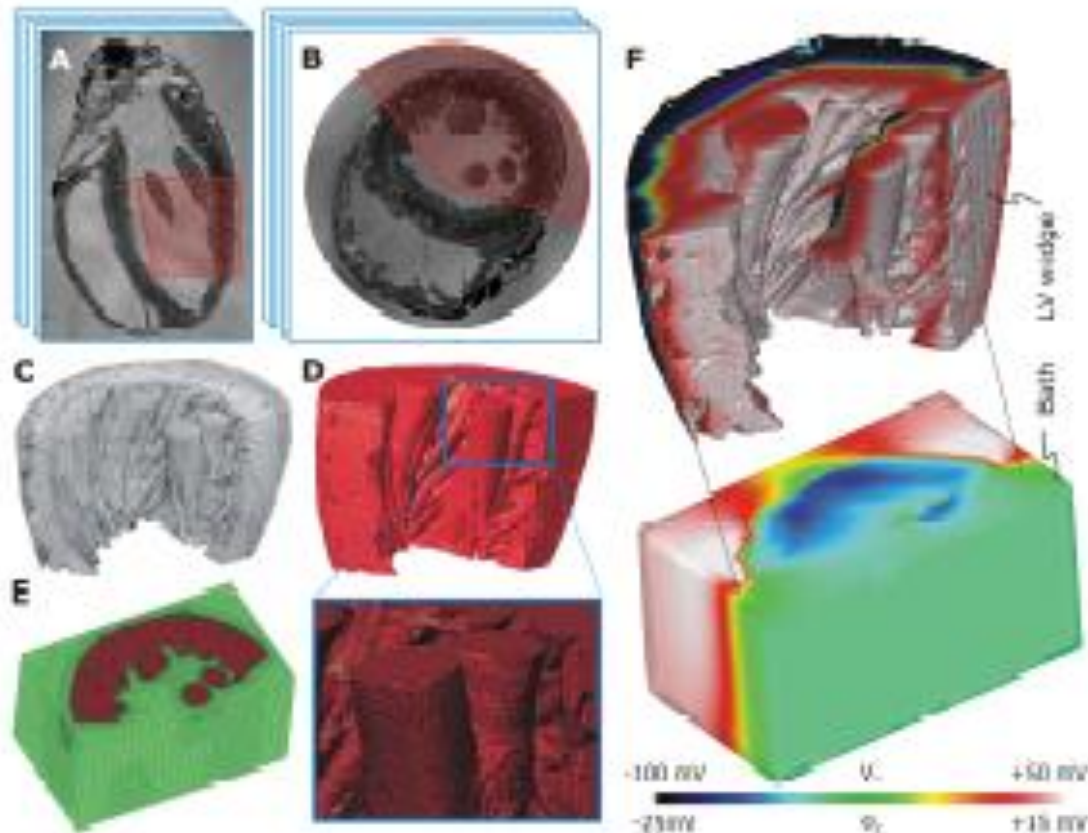
Generate mesh movement



# Models of Cardiac Electro-Mechanics

- Bottom-up design

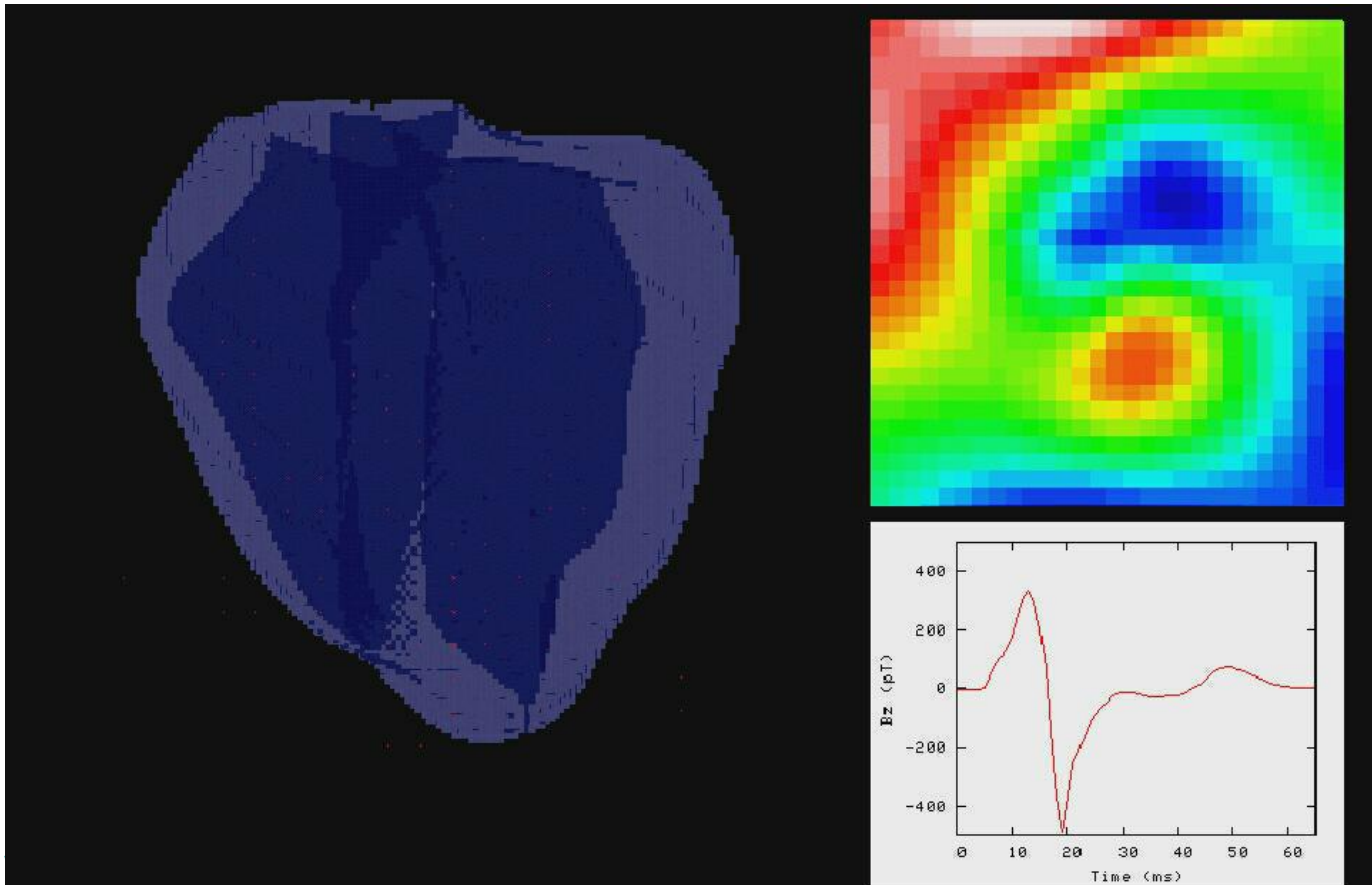
## Organ Modeling



# Models of Cardiac Electro-Mechanics

- Bottom-up design

## Organ Modeling



# Complex Models

- Modeling Challenges: Multi-scale and Multiphysics
- Computational Challenges: Simulations are computationally expensive (one heart beat = a couple of days in a parallel machine)
- Computer Challenges: Involves the coupling of several components (submodels) and data (geometry, biophysical parameters)



# Heterogeneous models for electrical propagation and mechanical contraction in the heart

## PART III

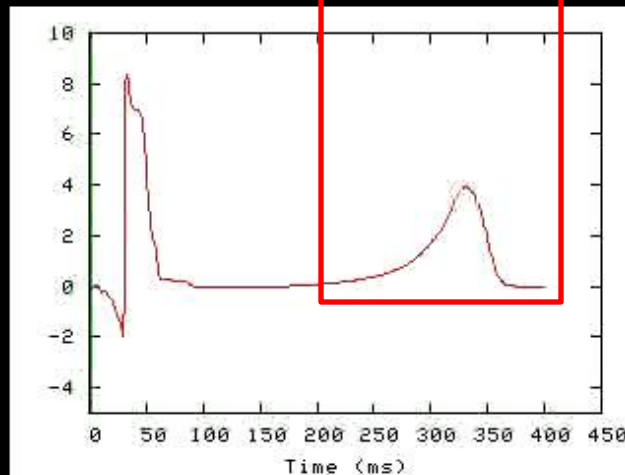
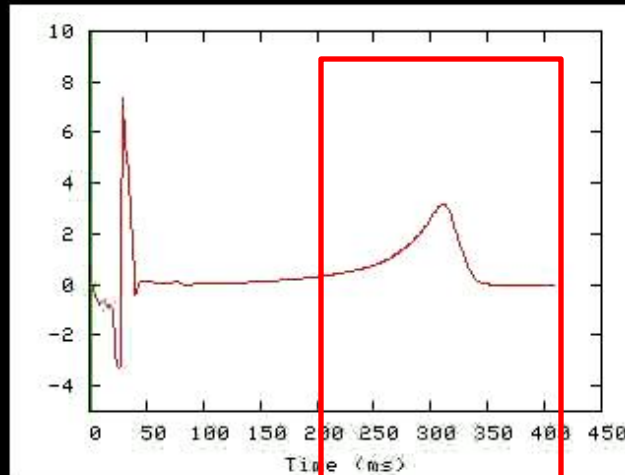
### Some **2D** Applications

Velocity of the wave front = Depolarization + tissue properties  
Simulation of fibrosis and of low gap junctional coupling



Dispersion of refractory period = Repolarization (APD) +  
tissue properties + Mechanical function

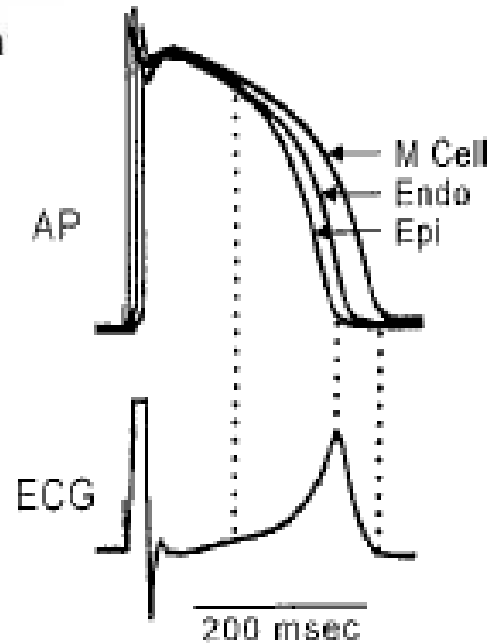
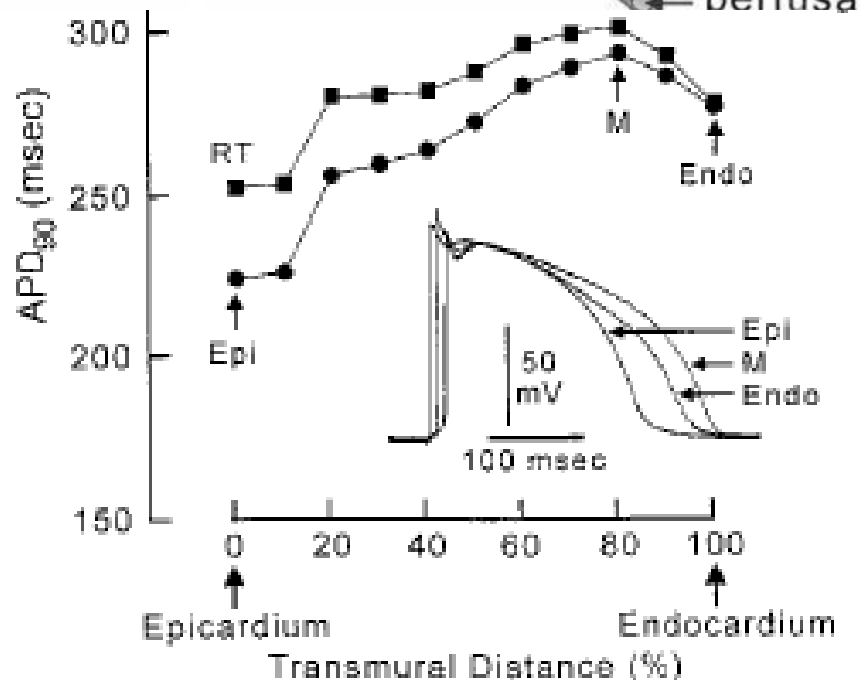
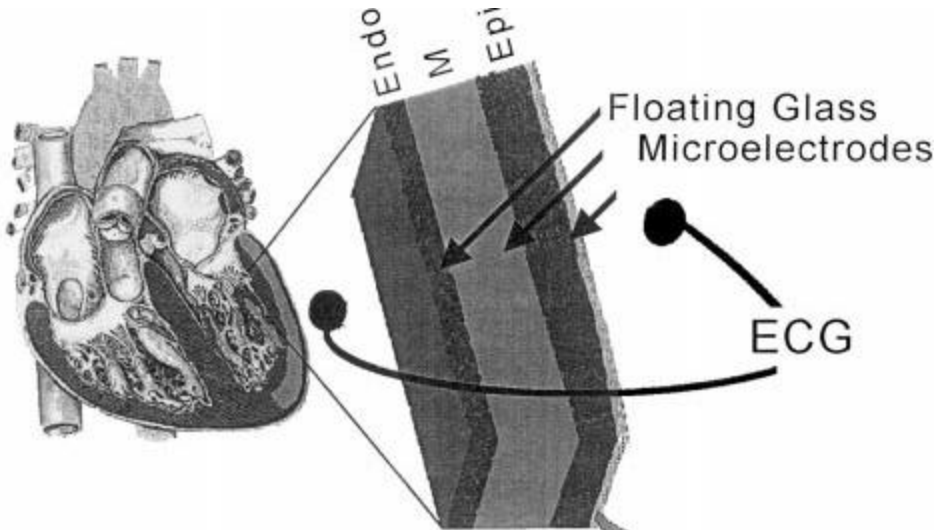
# ECG – T-Wave = Repolarization. Waveform?



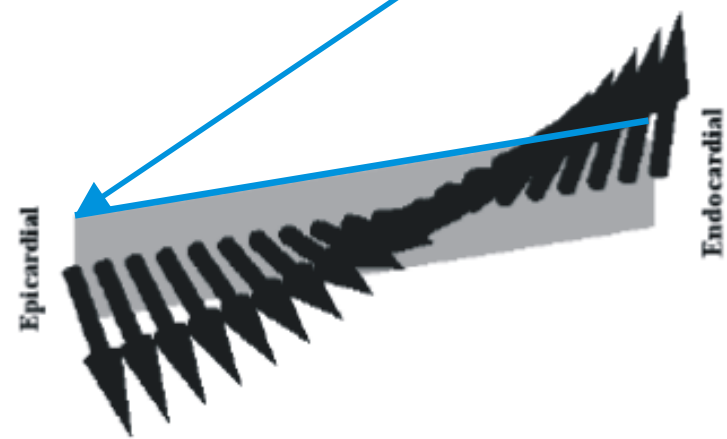
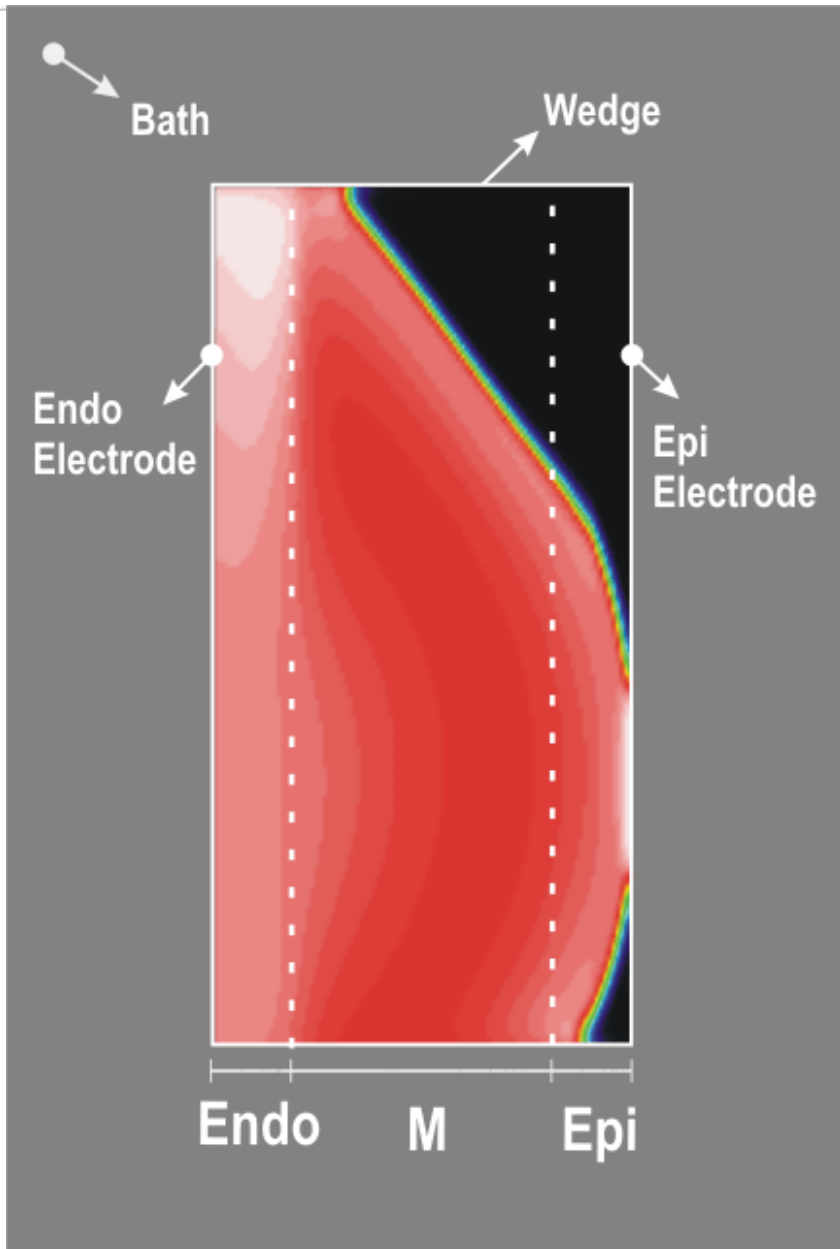
# LV Wedge

- Transmural Gradients
- M cells

-Key ingredients to understand Repolarization (T-Wave) and Arrhythmia (Tend-Tpeak index for transmural dispersion)



from Yan et al. Circ. 98

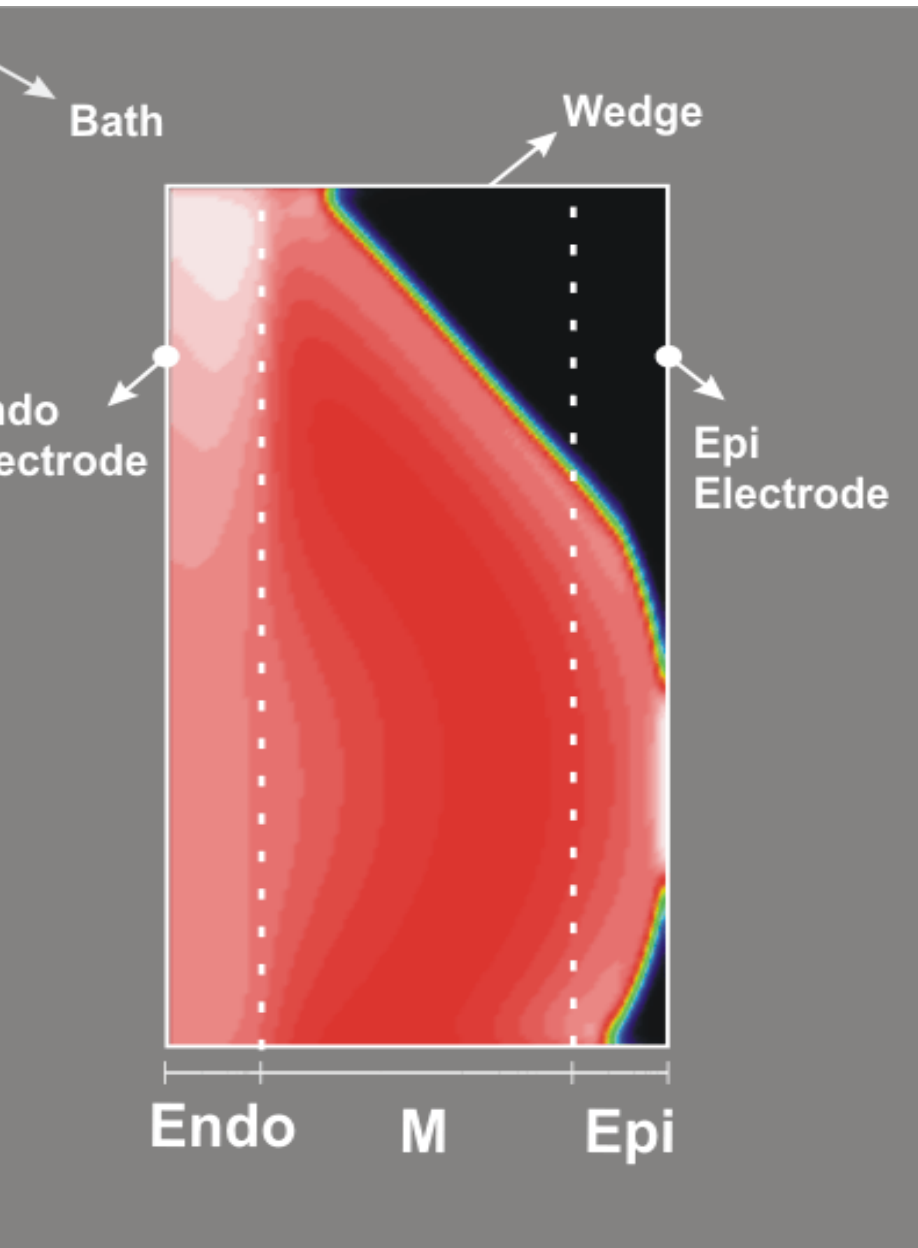


**Anisotropic Tissue –  
Transverse Anisotropy  
Fiber Transmural Rotation**

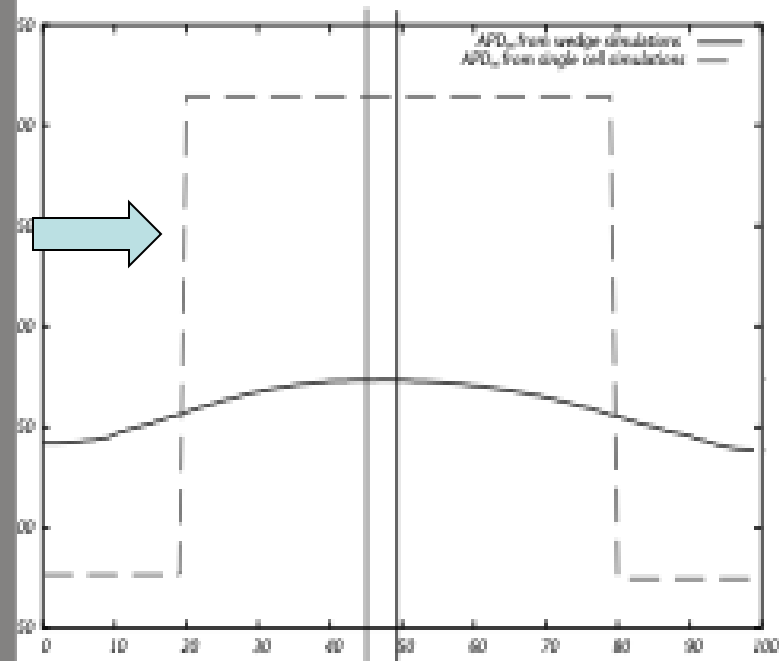
**T-waves are near flat**



# Computational wedge for human LV



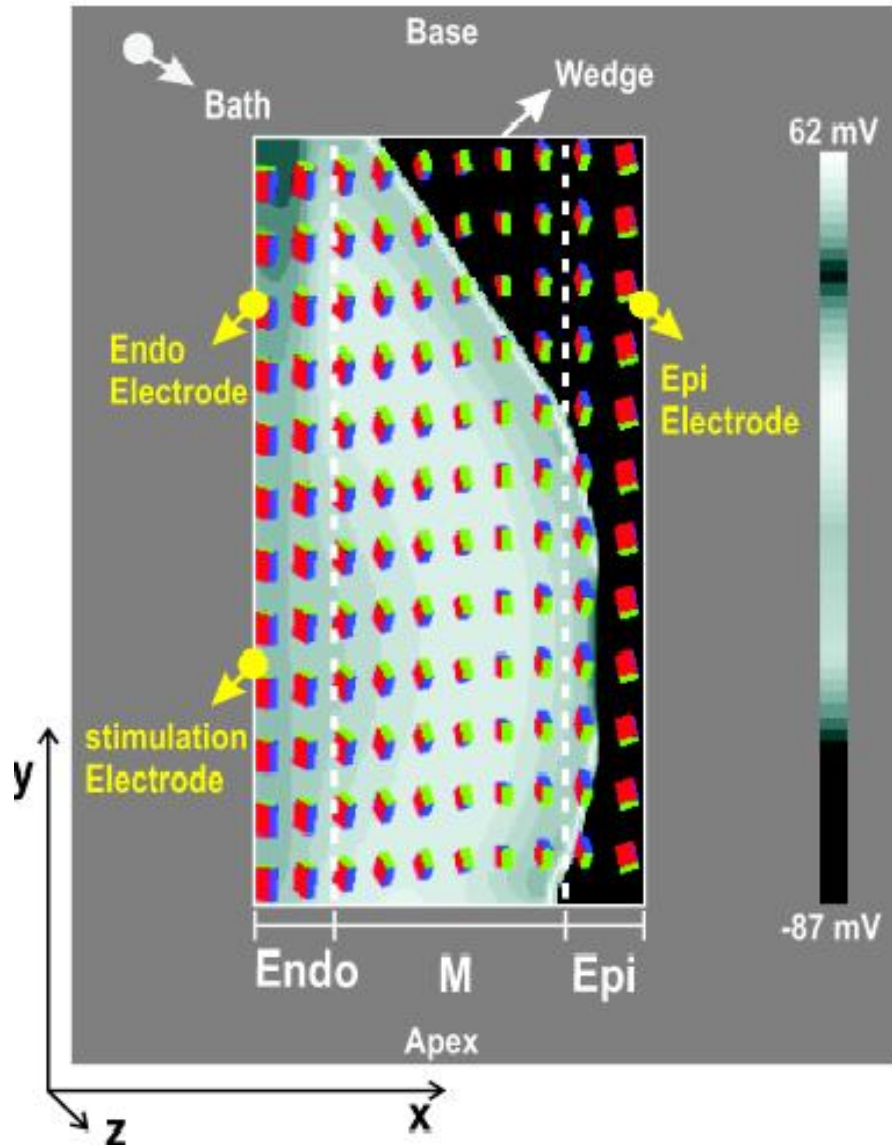
## APD90



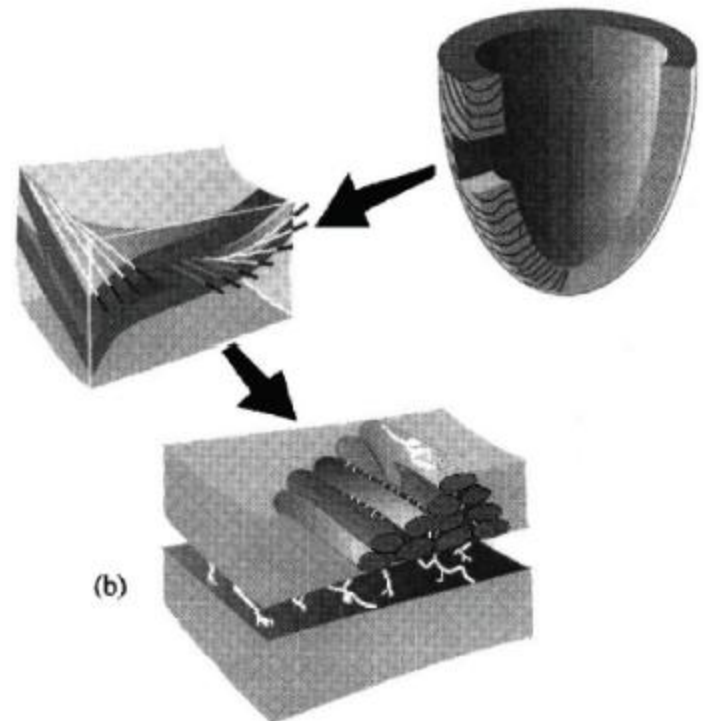
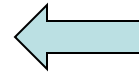
**Electrotonic Effect of the Diffusion Operator**

# Low Conduction of Epicardial Region

## Laminar-fiber structure

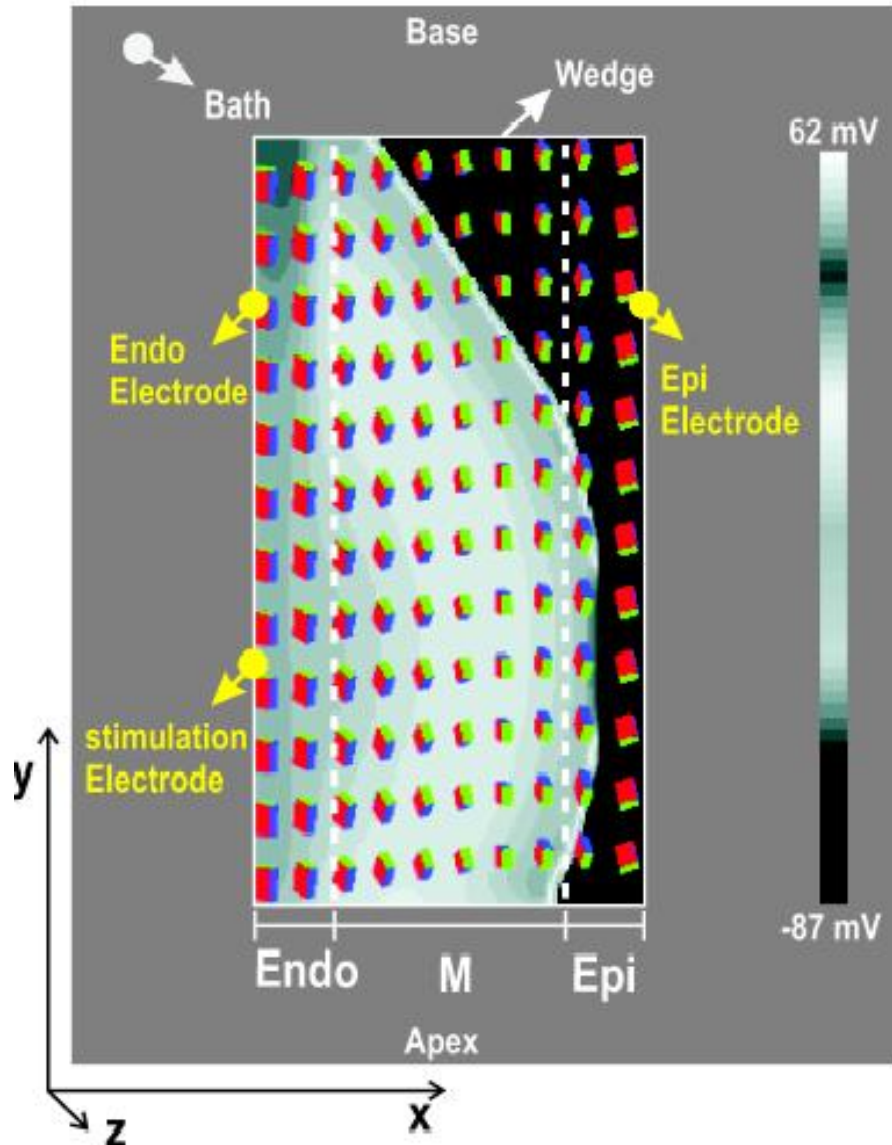


Costa et al. AmJ Physiol Heart Circ Physiol 1999;.

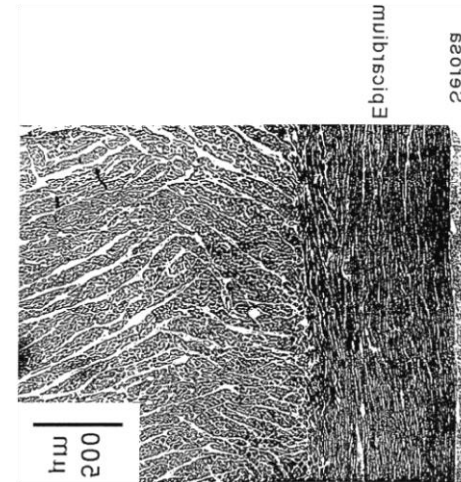
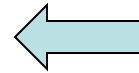


# Low Conduction of Epicardial Region

## Laminar-fiber structure

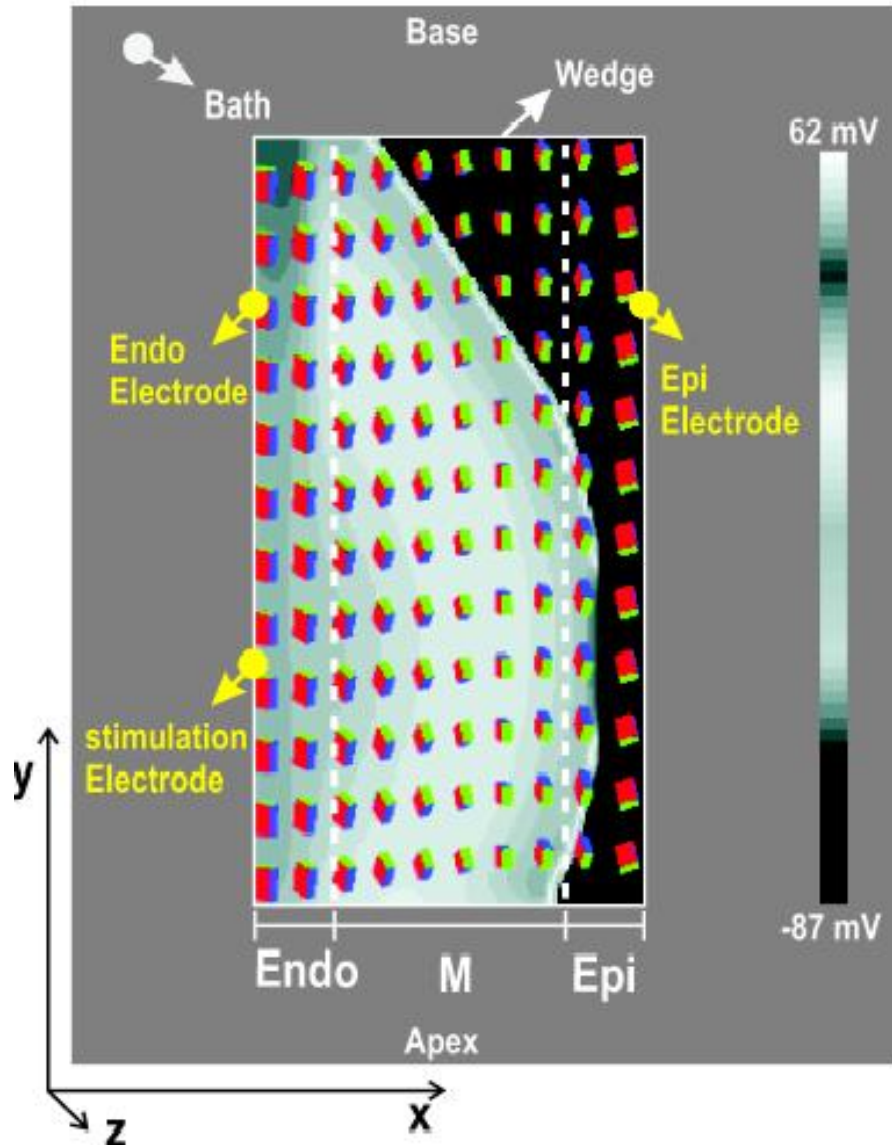


Costa et al. AmJ Physiol Heart Circ Physiol 1999;.

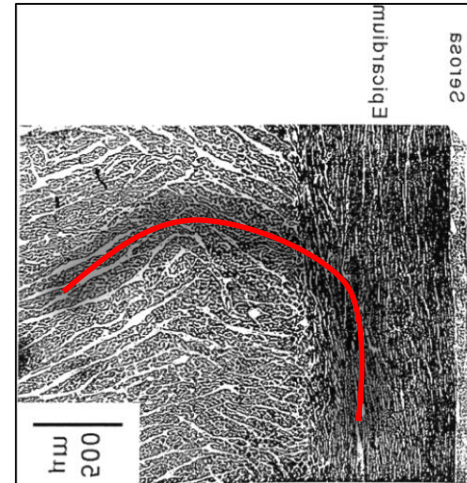
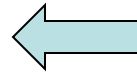


# Low Conduction of Epicardial Region

## Laminar-fiber structure

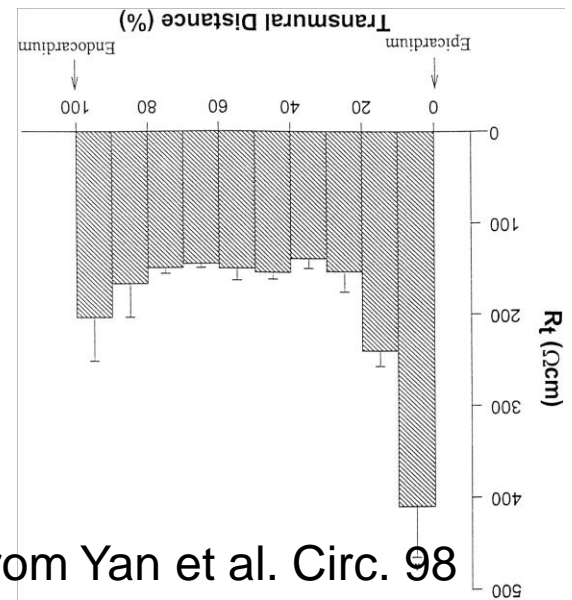
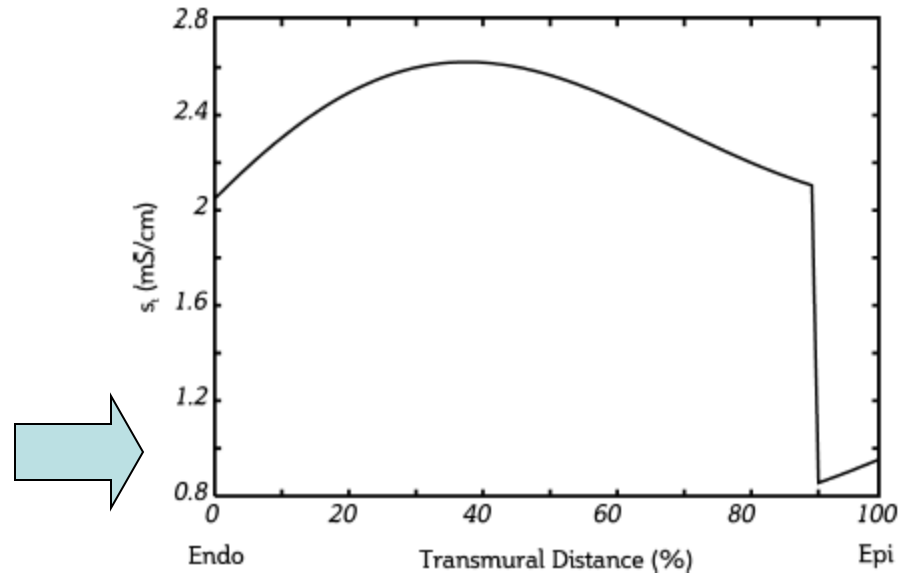
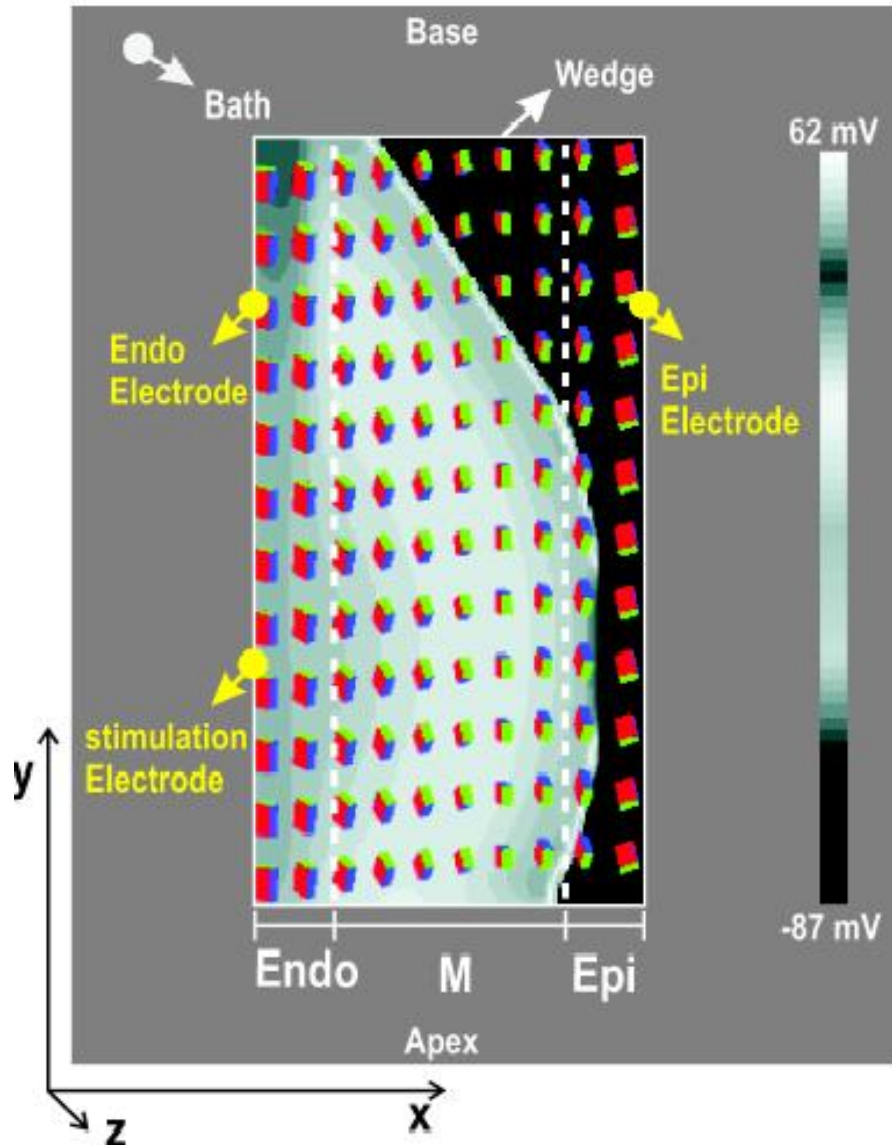


Costa et al. AmJ Physiol Heart Circ Physiol 1999;.





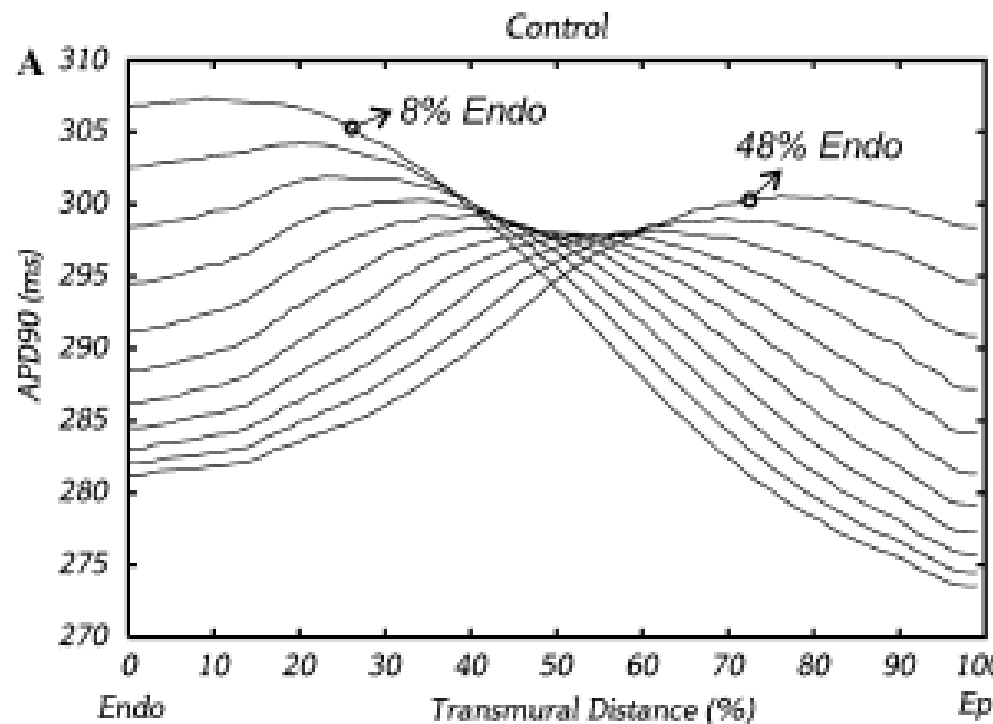
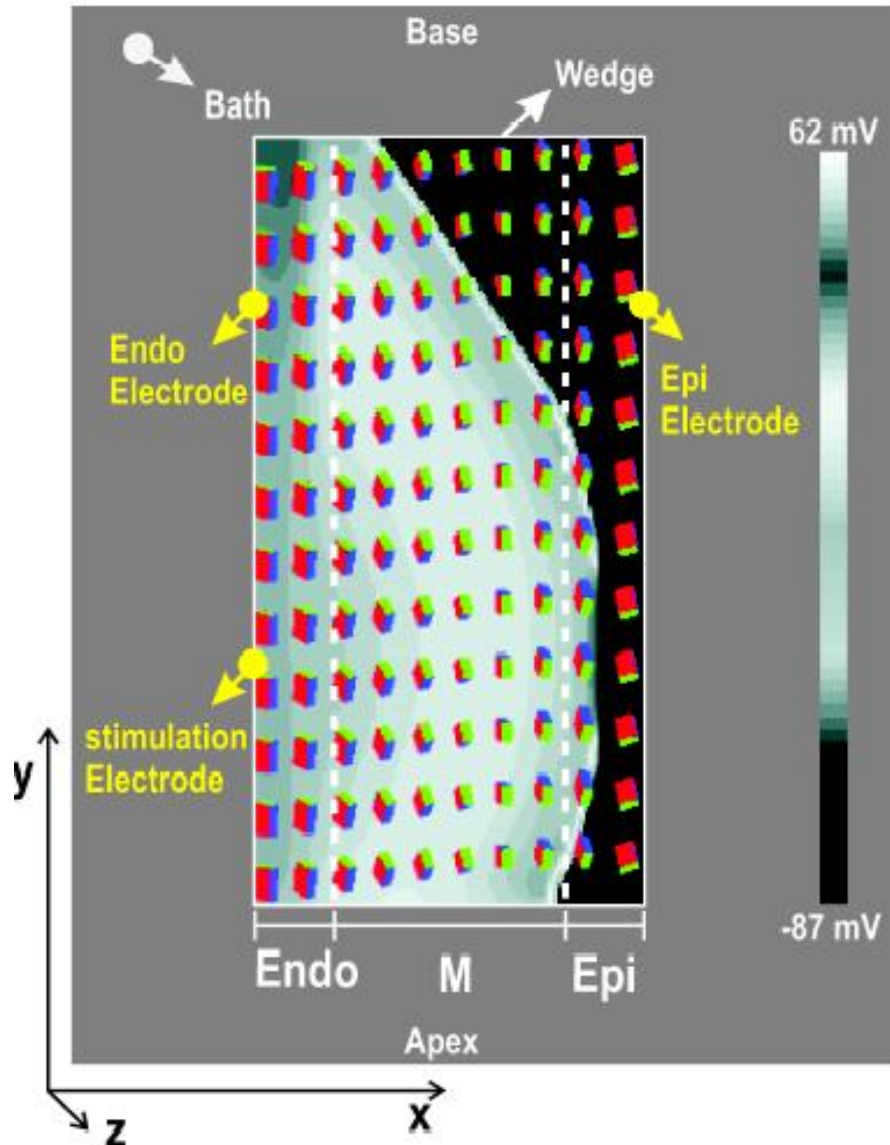
# Epicardial Region Low Conduction: Laminar-fiber Architecture



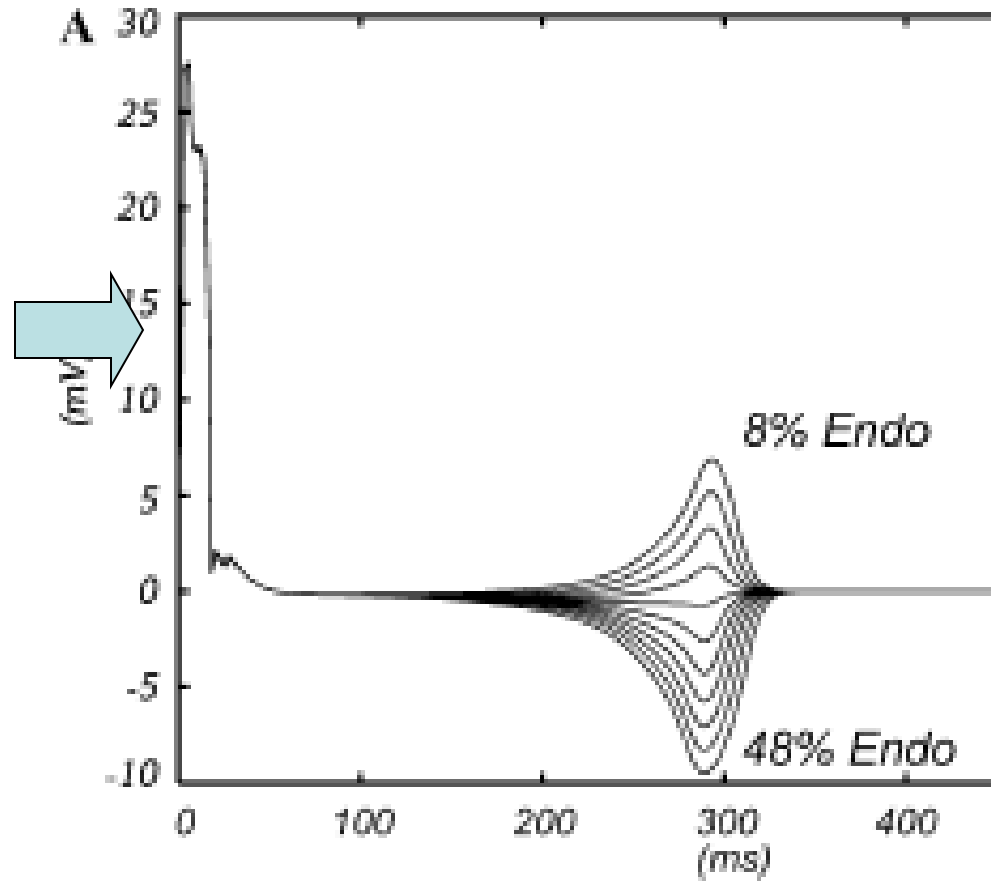
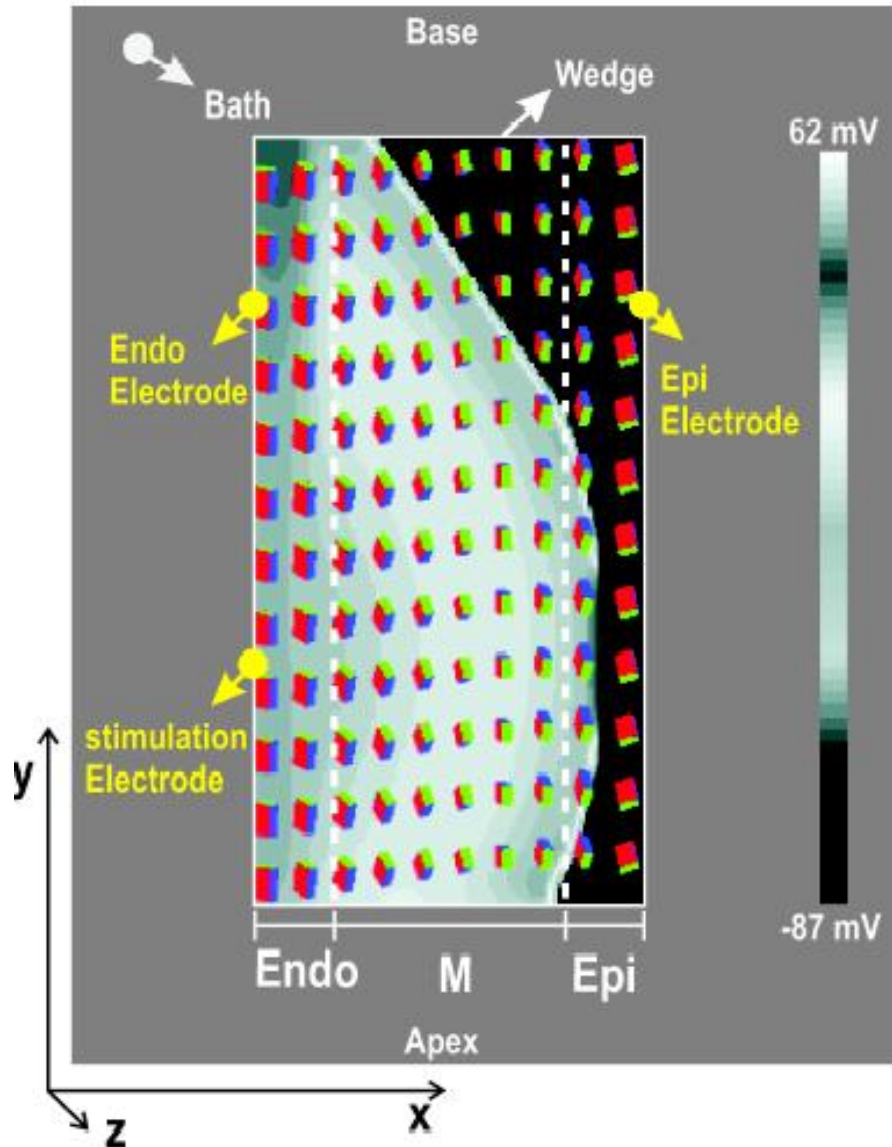
from Yan et al. Circ. 98



M-cells = 44%



M-cells = 44%



# A Computational Wedge model for the human LV

- T-wave format results from the Interplay of functional (APD, epi, endo M) and anatomical heterogeneities (fiber-sheet transmural rotation).

dos Santos, Rodrigo Weber ; OTAVIANO CAMPOS, FERNANDO ; NEUMANN CIUFFO, LEANDRO ; NYGREN, Anders ; GILES, Wayne ; KOCH, Hans . ATX-II Effects on the Apparent Location of M Cells in a Computational Model of a Human Left Ventricular Wedge. **Journal of Cardiovascular Electrophysiology**, New York, v. 17, n. Suppl 1, p. S86-S95, 2006.

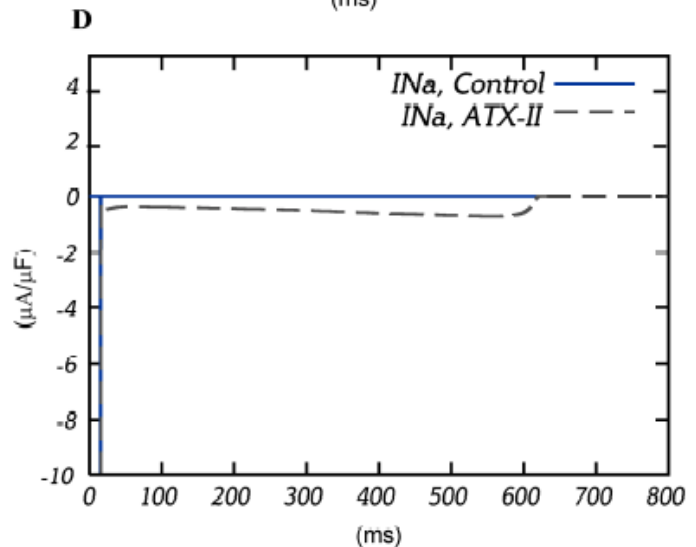
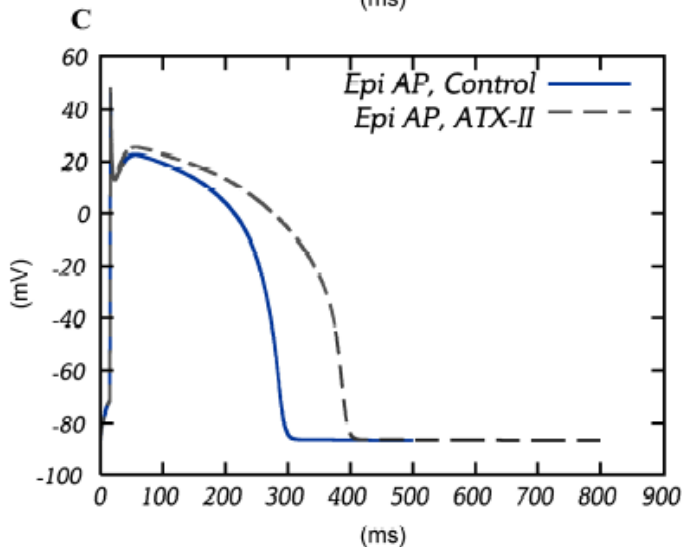
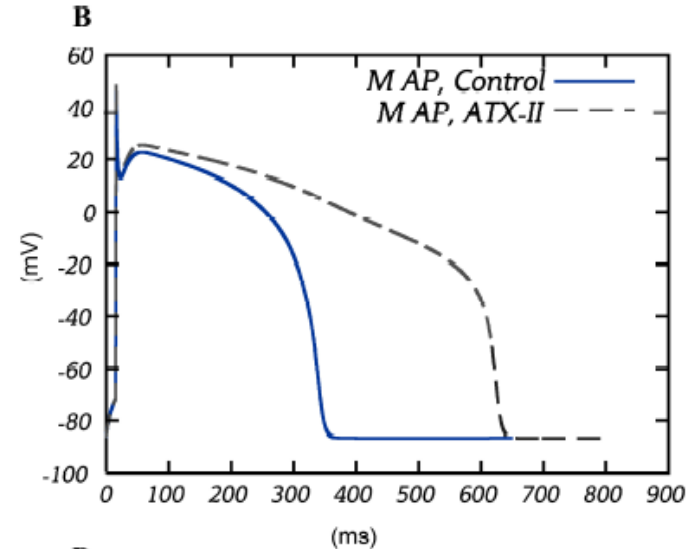
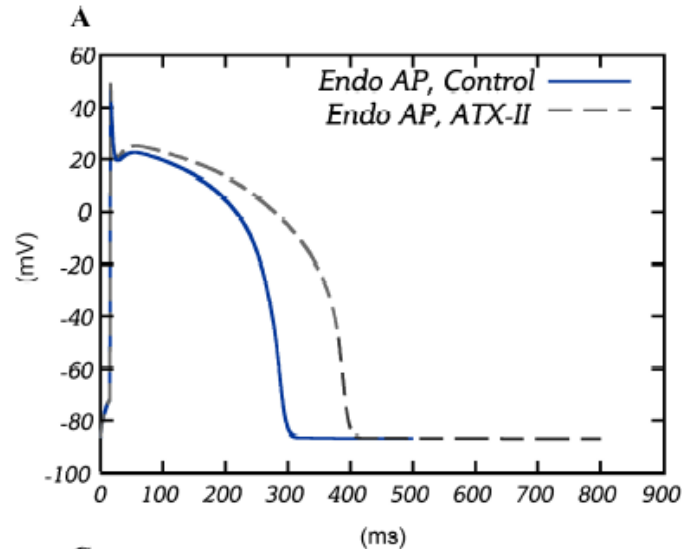
## A Computational Wedge model for the human LV

- Administration of anemone toxin II (ATX-II) alters the dynamics of late  $\text{Na}^+$  currents,  $I_{\text{Na}}$  in ventricular cells.
- Experiments using isolated canine ventricular wedge preparations can mimic LQT3 (Genetic disease – Deathly arrhythmia).

# Simulation of ATX-II for the ten-Tusscher cell models

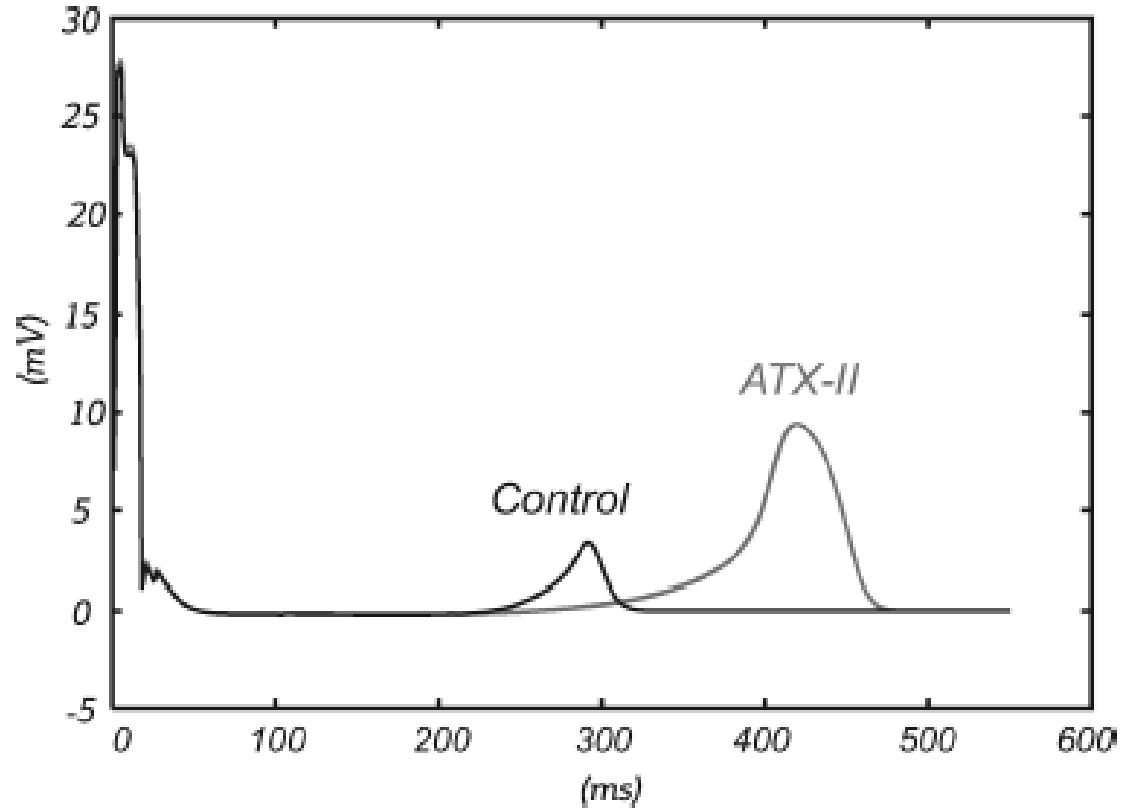
The effects of ATX-II on  $I_{Na}$  were simulated by altering the inactivation parameter:  $h$  (fast gate) and  $j$  (slow gate).

Crossing scales from protein (ion channels) to electrograms

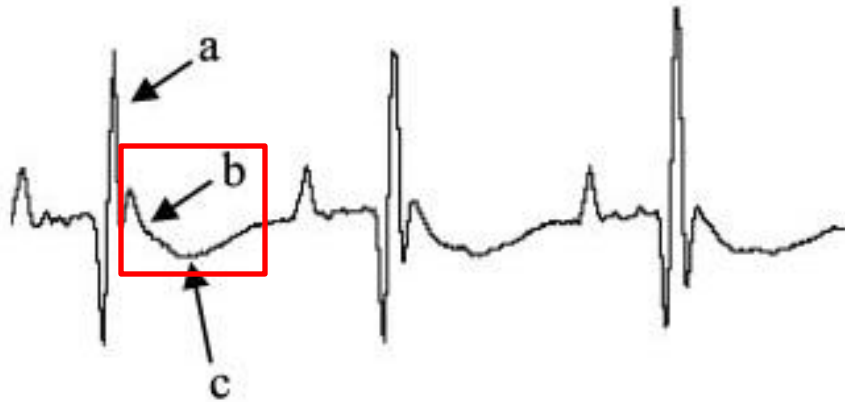




# Transmural Electrograms from the computational wedge: Control and ATX-II



# Computational wedge model for the rat LV



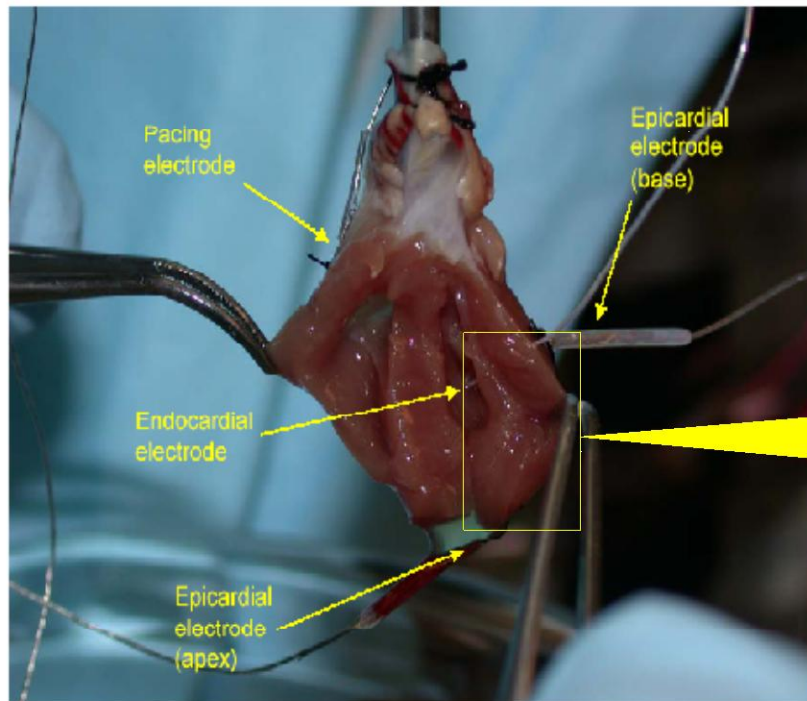
Danik et al. AmJ Physiol Heart Circ  
Physiol 2002;

Biphasic T-wave

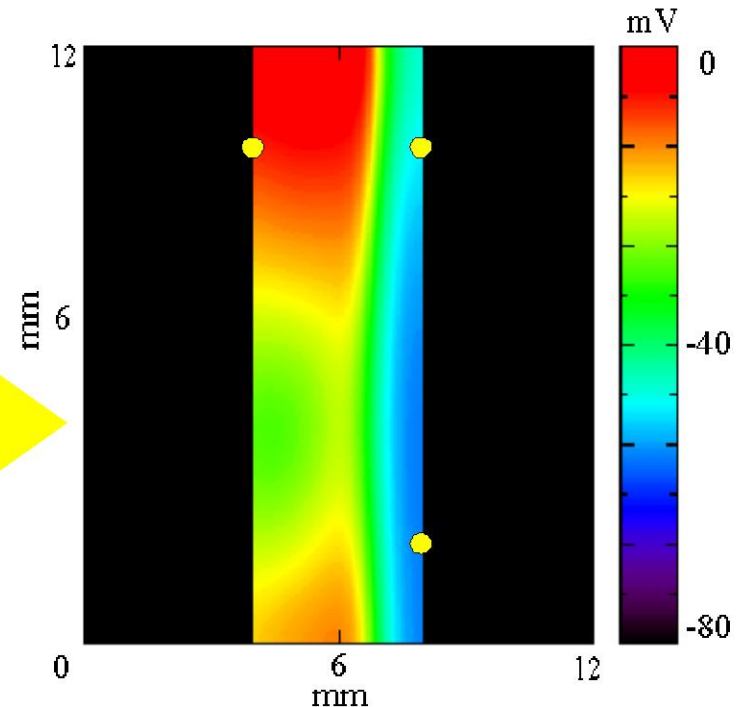


# Computational wedge model for the rat LV

a) Experiment

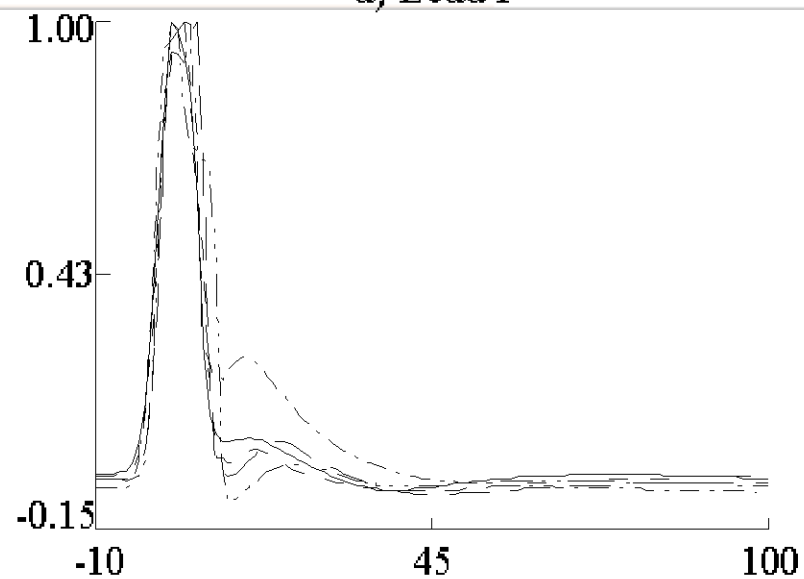


b) Simulation

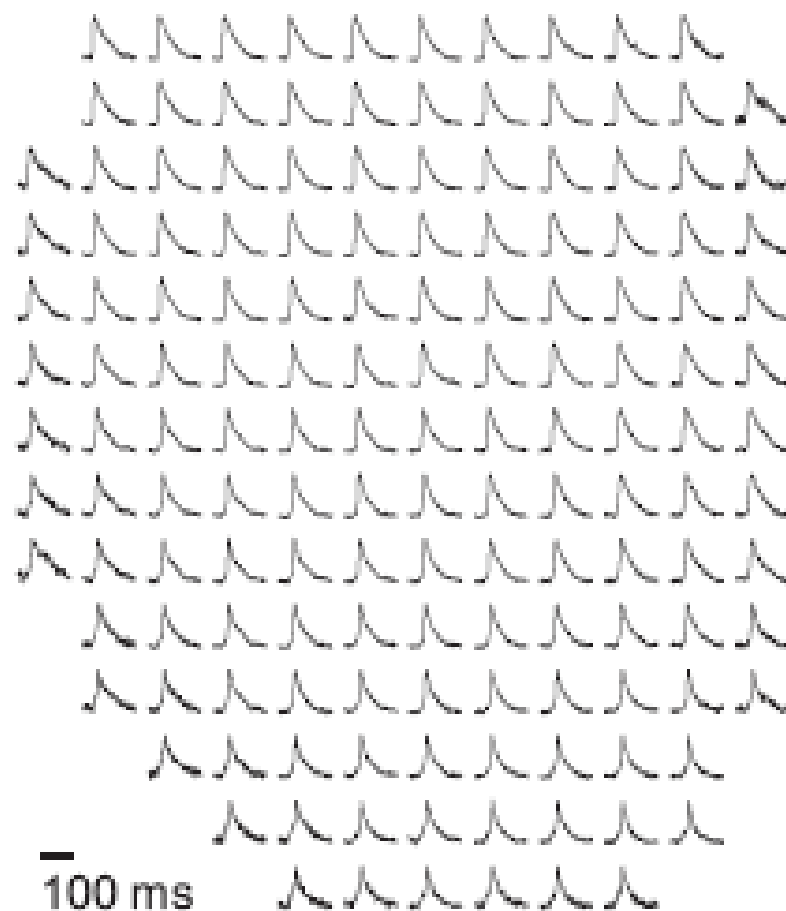
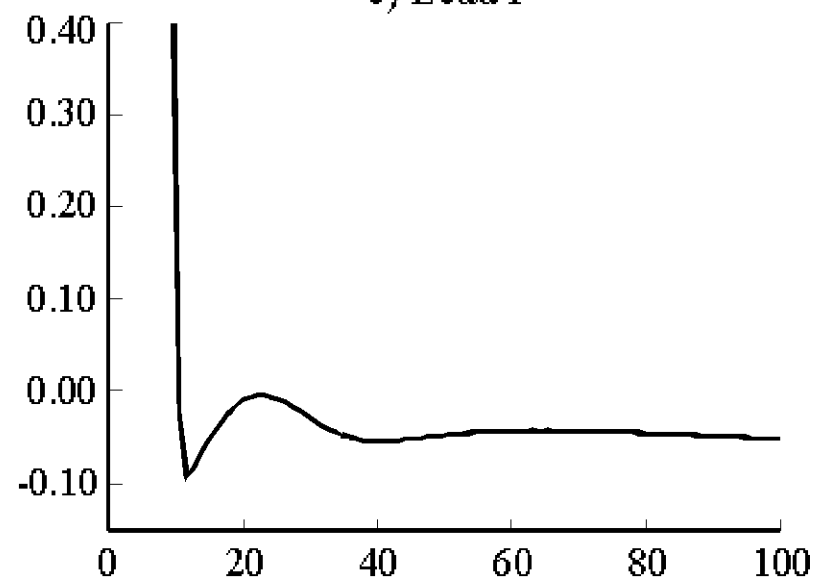


a) Setup of the Rat experiment. b) Simulation setup. The perfusing bath is shown in black. A transmembrane potential (mV) distribution taken during the repolarization phase is presented on the tissue. The simulated electrodes are shown as yellow circles.

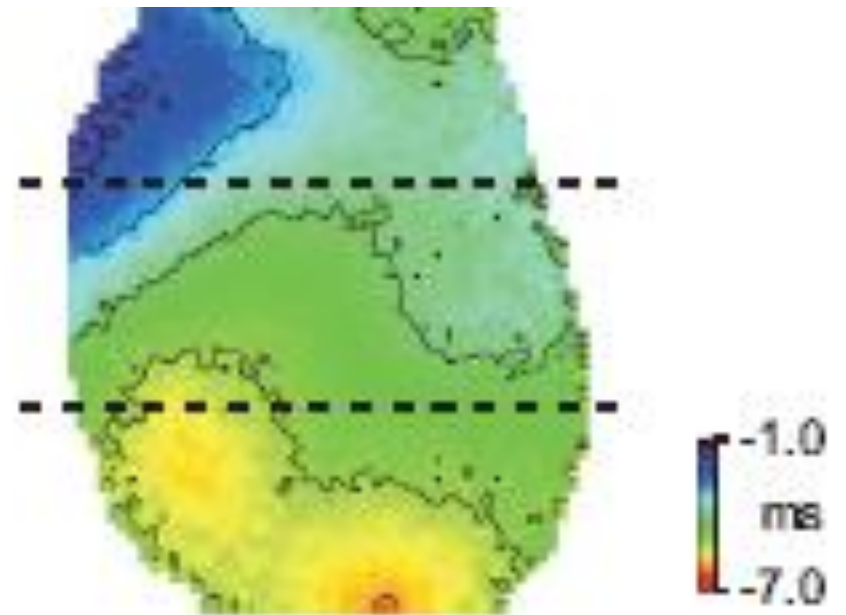
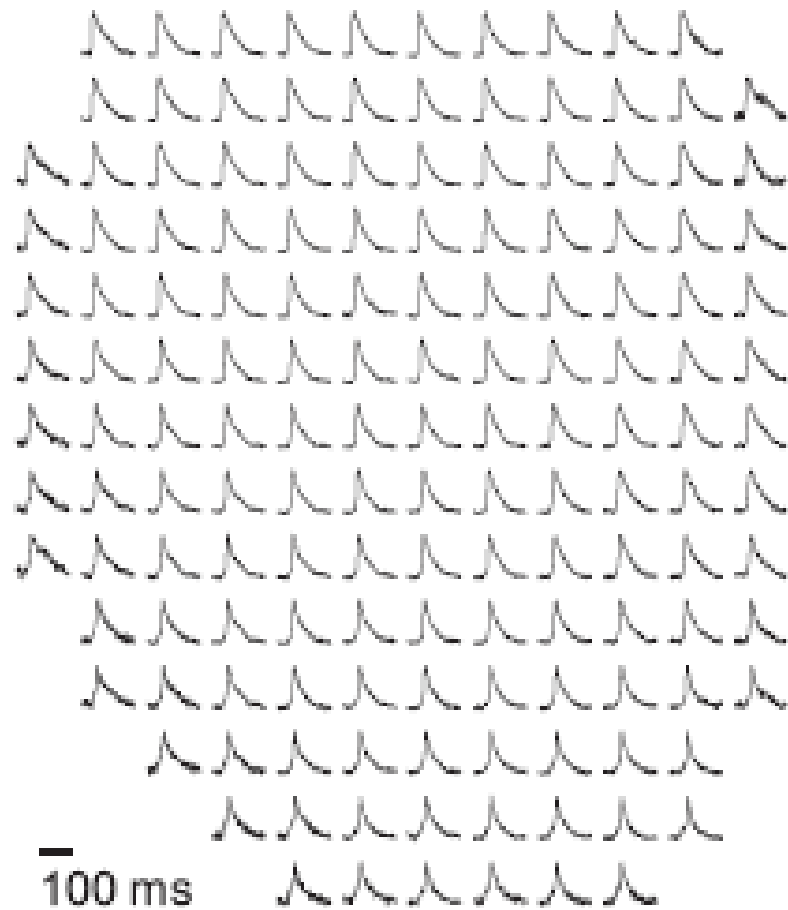
a) Lead I



c) Lead I

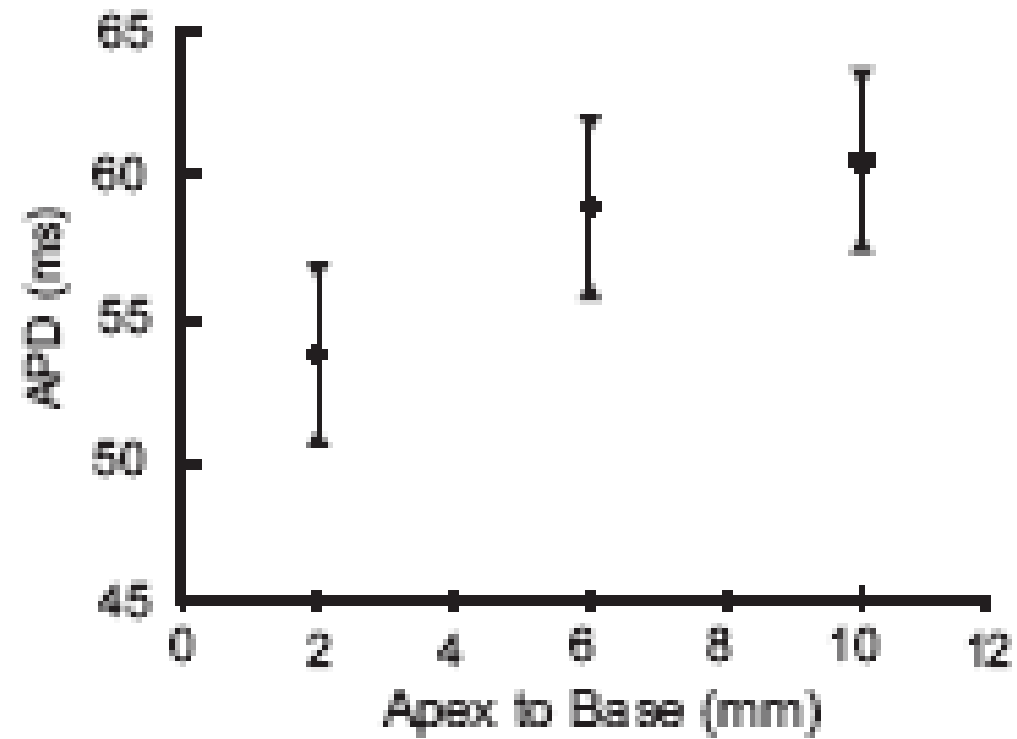


# Optical Maps

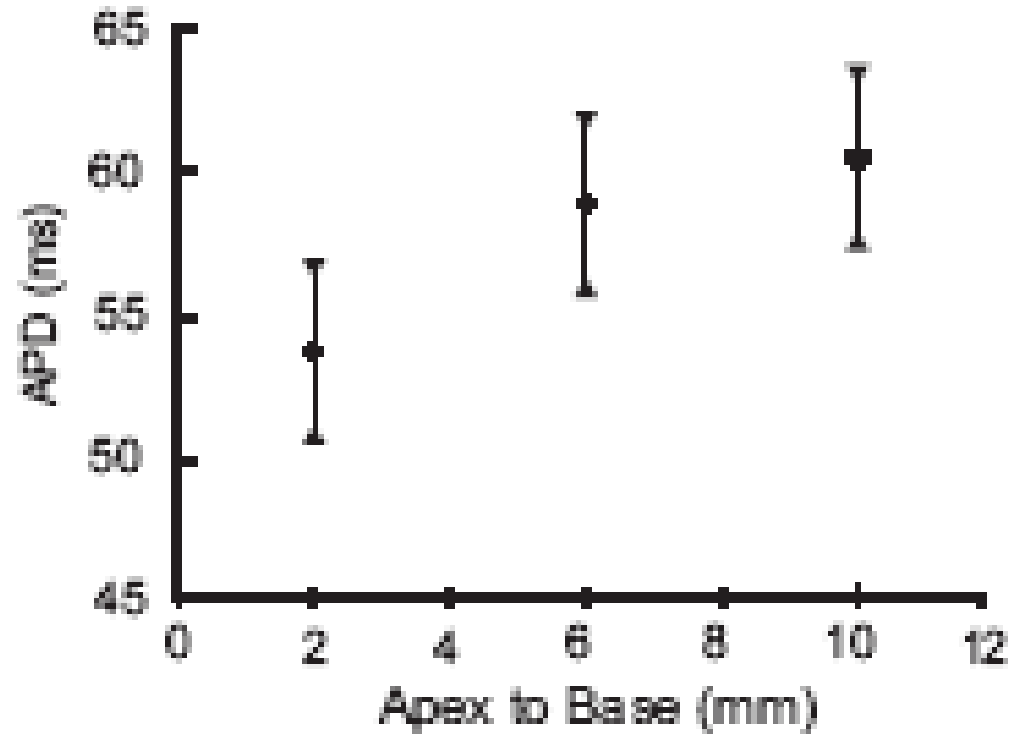
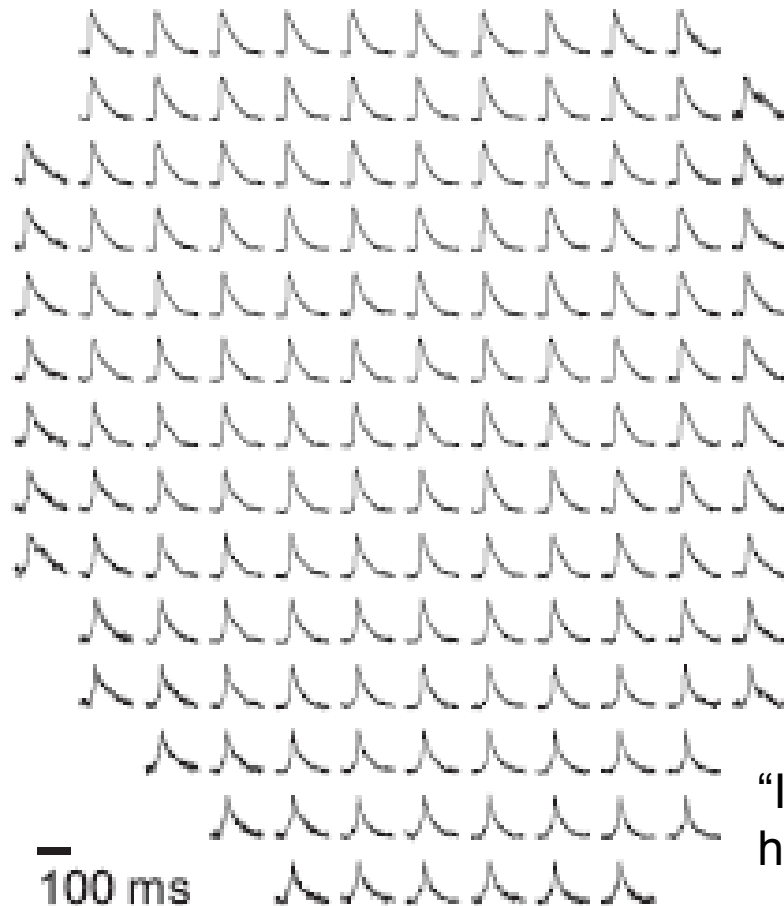




# APD Distribution

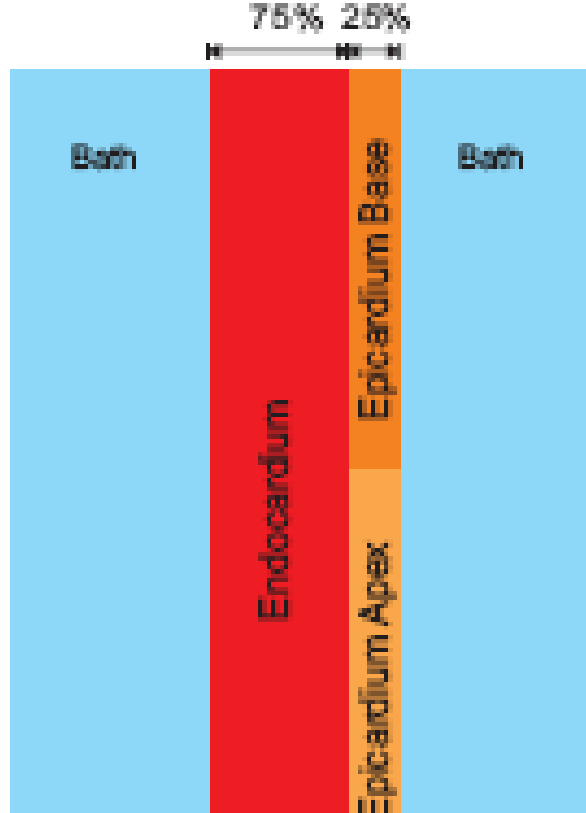


# APD Distribution

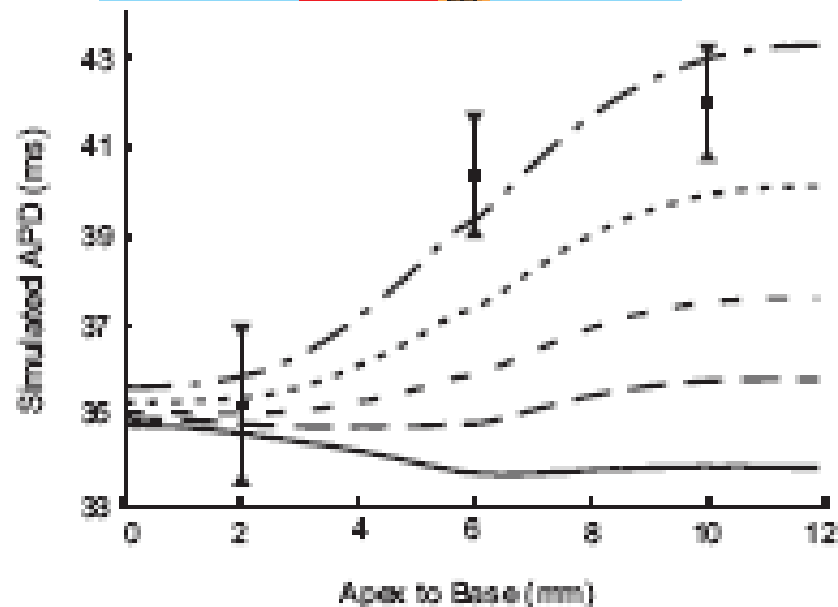


“Ito densities were found to be significantly higher in apex than in base myocytes”

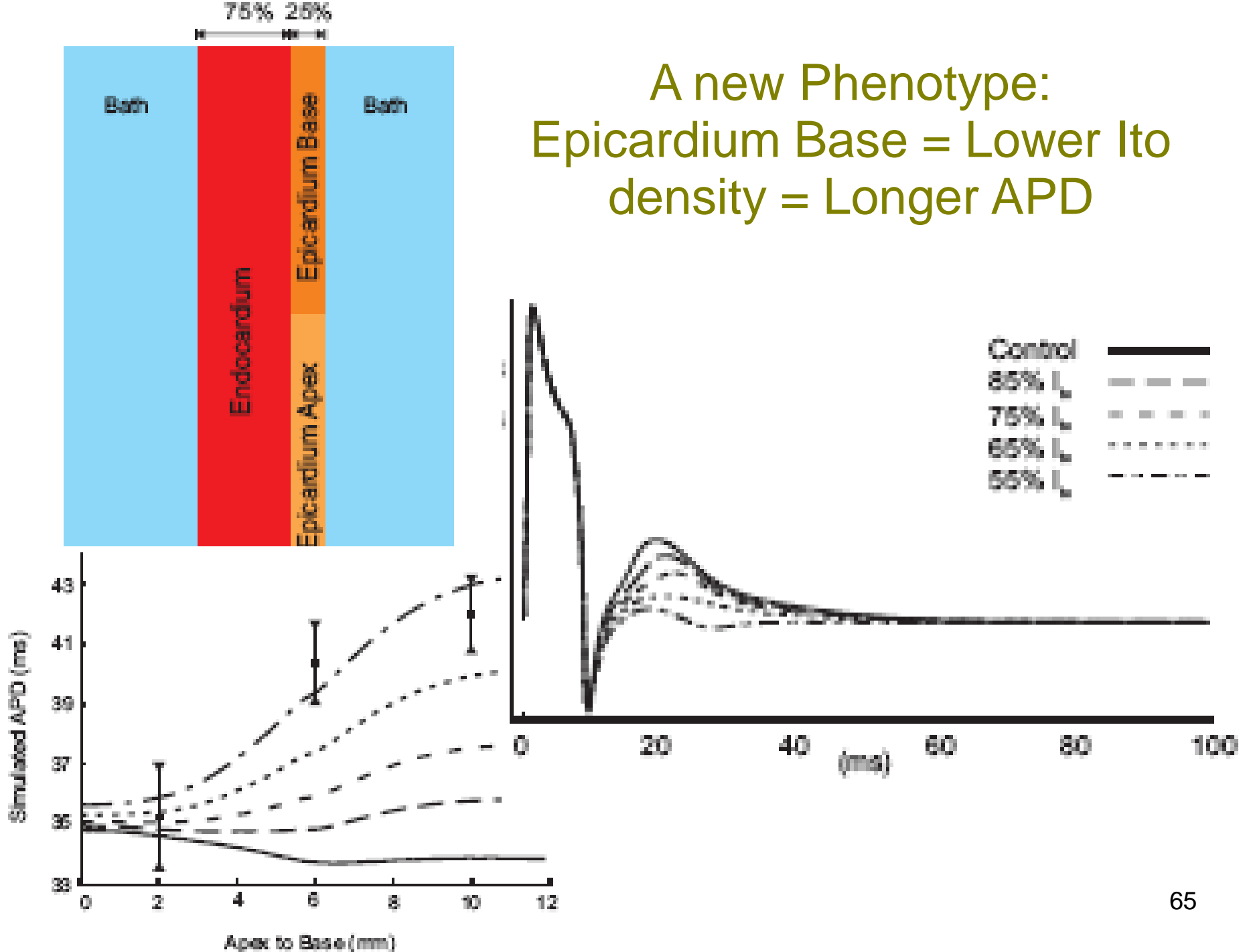
Brunet et al. *J Physiol* 559: 103-120, 2004.

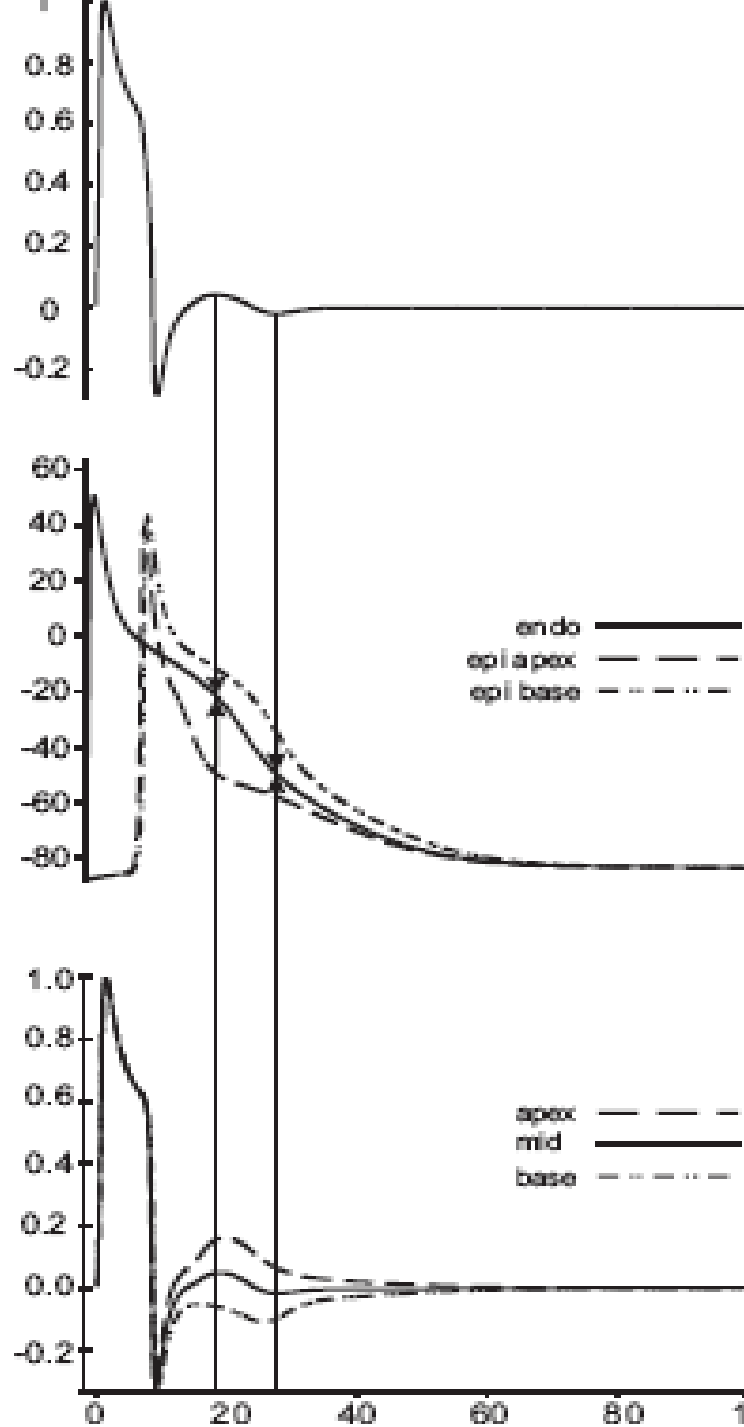


A new Phenotype:  
Epicardium Base = Lower Ito  
density = Longer APD



A new Phenotype:  
Epicardium Base = Lower  $I_{to}$   
density = Longer APD



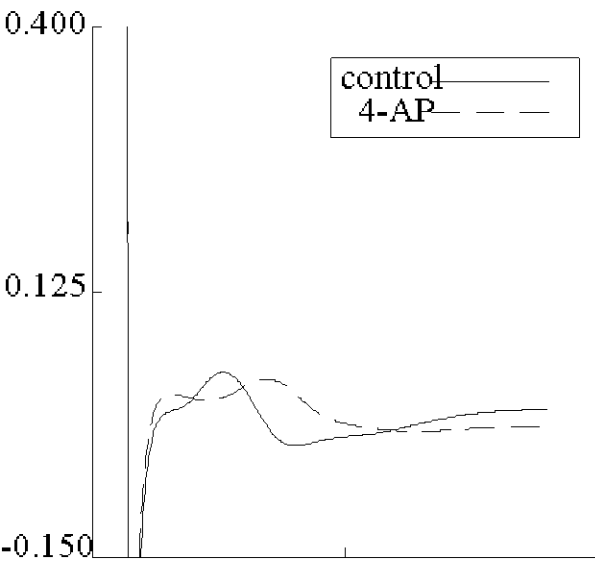


Weber dos Santos, R. ; Nygren, A. ; Otaviano Campos, F. ; Koch, H. ; Giles, W. R. . Experimental and theoretical ventricular electrograms and their relation to electrophysiological gradients in the adult rat heart. **American Journal of Physiology. Heart and Circulatory Physiology**, v. 297, p. H1521-H1534, **2009**.

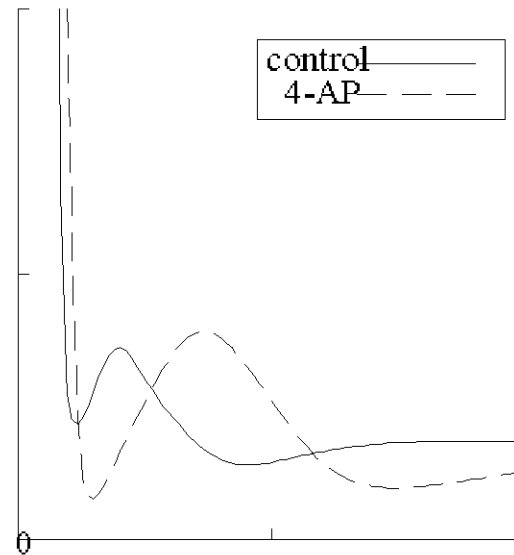


# Reproducing drug effects

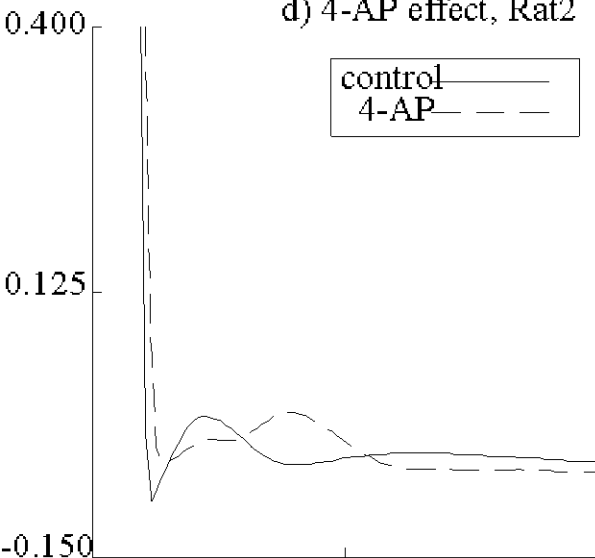
a) Simulated 4-AP effect, Lead I



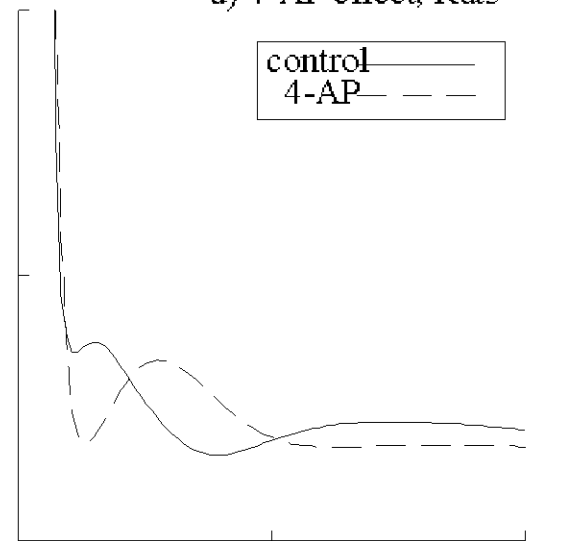
b) 4-AP effect, Rat 1



d) 4-AP effect, Rat2



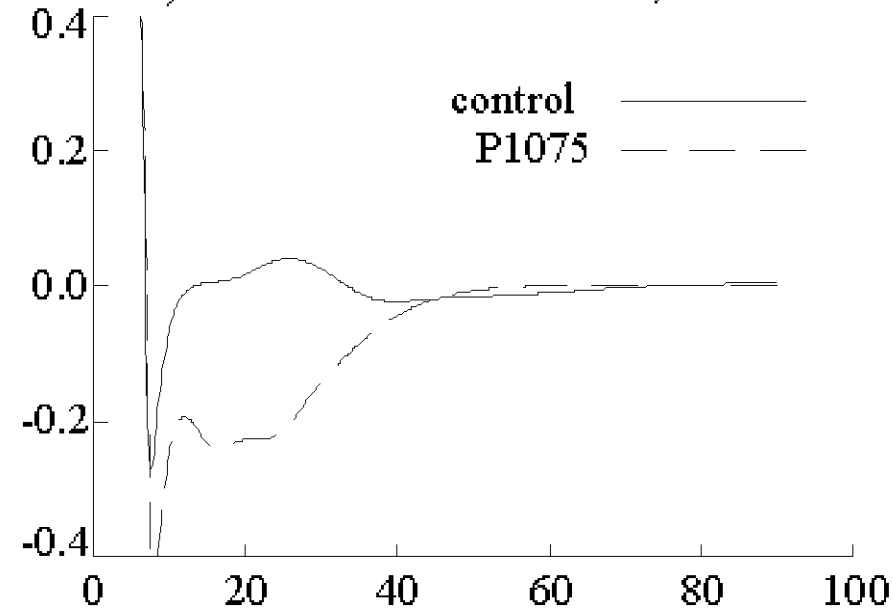
d) 4-AP effect, Rat3



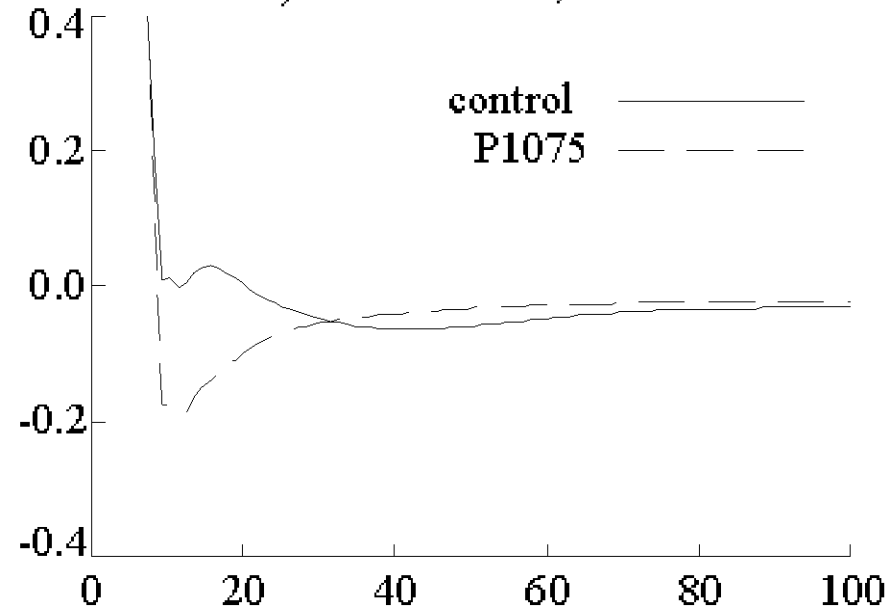
Experiment and computer simulation results.  
The drug 4-AP was used to block  $I_{to}$  in the Langendorf experiment preparations.

# Reproducing drug effects

a) Simulated P1075 effect, Lead I



b) P1075 effect, Rat 4



Experiment and computer simulation results.

The drug P1075 was used to open I<sub>K</sub> ATP in the Langendorf experiment preparations.

# Cardiac Mechanics

# Effects of Mechanical Deformation on Simulated Electrograms of a Human Left Ventricular Wedge

B. L. de Oliveira, B. M. Rocha, L. P. S. Barra, E. M. Toledo, J. Sundnes and R. Weber dos Santos

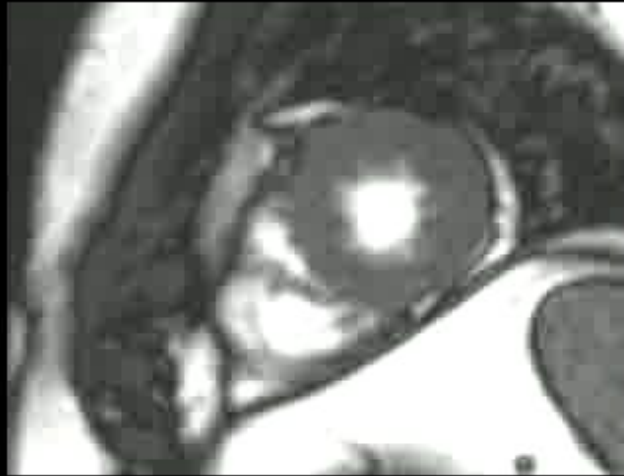
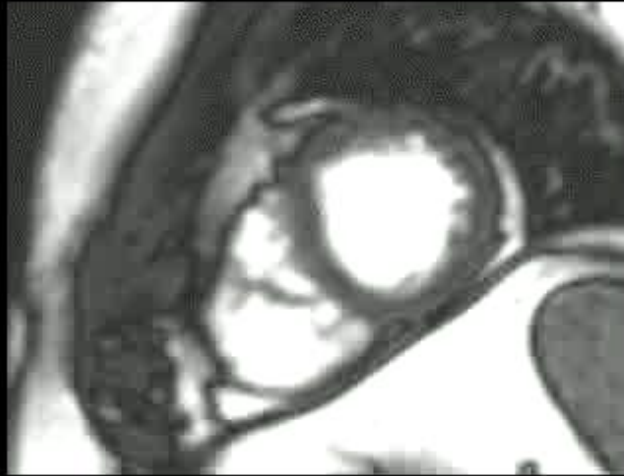
**Abstract**—Mechanical deformation affects the electrical activity of the heart through multiple feedback loops. The purpose of this study is to quantify the effect of deformation on simulated electrograms from an in silico human ventricular wedge. To achieve this purpose we developed a strongly coupled electromechanical cell model by coupling a human left ventricle electrophysiology model and an active contraction model parametrized for human cells. This model was then embedded in tissue simulations based on bidomain equations and non-linear solid mechanics. The effects of mechanical deformation on simulated electrograms were then evaluated. Our results indicate that the feature of the electrogram that is most influenced by deformation is the T-wave. Our findings are that there is an increase on the amplitude of the T-wave on simulations that account for the effects of cardiac deformation.

**Index Terms**—human electromechanical model, bidomain, solid mechanics, mechanoelectrical feedback, T-wave

the ventricles have contracted and are in the relaxation phase. The morphology of the T-wave has an important clinical significance as changes to it can be associated with several diseases and clinical conditions.

A 2D mechano-electric model was developed by Smith et al. to evaluate how deformation affects the T-wave [4]. The conclusion was that heart deformation slightly decreases the T-wave amplitude. However, this study did not consider any type of Action Potential (AP) heterogeneity which is well known to play an important role on T-wave morphology [6], [7].

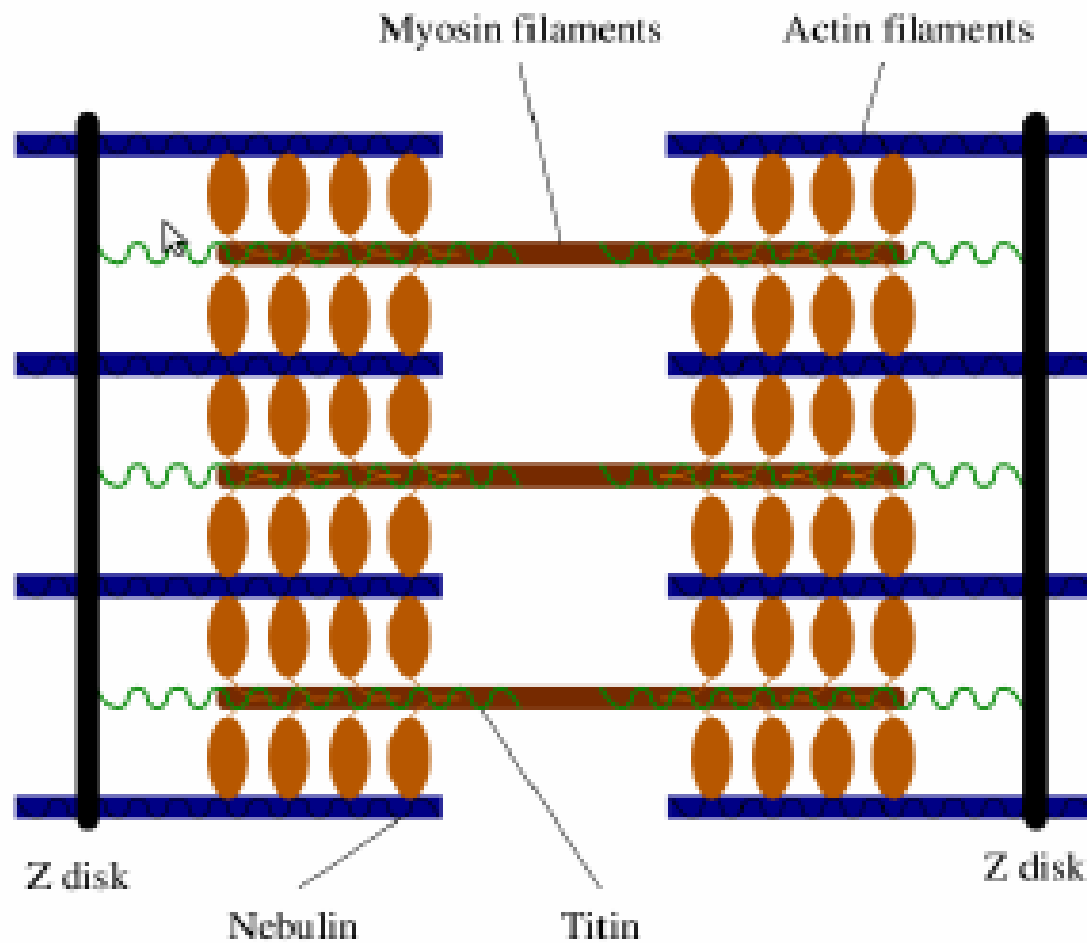
Another study with the same purpose was developed by Keller et al. [5]. In this study different phenotypes expressing different types of cardiac myocytes with heterogeneous action potentials were considered and a detailed 3D anatomical model of the heart was developed. This study also concluded that the inclusion





# Cardiac Mechanic

## Force Generation

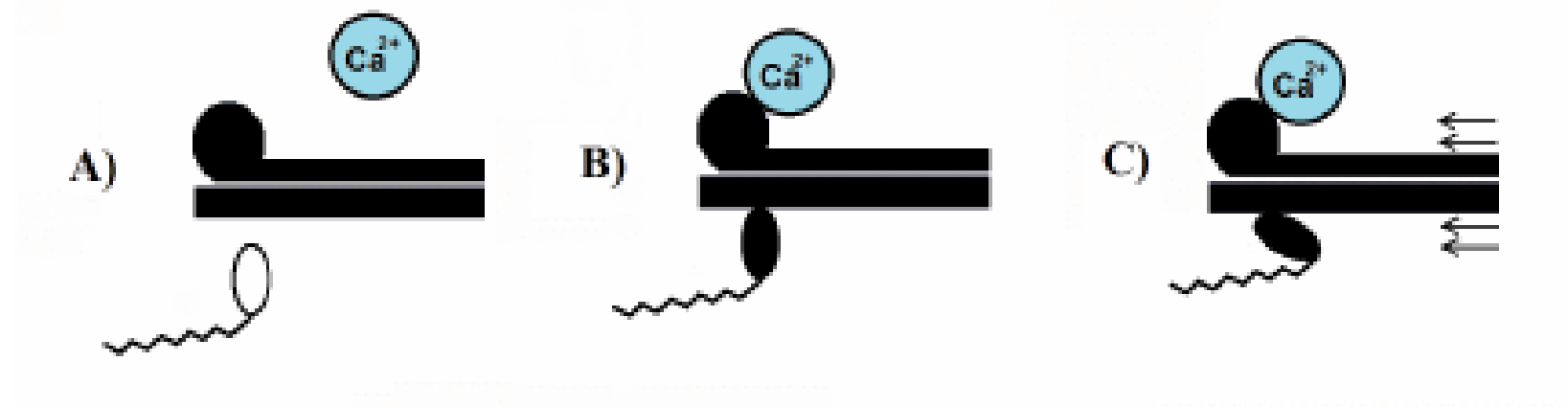


(Sachse 2004)

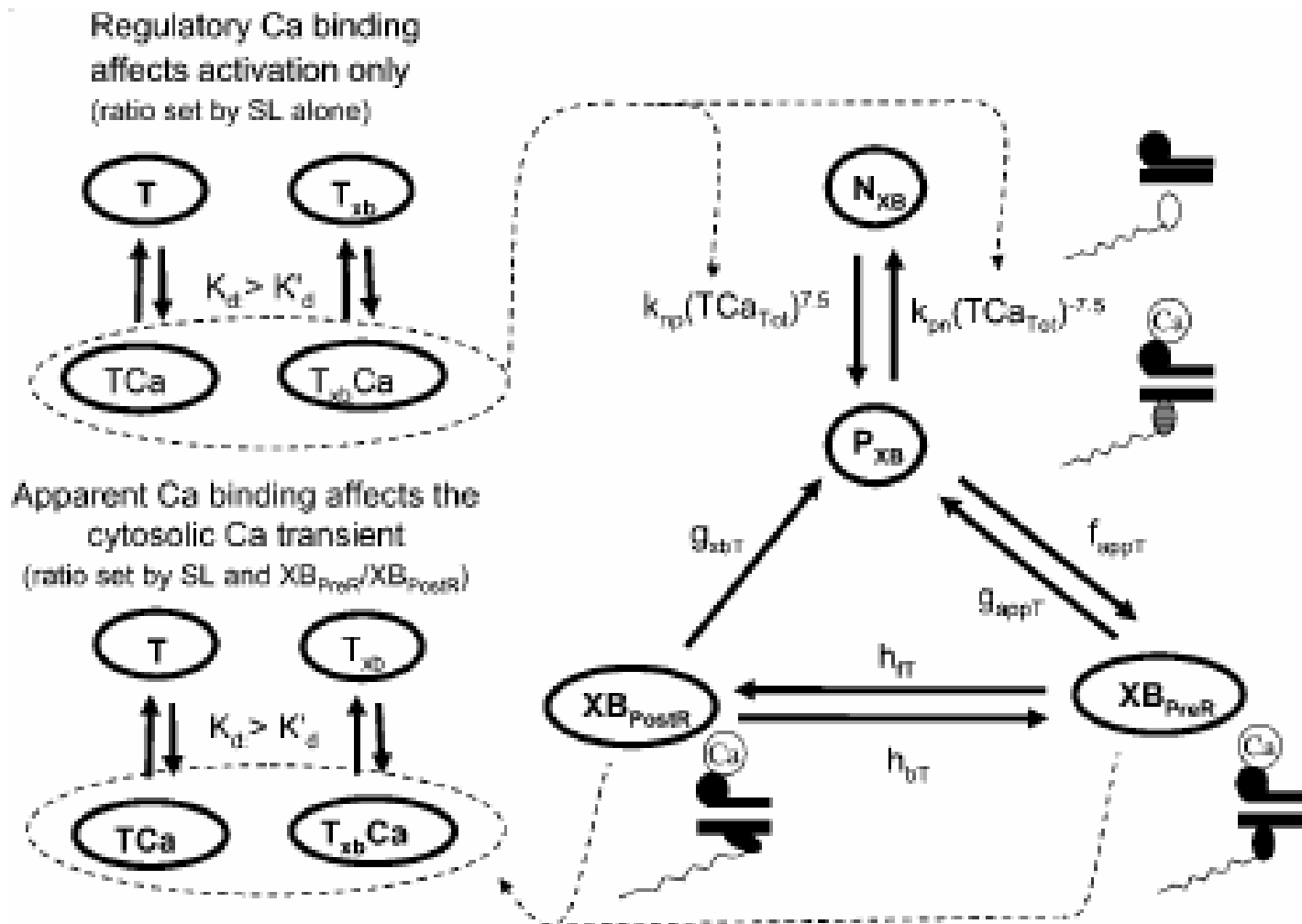
# Cardiac Mechanic

## Cross Bridge

- Force is developed by a process known as cross-bridge cycling
- The rotation of myosin head generates force.
- The myofilaments slide and overlap.



## Rice model



# Coupling Method

## Coupled System

$$\frac{1}{\sqrt{C}} \frac{\partial}{\partial X^M} \left( \sqrt{C} D_{iN}^M C^{NL} \frac{\partial V_m}{\partial X^L} \right) = - \frac{1}{\sqrt{C}} \frac{\partial}{\partial X^M} \left( \sqrt{C} D_{iN}^M C^{NL} \frac{\partial V_e}{\partial X^L} \right) + \beta I_m(V_m, s)$$
$$\frac{1}{\sqrt{C}} \frac{\partial}{\partial X^M} \left( \sqrt{C} (D_{iN}^M + D_{eN}^M) C^{NL} \frac{\partial V_e}{\partial X^L} \right) = - \frac{1}{\sqrt{C}} \frac{\partial}{\partial X^M} \left( \sqrt{C} D_{iN}^M C^{NL} \frac{\partial V_m}{\partial X^L} \right)$$

$$\frac{ds}{dt} = f(V_m, s)$$

$$\operatorname{div} \sigma + f = 0$$

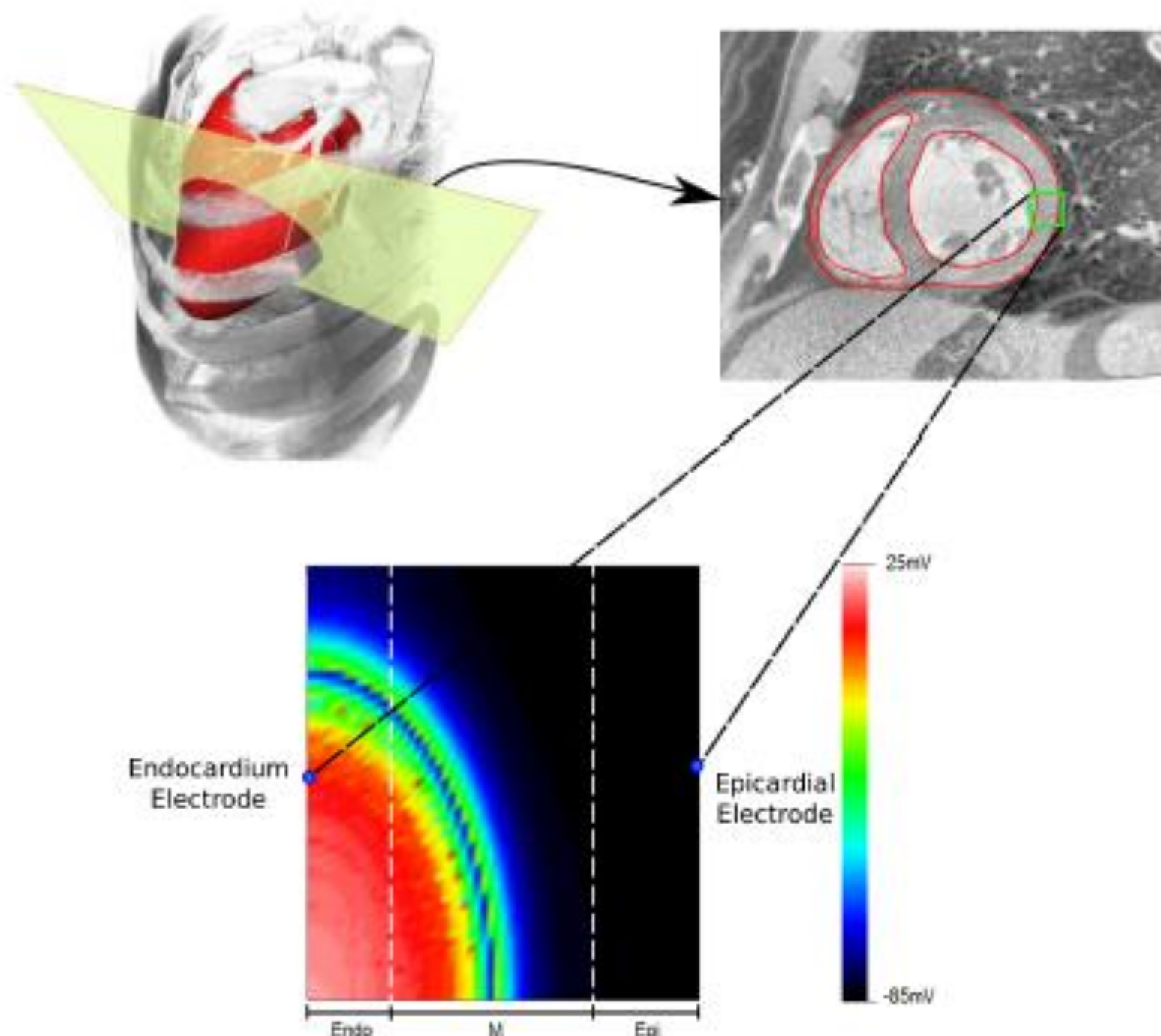
$$\sigma = \sigma_p + \sigma_a$$

$$\sigma_a = R^T \sigma_{al}(s) R$$

$$\sigma_p = J^{-1} F S F^T$$

$$S = \frac{\partial W}{\partial C}$$

$$W(I_1) = c_1(I_1 - 3)$$



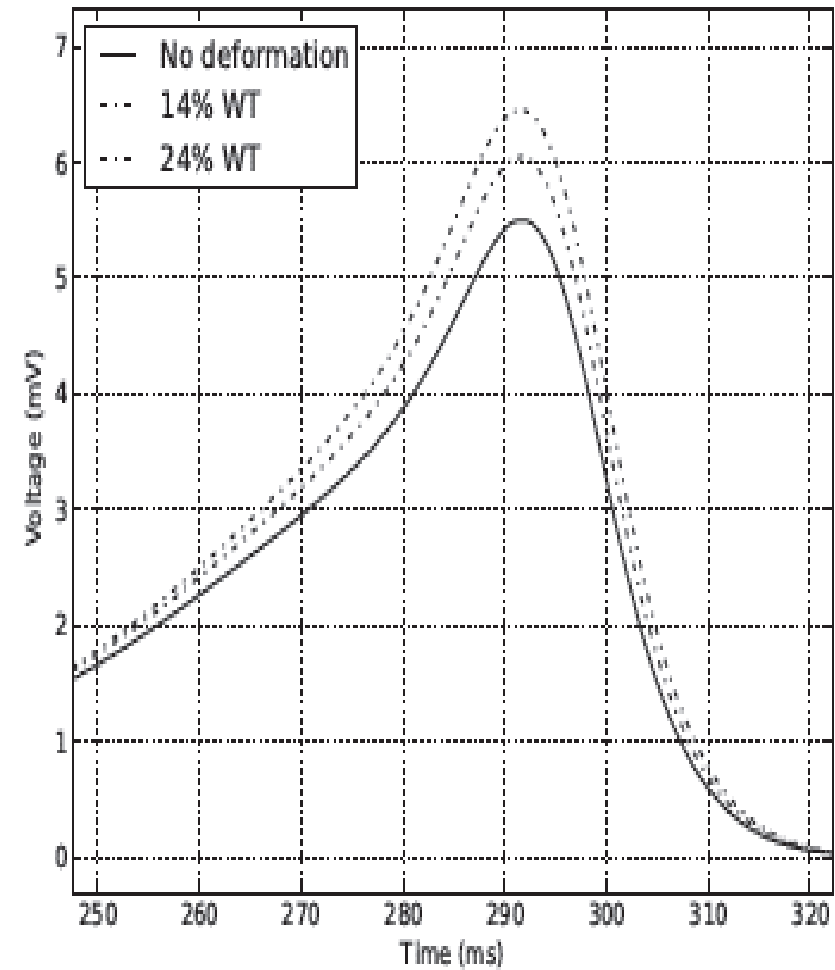
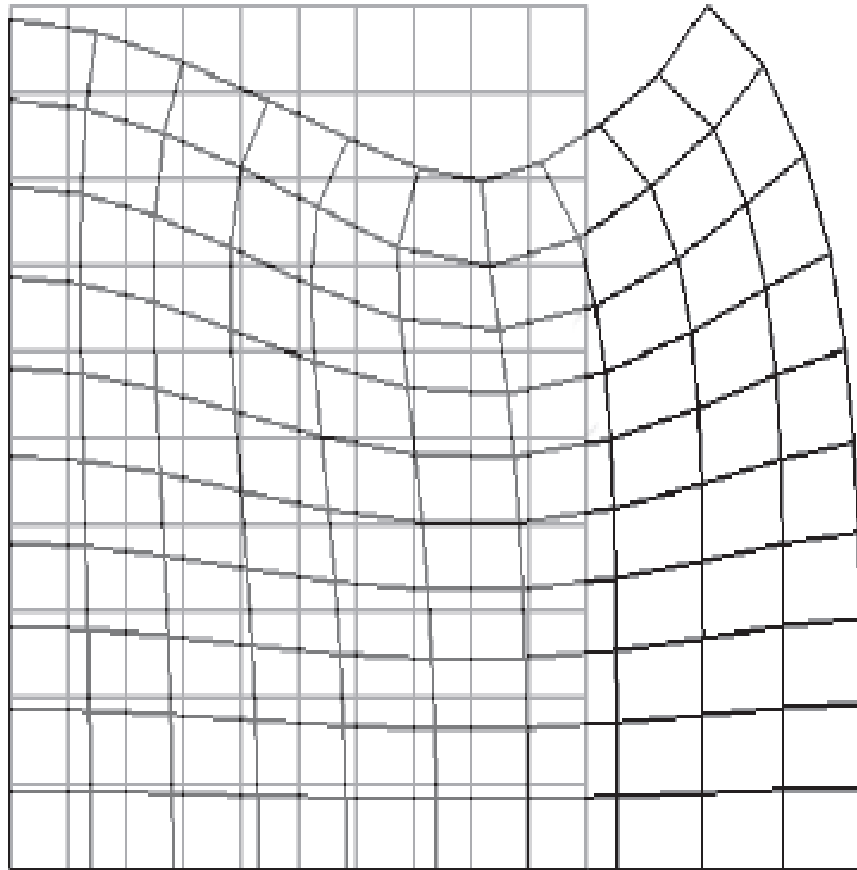
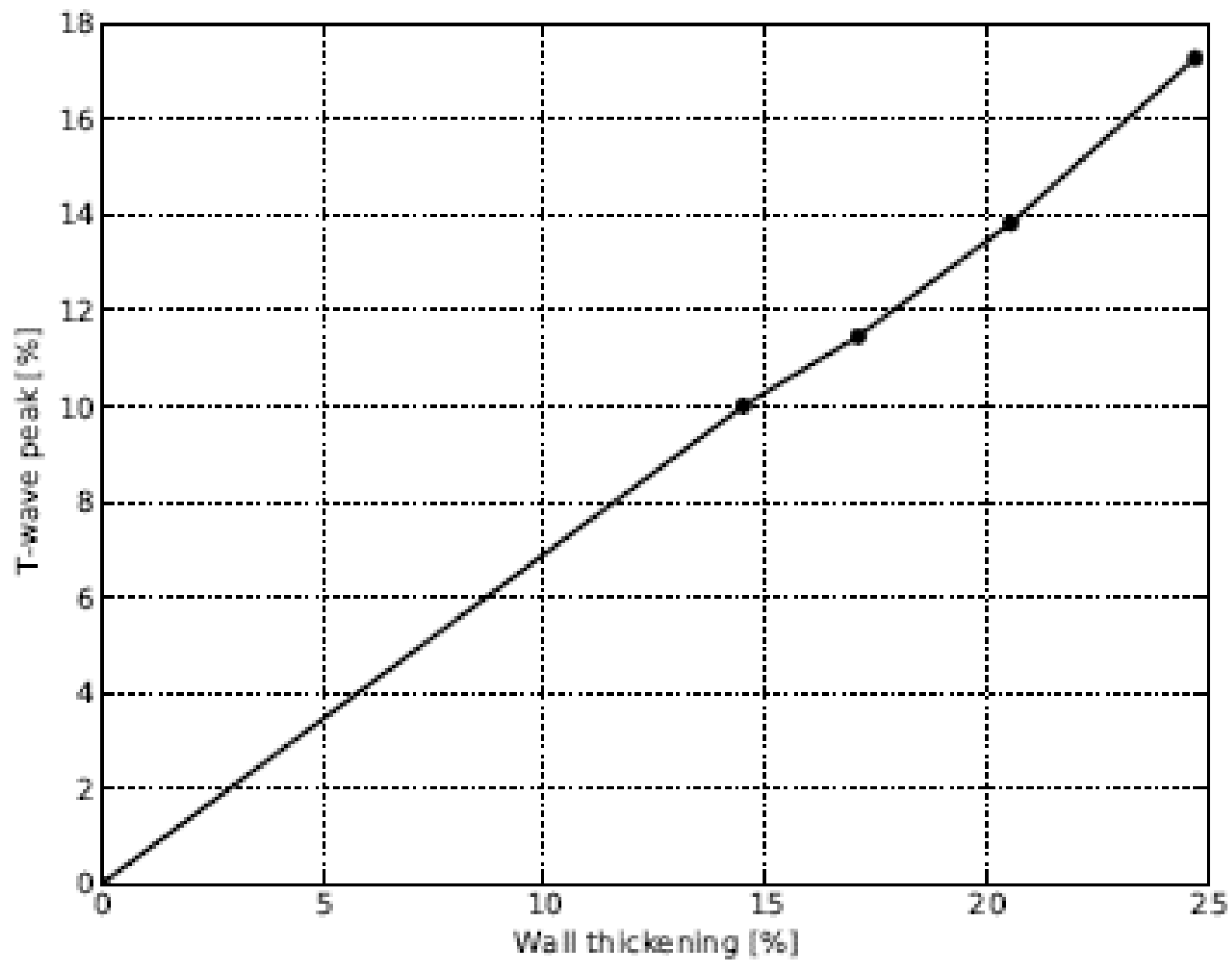


Fig. 3. Initial and deformed geometry of the human left ventricle wedge. This deformation was obtained at 110 ms of simulation, where we obtained the maximum WT.





# Repolarization summary

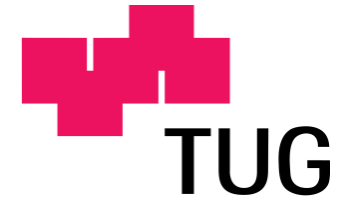
- T-wave format is influenced by different functional and anatomical heterogeneities of cardiac tissue as well as by the mechanical contraction of the heart.
- The computational models offer important insights that contribute to the better understanding of cardiac physiology and to the better interpretation of electrophysiological signals such as ECG, both for the case of normal and pathological conditions

Wave Speed, slow conduction,  
fractionation, Saltatory effects



Medical University of Graz

FWF



# Electro-anatomical Characterization of Microfibrosis in a Histologically Detailed Computer Model

Fernando Campos

*Supervisor:*

Univ.-Prof. Dipl.-Ing. Dr. techn. Paul Wach

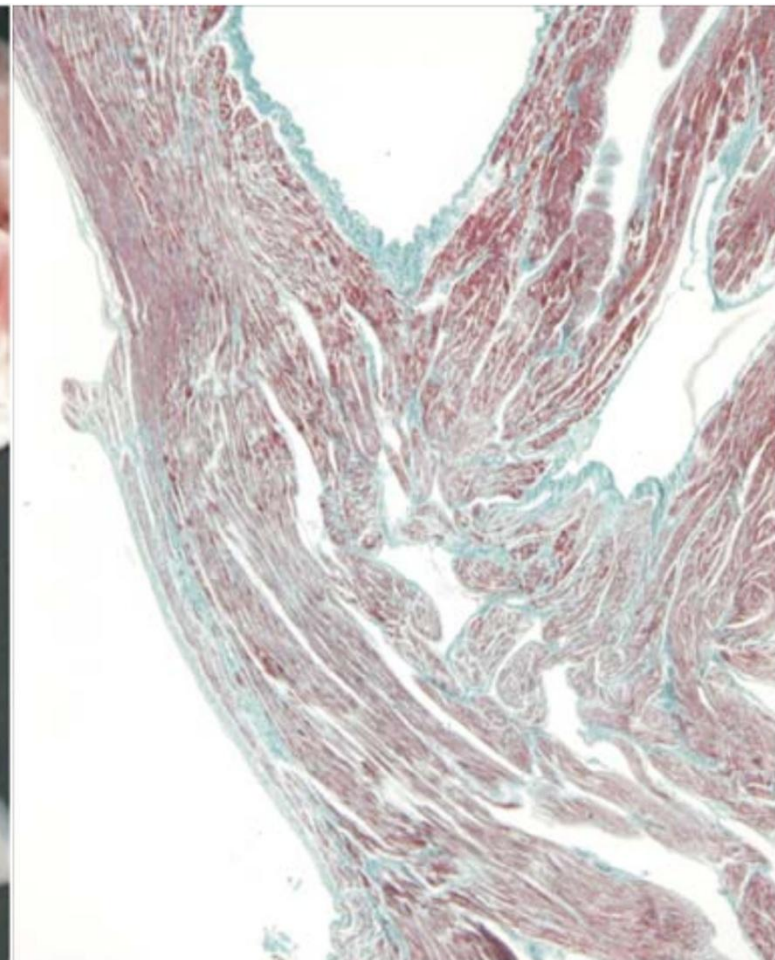
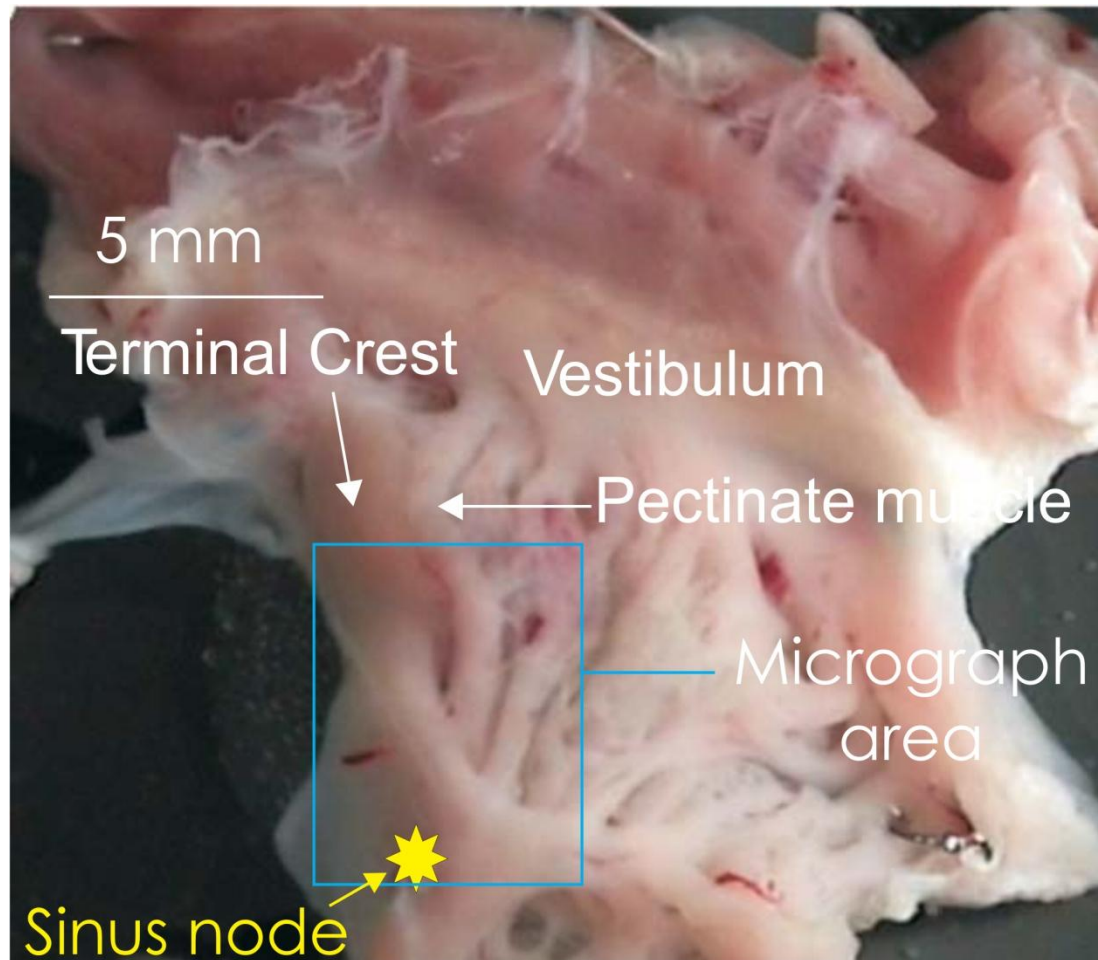
*Co-supervisors:*

ao. Univ.-Prof. Dipl.-Ing. Dr. techn. Ernst Hofer

assoz. Prof. Priv.-Doz. Dipl.-Ing. Dr. techn. Gernot Plank

# The Lower Right Atrial Isthmus

## Macro- and Microstructure



Aging → Fibrosis → Atrial fibrillation (AF)

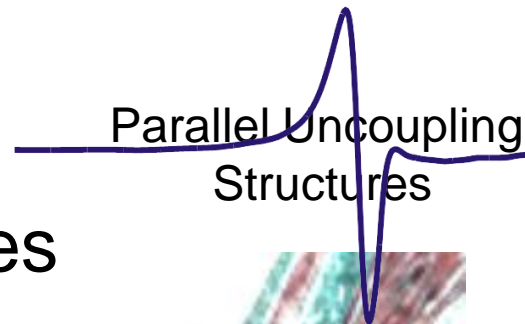
Fibrosis may change conduction

- Uniform Atrial electrograms (UAE) → complex fractionated atrial electrograms (CFAE)

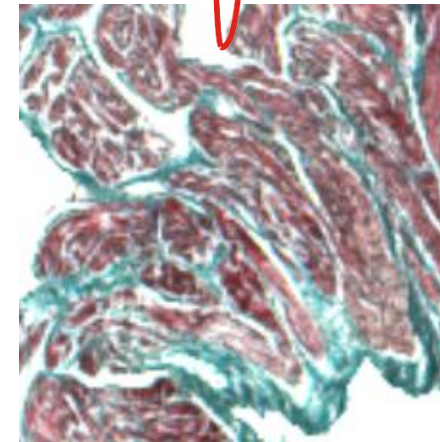
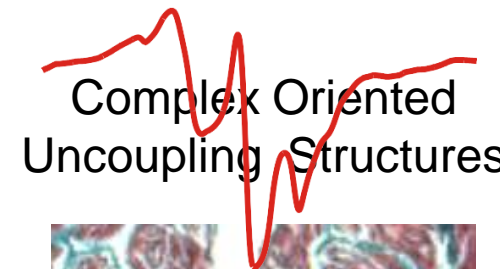
## CFAE

- Uncoupling structures
- Geometry of the structure
- Direction of the wavefront

UAE



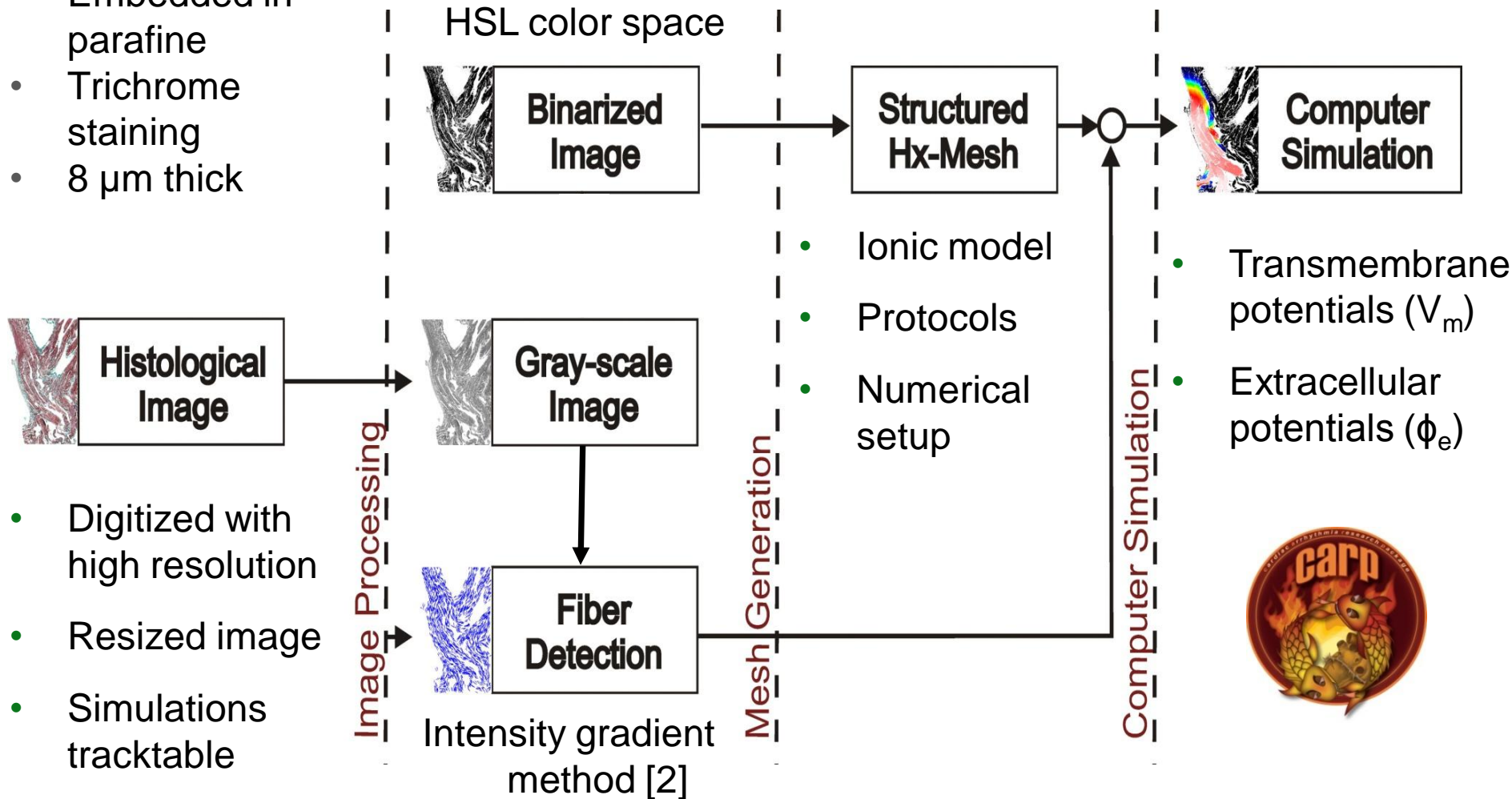
CFAE





# From Histograms to Computer Simulations

- Embedded in parafine
- Trichrome staining
- 8  $\mu\text{m}$  thick



## Monodomain Equations

$$\nabla \cdot (\bar{\sigma} \nabla V_m) = \beta I_m,$$

$$I_m = C_m \frac{\partial V_m}{\partial t} + I_{ion}(V_m, s_i) - I_{stim},$$

$$\frac{ds_i}{dt} = f(V_m, s_i)$$



STIM  
(1:12)

+50 mV



-80 mV



# Summary

- Investigate the relation between discontinuities in microstructure and CFAEs
- Support the development of a catheter tip for Multisite pacing to measure the degree of fibrosis

# Limitations of the homogenized cardiac Monodomain model for the case of low gap junctional coupling

Caroline Mendonça Costa and Rodrigo Weber dos Santos

# Our goal

- ✓ Revisit the classical homogenized monodomain formulation
  - ✓ Evaluate its ability to reproduce the situation of low gap junctional coupling
    - ✓ Implementation and comparison of the results of two models based on the monodomain formulation

# Motivation

- ✓ Pathological conditions
- ✓ Decrease of gap junctional coupling
  - ✓ Dilated cardiomyopathy
  - ✓ Ischemic cardiomyopathy
  - ✓ Myocarditis
  - ✓ **Myocardial infarcts (< 5%)**
- ✓ Gap junctional remodeling
  - ✓ Affected cells are “isolated”

# Microscopic Monodomain model

$$\nabla \cdot (\sigma(x) \nabla V_m) = \beta I_m(x)$$

with

$$I_m(x, V_m, \eta_i) = C_m \frac{\partial V_m}{\partial t} + I_{ion}(x, V_m, \eta_i) - I_{stim}$$

where

$$\frac{d\eta_i}{dt} = f(t, \eta_i)$$

$$I_{ion} = I_{Na}(x) + I_{si} + I_K + I_{K1} + I_{Kp} + I_b$$

$$\sigma(x) = \begin{cases} \sigma_c; & i < x \leq il - l_g \\ \sigma_g; & il - l_g < x, \leq il \end{cases}$$



# Homogenization

- ✓ Simplified model
- ✓ Large and complex simulations
  - ✓ No space variation
  - ✓ Effective values
- ✓ Macroscopic model that still captures the microscopic scale influence

# Homogenization process

$$\bar{\sigma} = \frac{L}{\int_0^L \frac{1}{\sigma(x)} dx}$$

Intracellular  
conductivity

# Macroscopic Monodomain model

$$\nabla \cdot (\bar{\sigma} \nabla V_m) = \beta I_m$$

with

$$I_m(V_m, \eta_i) = C_m \frac{\partial V_m}{\partial t} + I_{ion}(V_m, \eta_i) - I_{stim}$$

where

$$\frac{d\eta_i}{dt} = f(t, \eta_i)$$

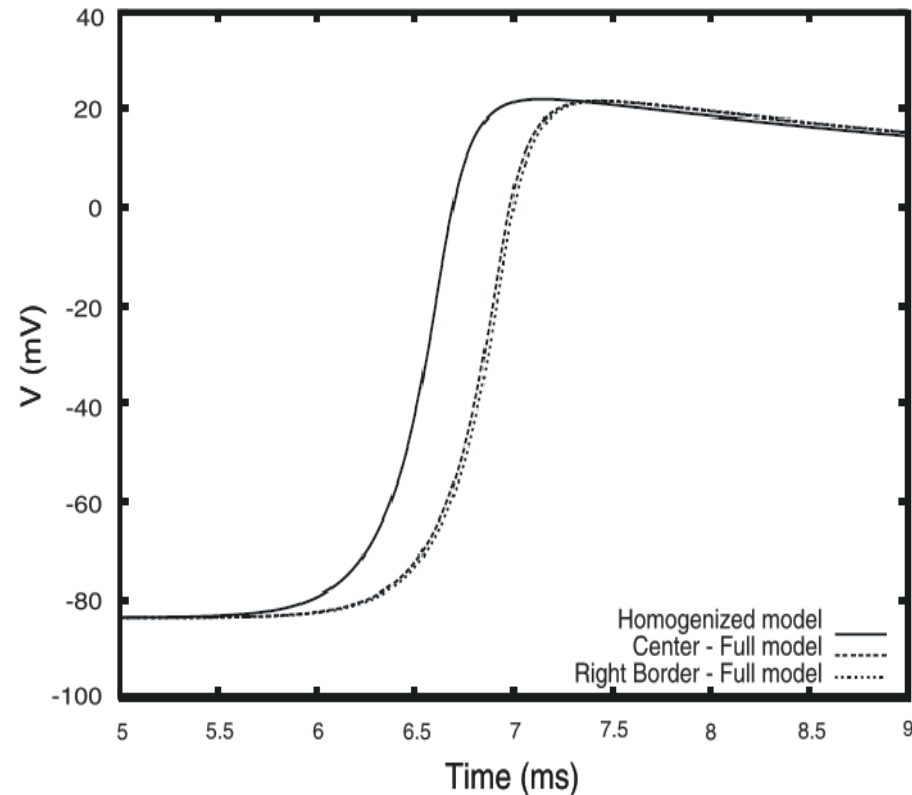
$$I_{ion} = I_{Na} + I_{si} + I_K + I_{K1} + I_{Kp} + I_b$$

# What we did

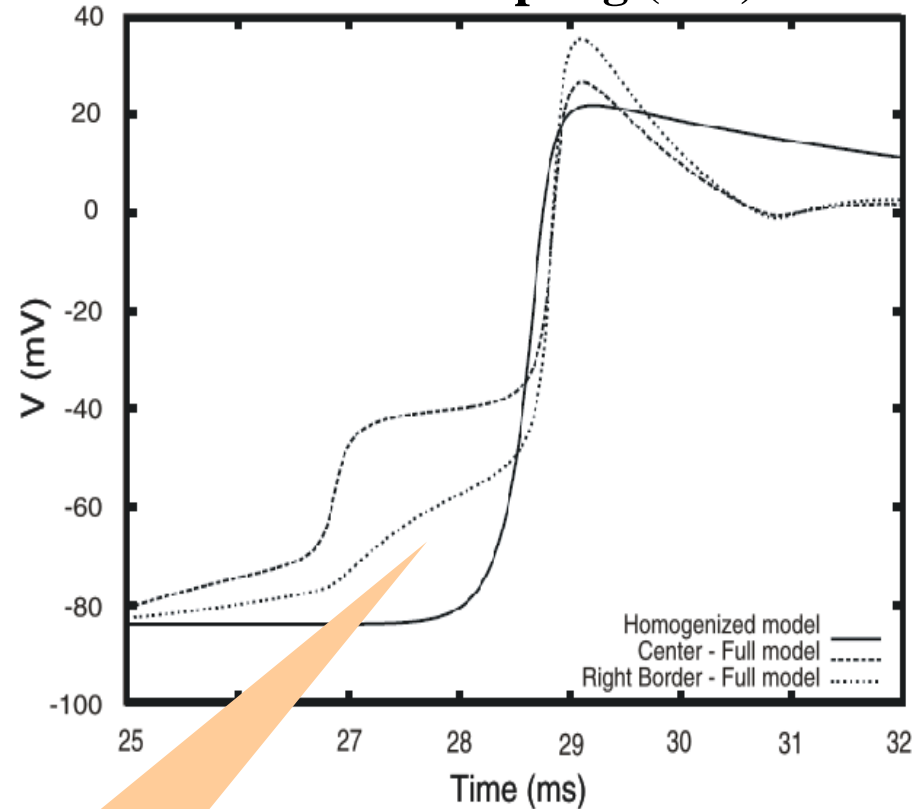
- ✓ We compared the simulation results of the two models for the case of low gap junctional coupling
  - ✓ This situations arises in many pathological conditions
  - ✓ Accurate models of these conditions are of extreme importance

# Action Potential

**Normal coupling (100%)**

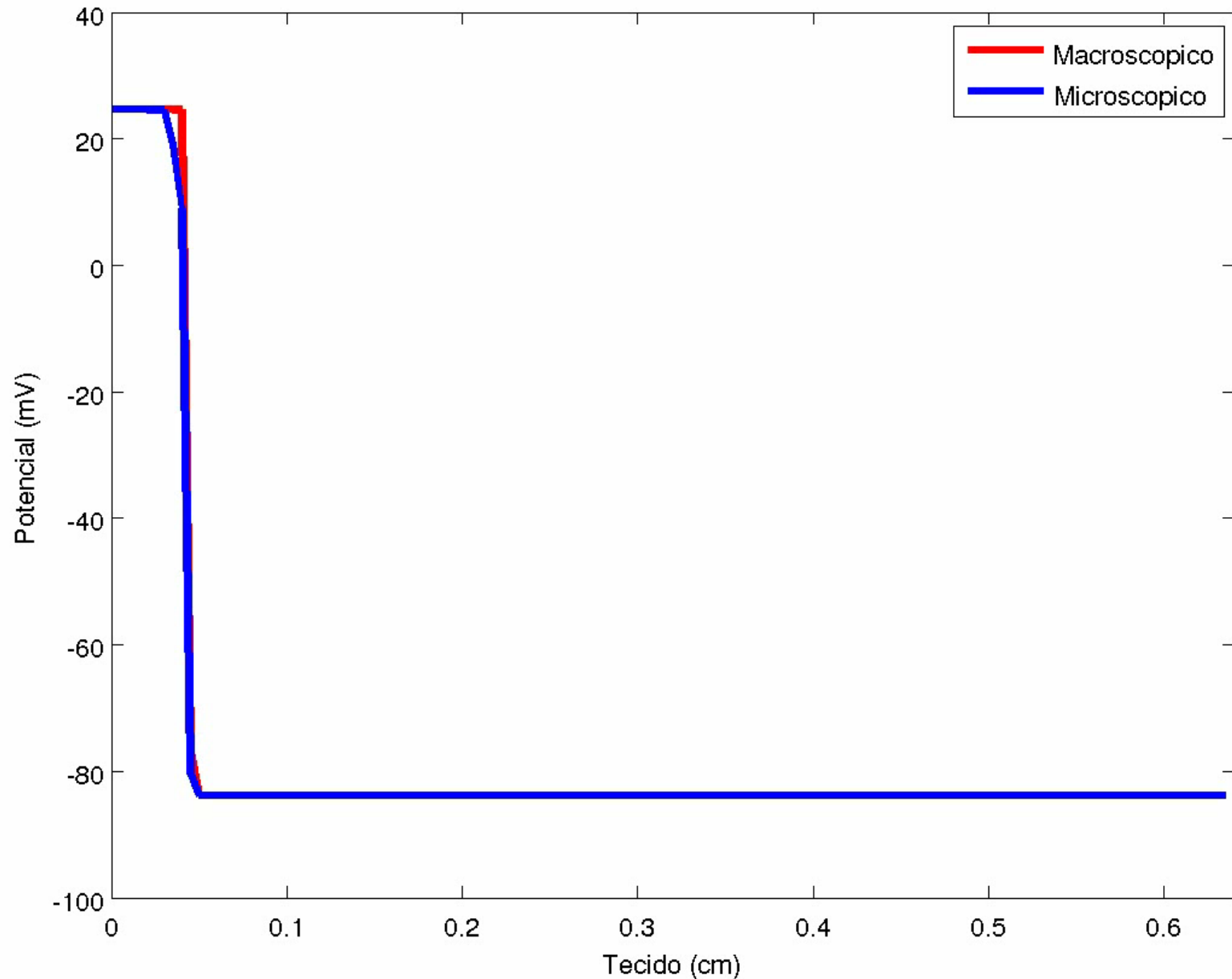


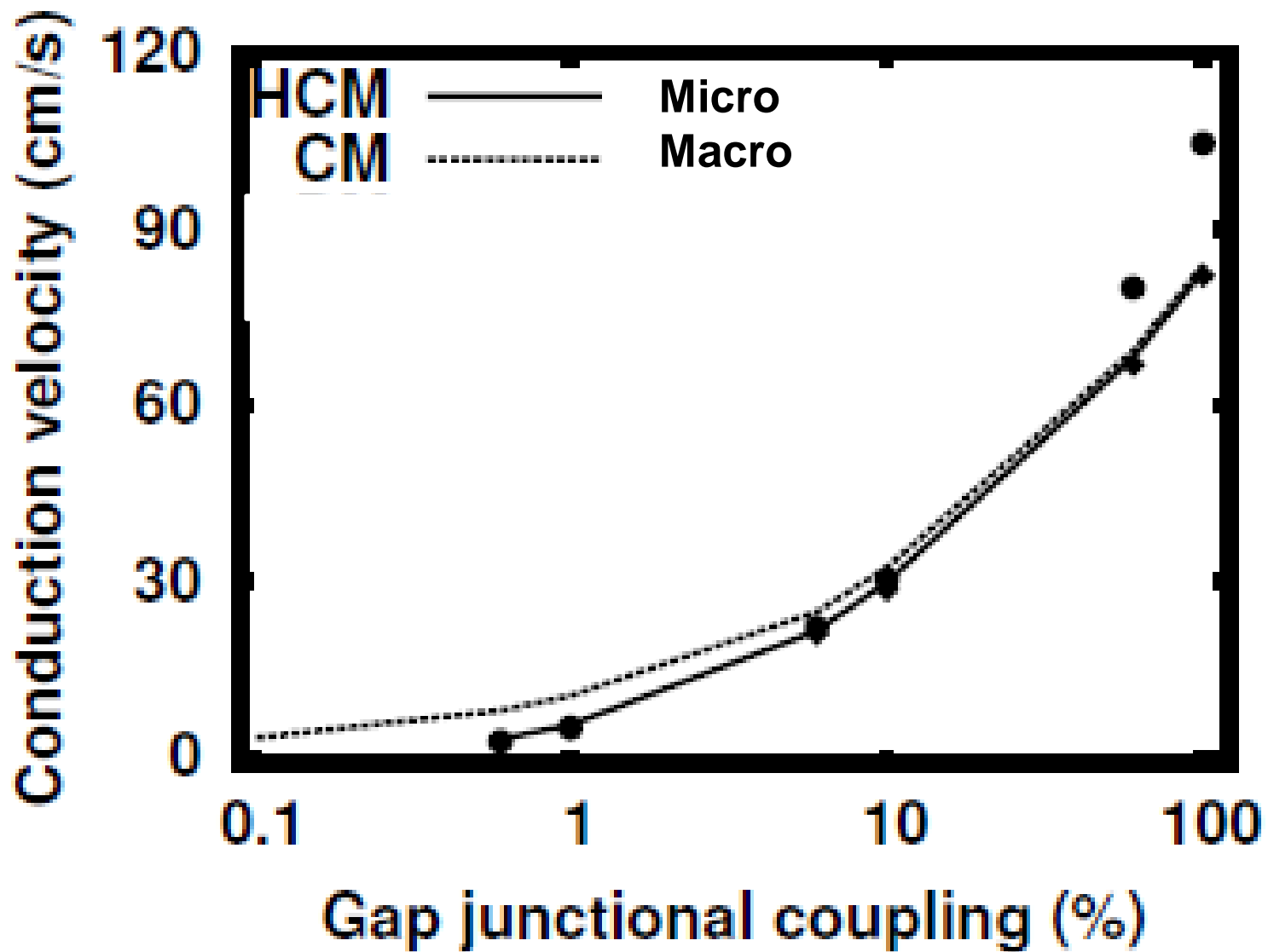
**Reduced coupling (1%)**



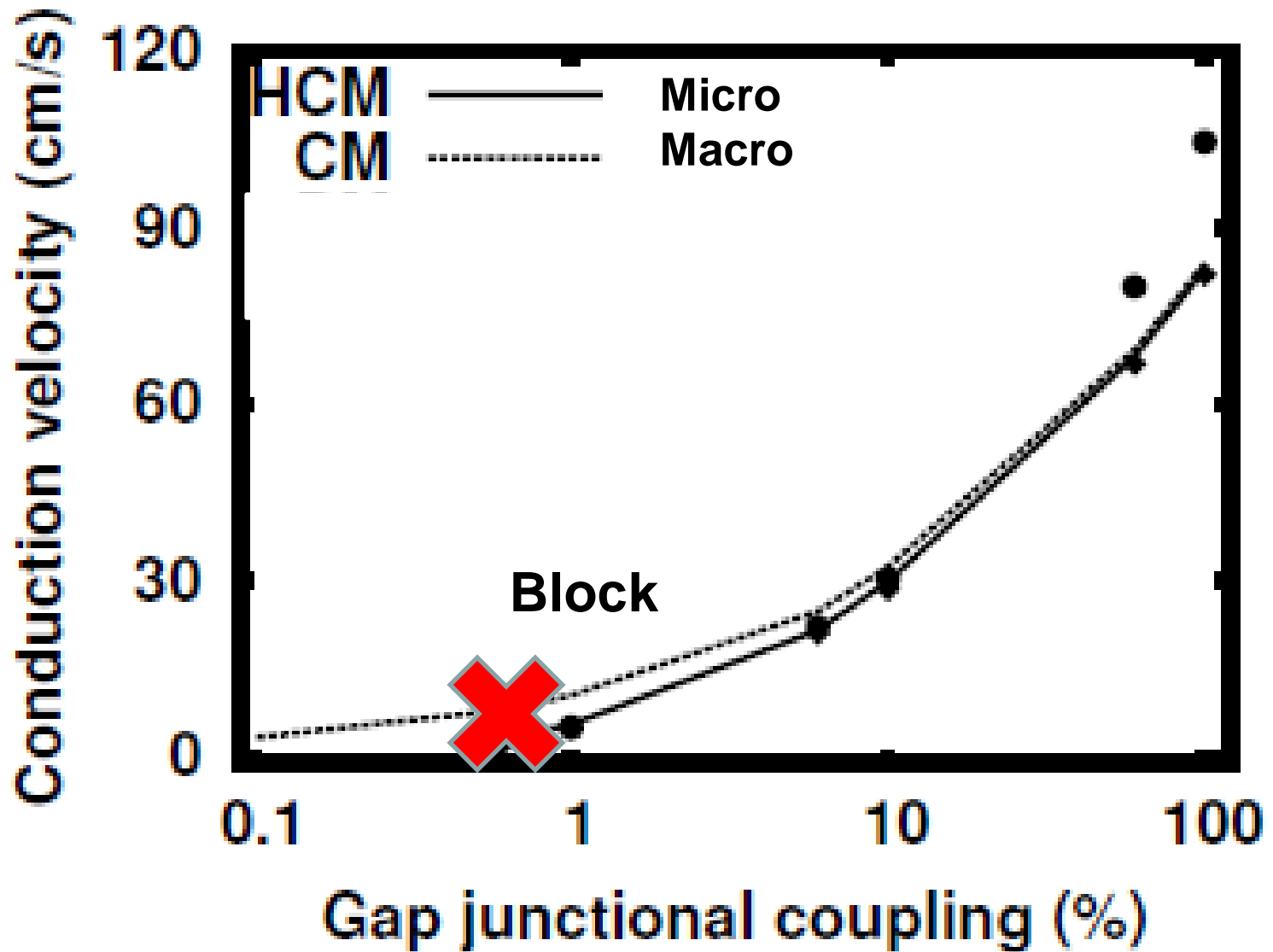
**Different shapes**

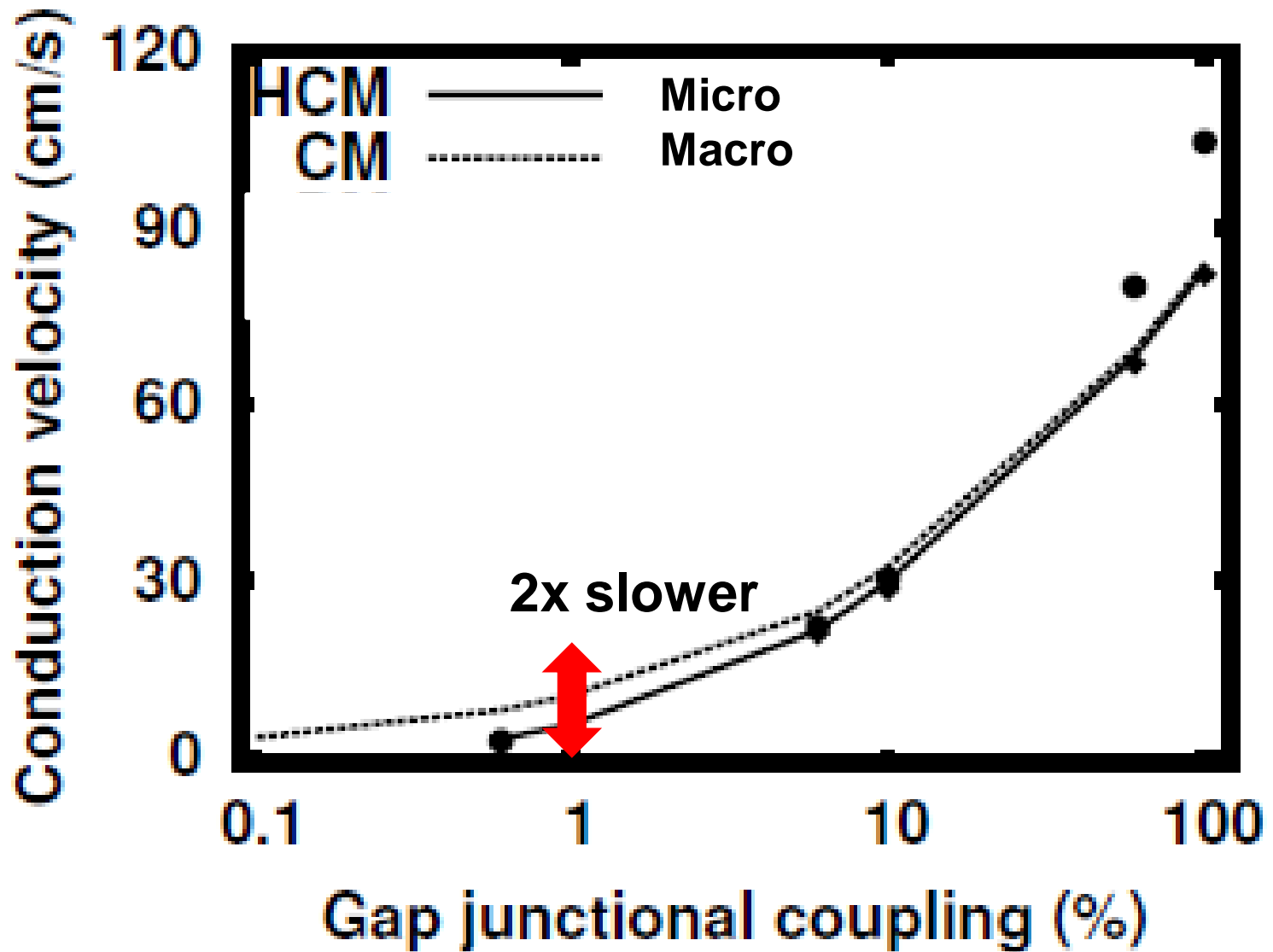
# Saltatory Conduction in 1D



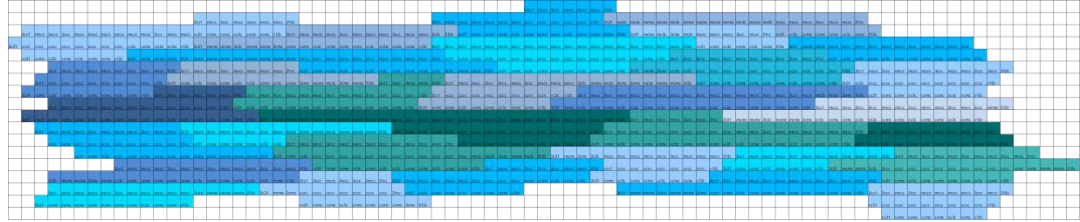






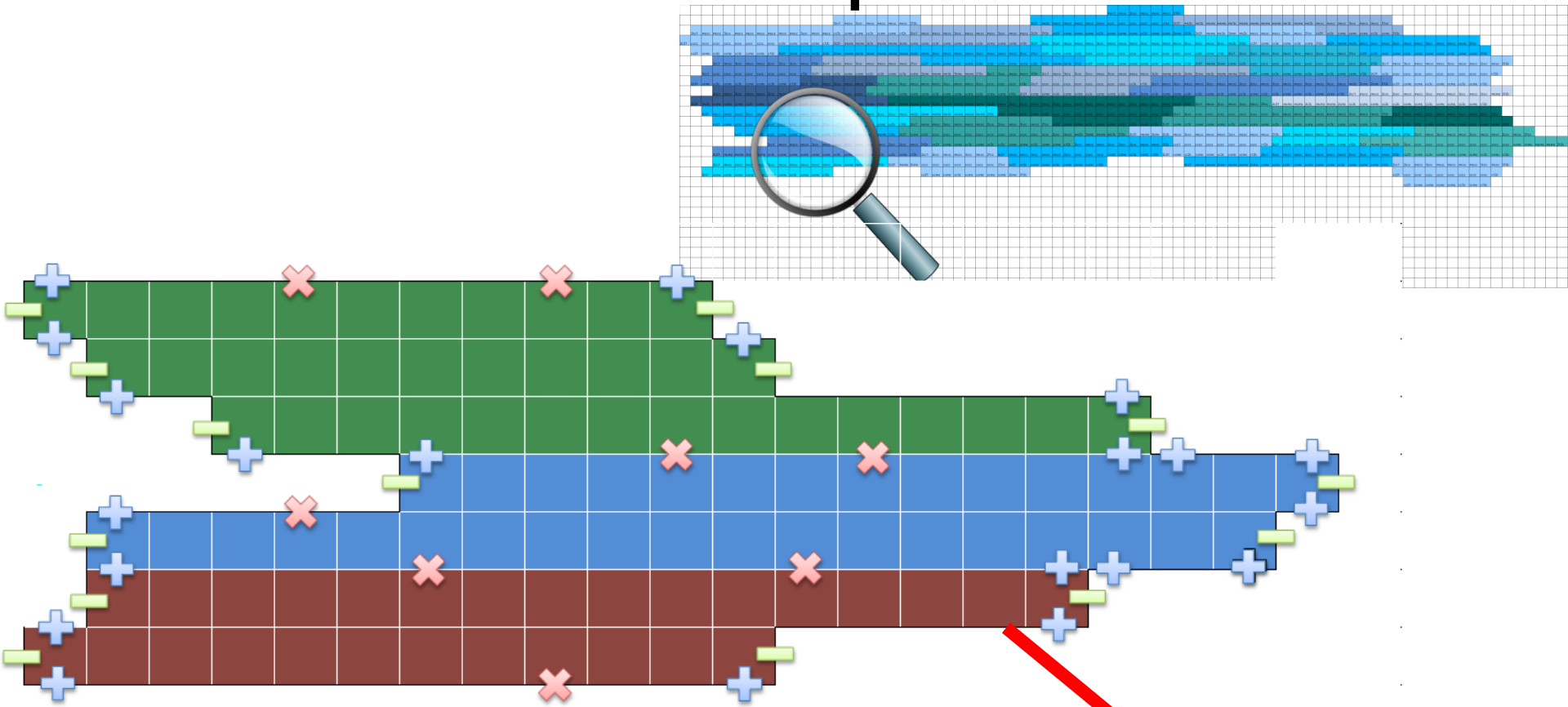


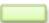


# 2D Microscopic Model



**Madison S. Spach, J. Francis Heidlage The  
Stochastic Nature of Cardiac Propagation at a  
Microscopic Level  
Electrical Description of Myocardial Architecture and  
Its Application to Conduction , Circulation Research  
76:366-380 (1995)**

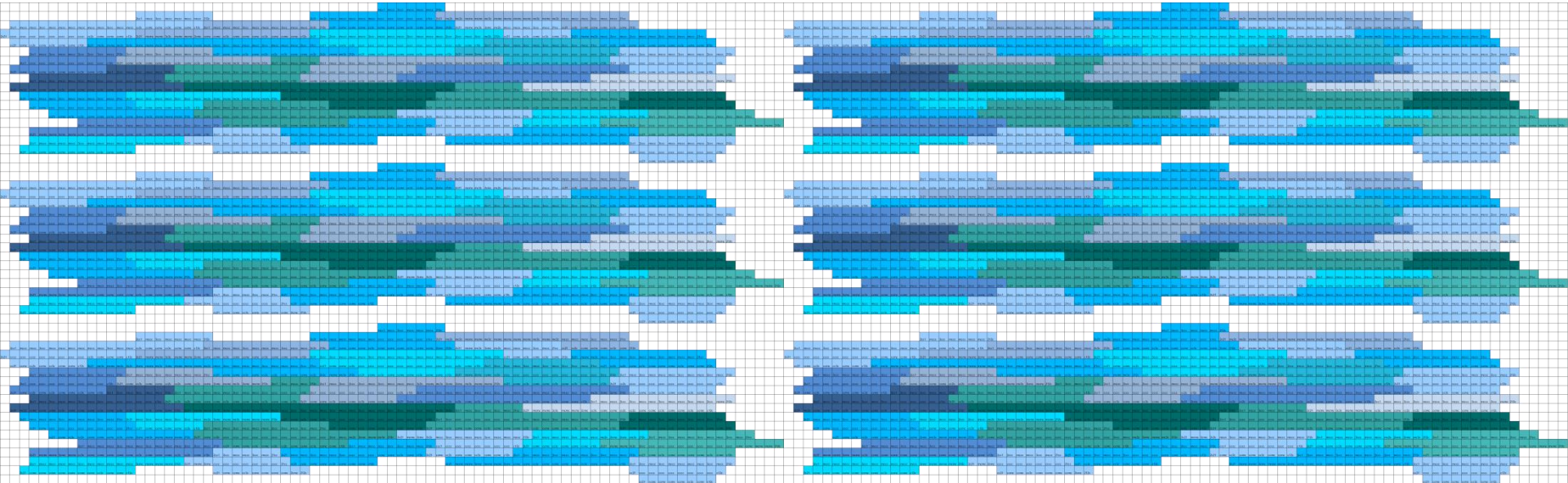
# 2D Microscopic Model



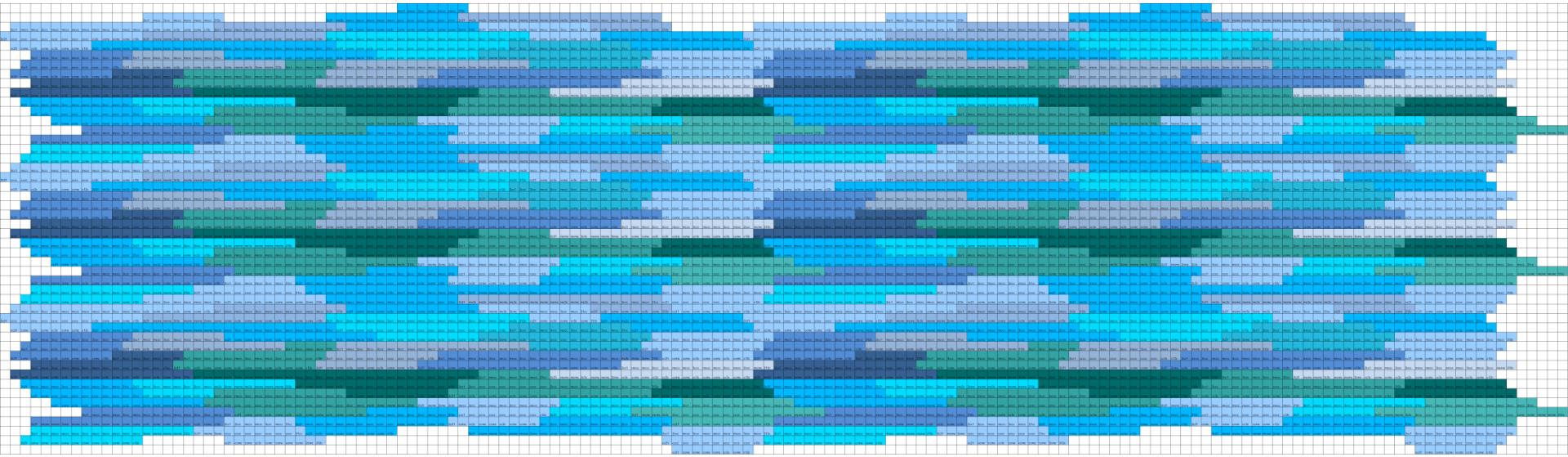
Legenda	
	PLICATE GAP JUNCTION
	INTERPLATE GAP JUNCTION
	COMBINED PLICATE GAP JUNCTION

8x8um

# 2D Microscopic Model

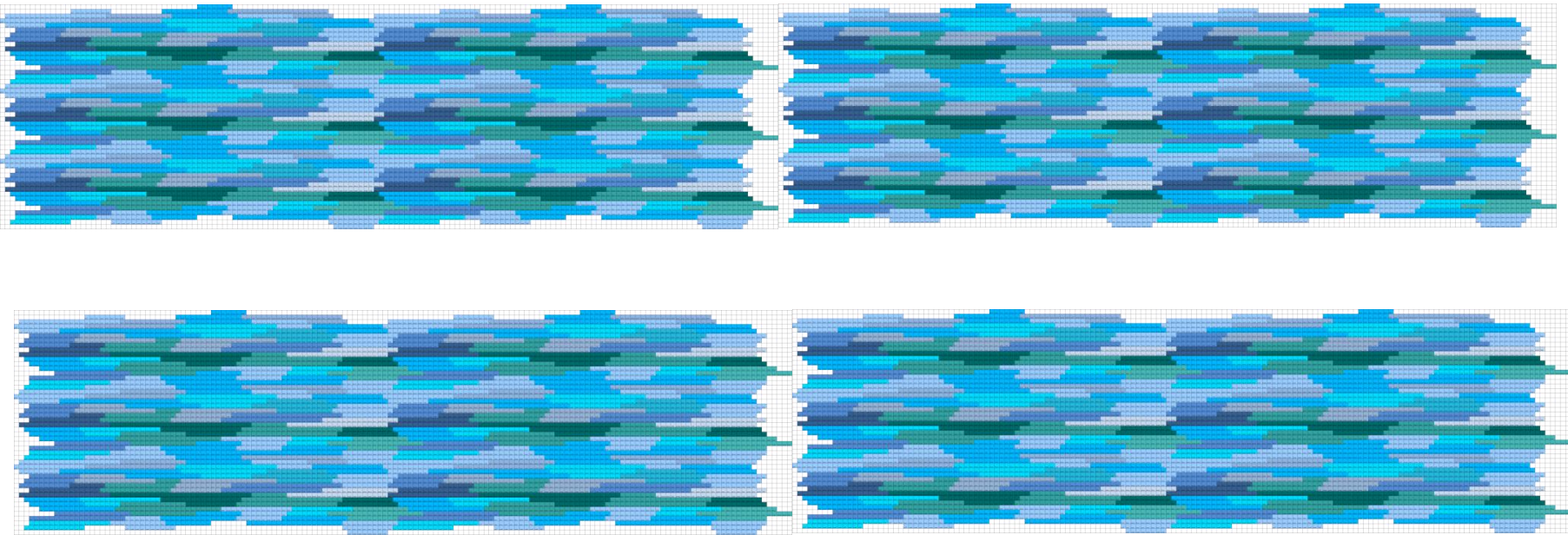


# 2D Microscopic Model





# 2D Microscopic Model

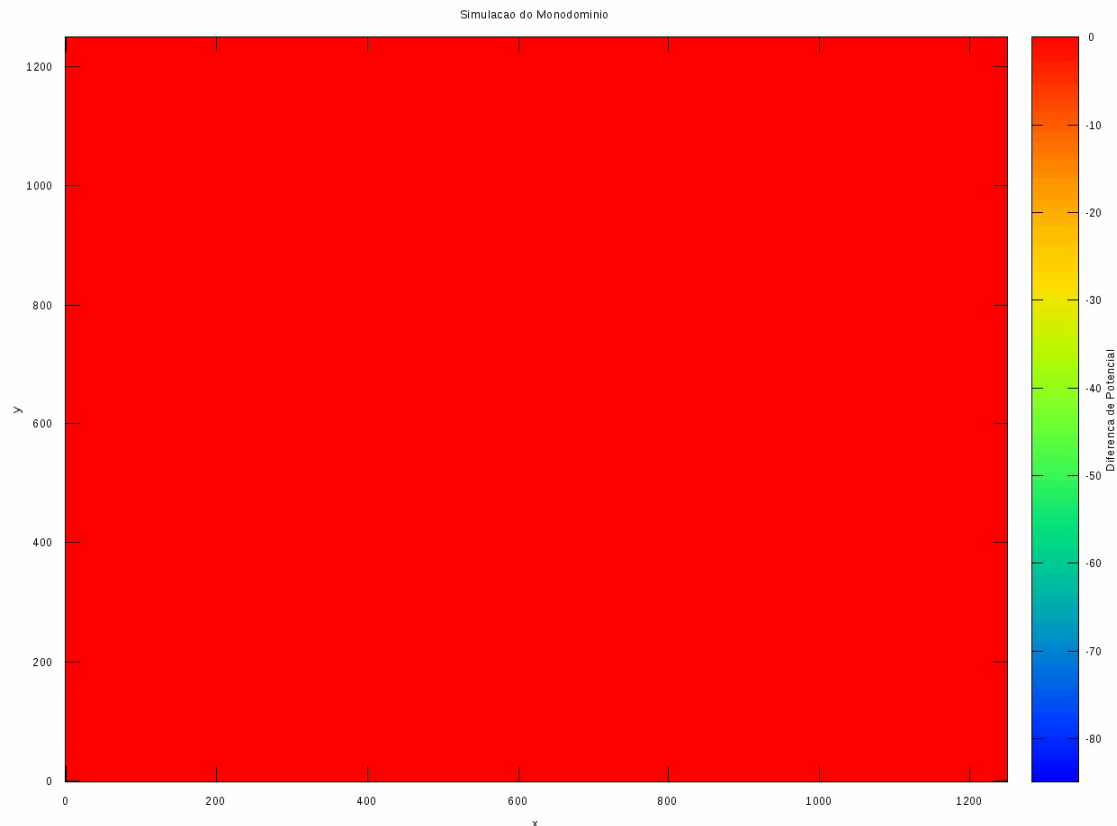




# 2D Microscopic Model

1x1cm tissue with 8x8um discretization

No. Unknowns =  $1250 \times 1250 \times 41 = 64\text{Millions}$

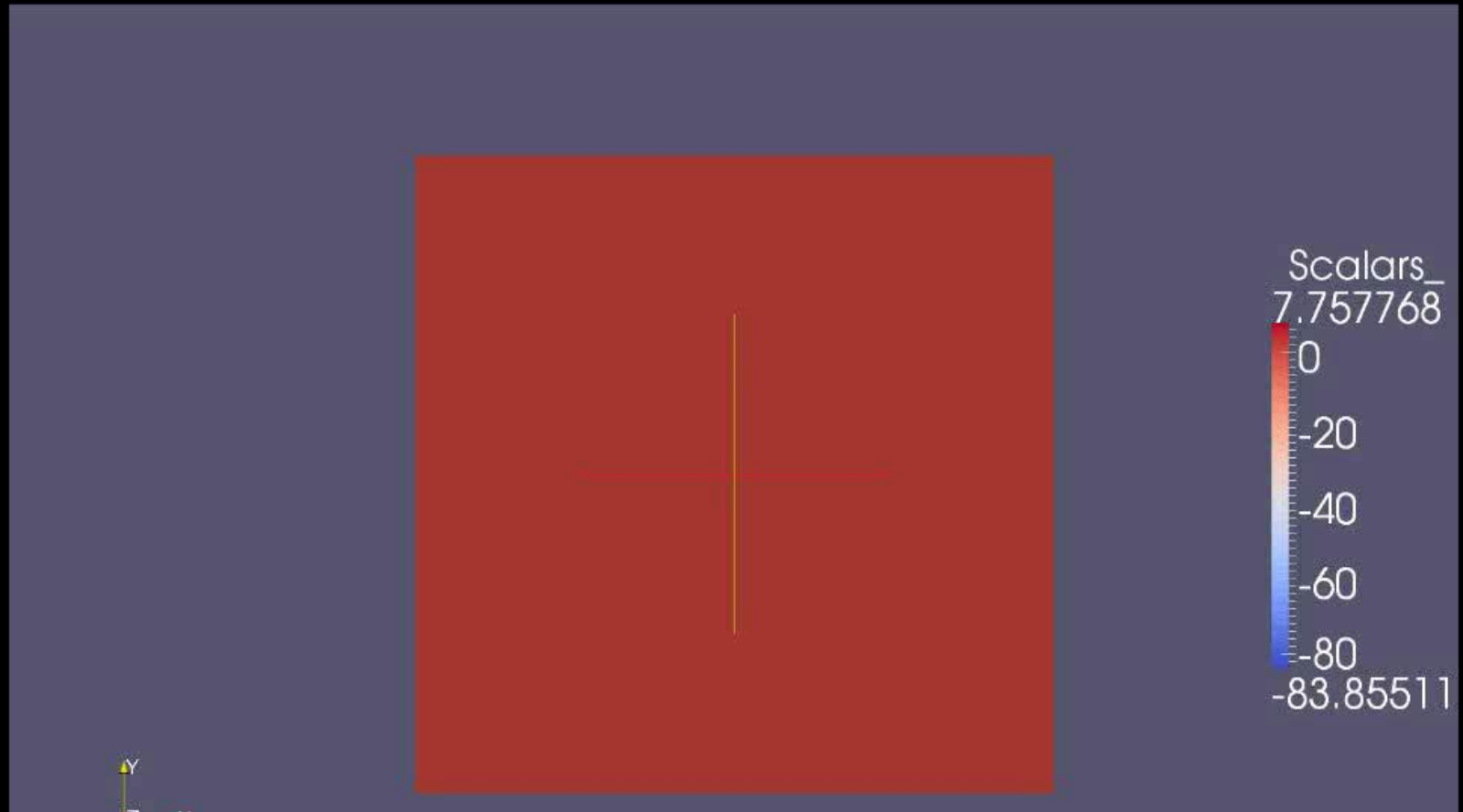


# 2D Microscopic Model

1x1cm tissue with 8x8um discretization

No. Unknowns =  $1250 \times 1250 \times 41 = 64\text{Millions}$

Zoom in: 2mmx2mm



# Efficient Solvers Based on Manycore computers and adaptive techniques for Cardiac Modeling

## PART IV

# Complex Models

- Modeling Challenges: Multi-scale and Multiphysics
- Computational Challenges: Simulations are computationally expensive (one heart beat = a couple of days in a parallel machine)
- Computer Challenges: Involves the coupling of several components (submodels) and data (geometry, biophysical parameters)

## Efficient Solvers Based **on Manycore computers** and adaptive techniques for Cardiac Modeling

**GPU and MultiGPU for Monodomain equation:**

$$\beta C_m \frac{\partial V_m}{\partial t} + \beta I_{ion}(V_m, \eta) - \nabla \cdot (\sigma_m \nabla V_m) + I_{stim}$$
$$\frac{\partial \eta}{\partial t} = \mathbf{f}(V_m, \eta)$$

# Methods

- Cell Model: LR1
- Tissue: 0.5cmx0.5cm
- Non-linear system of PDE: Operator Splitting
- ODE System: Solved with explicit Euler
- PDE: Discretized with Finite Elements, Implicit Euler for time
- Discretization:  $dx = 50\mu\text{m}$ ,  $t = 0.01 \text{ ms}$
- Linear System: CG
- Parallelization: OPEMP, CUDA, OPENCL, OPENGL

## Numerical experiments - Environment

---

- Intel Core i7 860 2.80GHz, 8GB of memory
- GPUs:
  1. NVIDIA GeForce GTX 470, 448 CUDA cores, 1 GB GDDR5 memory and 133.9 GB/s of memory bandwidth
  2. AMD Radeon 6850, 960 Stream processors, 1 GB GDDR5 memory and 128 GB/s of memory bandwidth



Figure: NV-GTX470



Figure: AMD-R6850



## Results - Comments on ODE problem

---

- **Embarrassingly parallel** problem. High ratio of Comp/Mem
- Good performance of the GPU solvers.
- OpenGL was faster in all tests using NVIDIA GTX 470.
- Mathematical optimization flags really **improves** the performance of the ODE solver (GTX 470).
- We observed a good performance of the OpenCL implementation.

Speedup	
NV-GTX470 - OpenGL	449
NV-GTX470 - CUDA	286
NV-GTX470 - OpenCL	277
AMD-R6850 - OpenCL	109

Compared to OPENMP  
with 4 cores

## Results - Comments on PDE problem

---

- Non-embarrassingly parallel
- Building blocks: SpMV, DotProduct, Conjugate Gradient.
- Poor performance when using the "traditional" CSR format.
- Significant improvements using formats that exploits the structure of the matrix, i.e., DIA format (or even ELLPACK)
- CUDA outperforms the other implementations using NV-GTX470

Speedup	
NV-GTX470 - CUDA - DIA	8.6
NV-GTX470 - CUDA - CSR	1.5
NV-GTX470 - OpenCL - DIA	4.8
NV-GTX470 - OpenCL - CSR	1.3
NV-GTX470 - OpenGL - DIA	4.1
AMD-R6850 - OpenCL	2.1

Compared to OPENMP  
with 4 cores

- OpenCL was slower than CUDA:
  - CSR ~14%
  - DIA ~76%

OPENMP was 2.5 faster  
than seq. code

GPGPU implementation using CUDA with **1 GPU** offered a total speedup of **35** (ODE + PDE) when compared to OPENMP running with **4 cores**

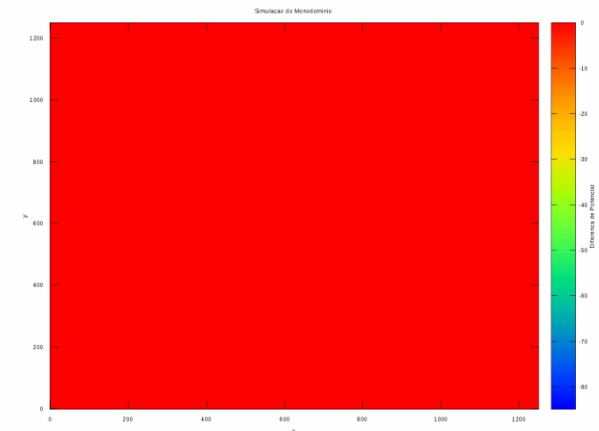
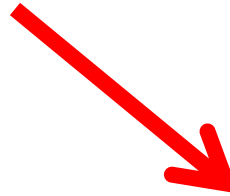
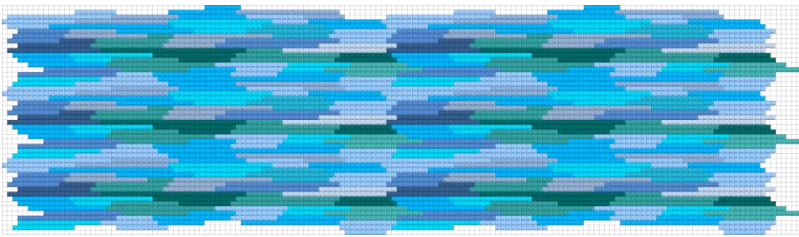
-- Rocha, B. M. ; Campos, F. O. ; AMORIM, R. M. ; PLANK, G. ; Santos, R. W. dos ; Liebmann, M. ; Haase, G. . Accelerating cardiac excitation spread simulations using graphics processing units. **Concurrency and Computation**, v. 23, p. 708-720, 2011.

# 2D Microscopic Model

1x1cm tissue with 8x8um discretization

(No. Unknowns =  $1250 \times 1250 \times 41 = 64\text{Millions}$ )

on MultiGPU platform



# Methods

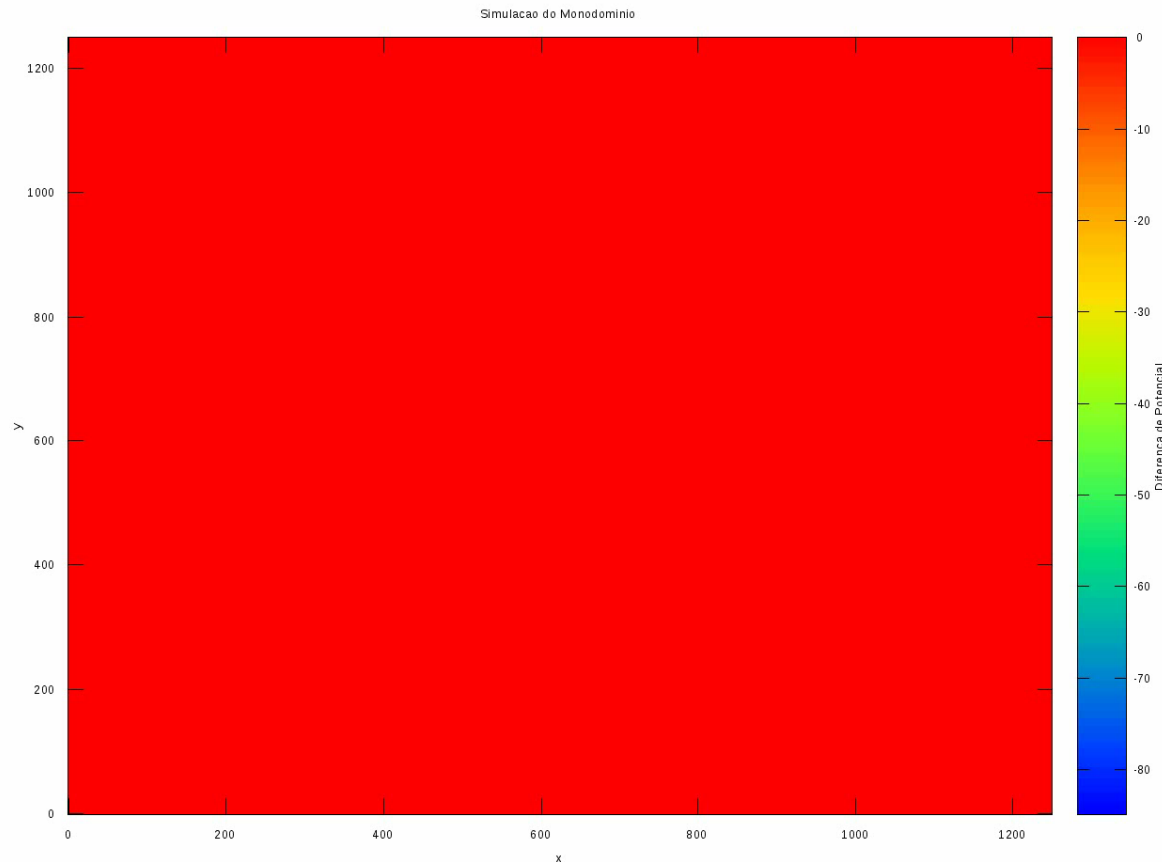
- Cell Model: Bondarenko et al.
- Simulation time: 10ms
- Non-linear system of PDE: Operator Splitting
- ODE System: Solved with explicit Euler
- PDE: Discretized with Finite Elements, Implicit Euler for time
- Linear System: CG
- **Parallelization:**
  - PETSc( MPI) for PDE + CUDA for ODEs**
- Small Cluster: 8 machines (2 quad-core Intel Xeon CPU E5420 2.50GHz 8 GB RAM + 1 Tesla C1060 GPU) = 64 cores + 8 GPUs

cores	Exec Time	Speedup
0.5cmx0.5cm -> # unknowns = $625 \times 625 \times 41 = 16$ millions		
1	<b>1.6day</b>	1
8	5.1h	7.5
16	2.6h	14
32	1.2h	31
64	<b>38min</b>	60
64 cores + 8 GPUs	<b>6.7min</b>	<b>343</b>
1cmx1cm -> # unknowns = $1250 \times 1250 \times 41 = 64$ millions		
1	<b>6.3days</b>	1
64	2.4h	61
64 cores + 8 GPUs	<b>21.7min</b>	<b>420</b>

# 2D Microscopic Model

1x1cm tissue with 8x8um discretization

No. Unknowns =  $1250 \times 1250 \times 41 = 64\text{Millions}$





## Efficient Solvers Based on Manycore computers and **adaptive techniques** for Cardiac Modeling

GPU and MultiGPU for Monodomain equation:

$$\beta C_m \frac{\partial V_m}{\partial t} + \beta I_{ion}(V_m, \eta) - \nabla \cdot (\sigma_m \nabla V_m) + I_{stim}$$
$$\frac{\partial \eta}{\partial t} = \mathbf{f}(V_m, \eta)$$

# AGOS – Automatic CellML To Numerical Solver (C, C++, CUDA, OpenMP))

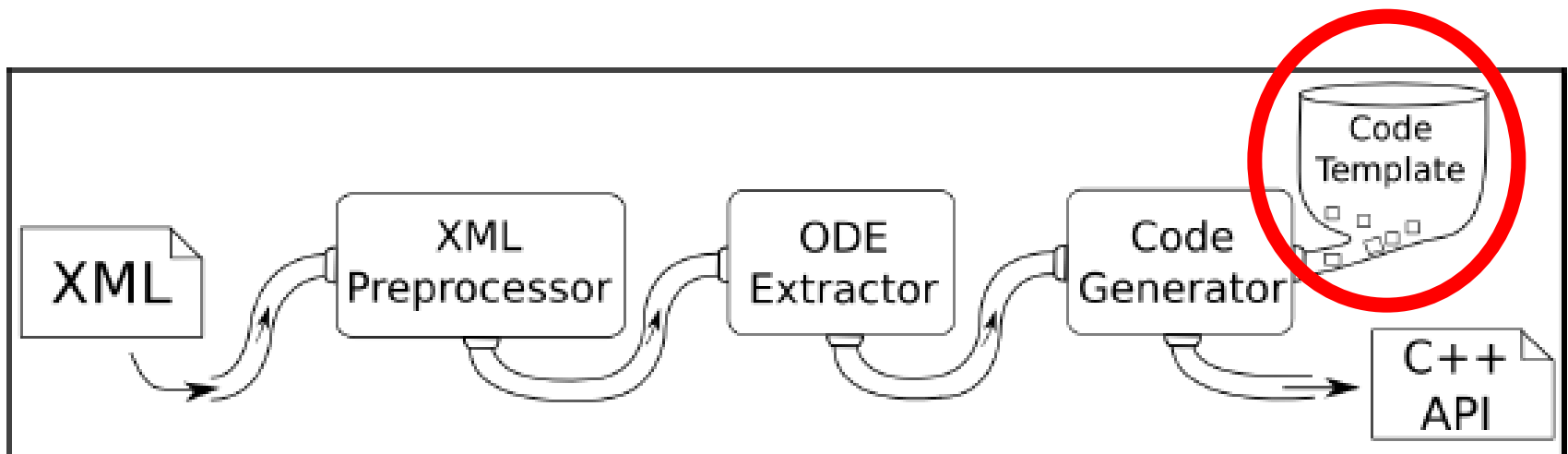
-- Garny, Alan ; Nickerson, David P. ; Cooper, Jonathan ; SANTOS, Rodrigo Weber dos ; Miller, Andrew K. ; McKeever, Steve ; Nielsen, Poul M.F. ; Hunter, Peter J. . CellML and associated tools and techniques. **Philosophical Transactions. Royal Society. Mathematical, Physical and Engineering Sciences**, v. 366, p. 3017-3043, 2008. .

-- Campos, Ricardo Silva ; Amorim, Ronan Mendonca ; Costa, Caroline Mendonça ; Lino de Oliveira, Bernardo ; BARBOSA, Ciro de Barros ; Sundnes, Joakim ; Weber dos Santos, Rodrigo . Approaching cardiac modeling challenges to computer science with CellML-based web tools. **Future Generation Computer Systems**, v. 26, p. 462-470, 2010

(Ricardo Campos Master Thesis)

# CELL-Level Simulations

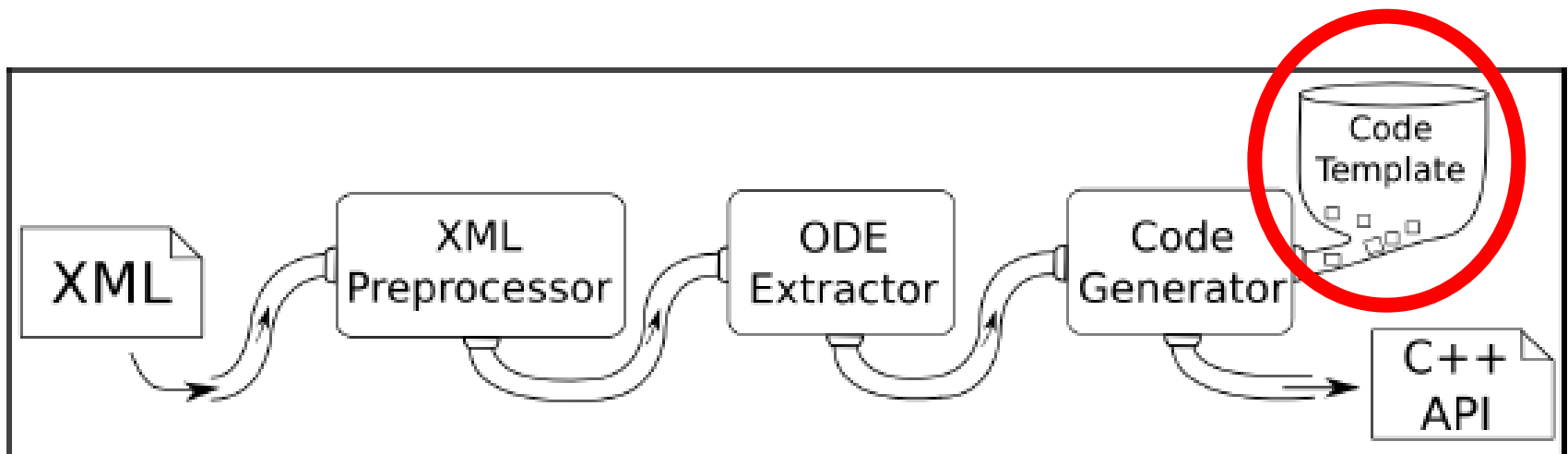
- Implement and merge different optimizations proposed before for the EULER method within the AGOS framework:
- Adaptive Time Step
- LUT + fine PE (PYCML)
- OPEMP
- Result: Light-weight explicit method more efficient than BDF (SUNDIALS) **for cardiac modeling**



(Ricardo Campos Master Thesis)

# CELL-Level Simulations

- Implement and merge different optimizations proposed before for the EULER method within the AGOS framework:
- **Euler with Adaptive Time Step**
- Result: Light-weight explicit method more efficient than BDF (SUNDIALS) **for cardiac modeling**



# Methods

- Four models were tested,  $h$  chosen so that errors (relative L2) compared to a simulation using very fine  $h$  were  $< 1\%$
- Computer: Intel Core i7 860 2.80GHz and 8GB

Model	Frequency(Hz)	Simulation(s)	Fixed $h$ (s)
Noble et al	1	100	1,0e-5
TenTusscher e Panfilov	2	100	1,0e-6
Garny et al	-	100	5,0e-6
Bondarenko et al	14	10	2,0e-7

# Stiff ODEs

- Cardiac models are based on Stiff ODEs
  - Cell-level simulations normally use BDF method from SUNDIALS with adaptivity for both time step and method order
  - However, these methods are usually not used in tissue simulations due to huge memory consumption (Jacobian, Newton , etc).
  - EULER or similar light-weight explicit methods (R-L): preferred methods for Tissue simulations due to simplicity and low memory consumption
- DRAWBACK: Demands small  $h$  -> many iterations

# Methods

- **Time Step adaptive method:**
  - Increase/decrease  $h$  based on comparison:
  - Euler x Heun 2<sup>nd</sup> order.

$$\tilde{y}_{i+1}^j = y_i^j + h_i f^j(t_i, \vec{y}_i)$$

$$y_{i+1}^j = y_i^j + \frac{h_i}{2} (f(t_i, \vec{y}_i) + f(t_{i+1}, \vec{\tilde{y}}_{i+1}))$$

$$error_i = \|\vec{y}_{i+1} - \vec{\tilde{y}}_{i+1}\|_{\infty}$$

$$h_{i+1} = get\_new\_h(error_i, tol, h_i)$$

Get a new  $h$  using the difference between Heun and Euler solution, a user-defined tolerance ( $tol$ ) and the current time step  $h$ .

$$h_{i+1} = h_i \sqrt{\frac{tol}{error_i}}$$

If  $error_i > tol$ :

Throw the iteration results away  
and compute them again with a  
new  $h$

Else:

Accept results and go on to the  
next iteration with the new  $h$ .



# Adaptive Time Step Results

BDF x Euler X AM

BDF from 4.5 to 23.7  
times faster than  
Euler

In average, BDF  
consumes 80%  
more memory;

AM: from 5.6 to 31.6  
times faster than  
Euler

Model		Euler	ATSH	BDF
NBL	Run-time(s)	28.0	5.0	6.2
	Memory(kB)	180	180	316
	Error(%)	0.07	0.17	0.9
TTP	Run-time(s)	317.0	48.7	40.8
	Memory(kB)	180	180	312
	Error(%)	0.02	0.5	0.8
GRN	Run-time(s)	47.4	1.5	2.0
	Memory(kB)	152	152	288
	Error(%)	0.9	0.9	0.2
BDK	Run-time(s)	165.4	10.0	11.5
	Memory(kB)	196	146	356
	Error(%)	0.003	0.6	0.6

Same memory

# Results

BDF x Euler X AM

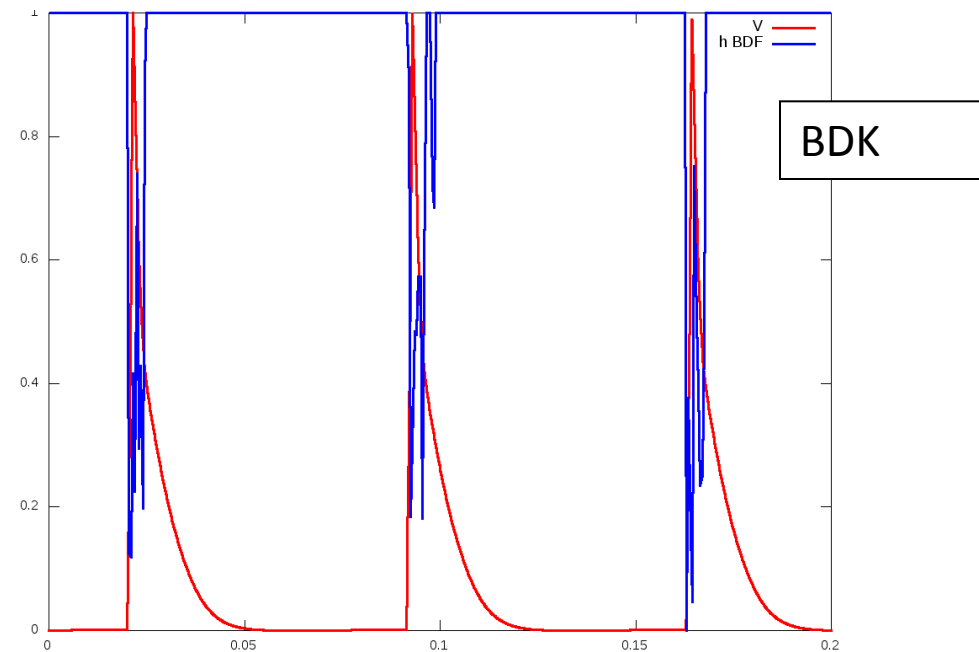
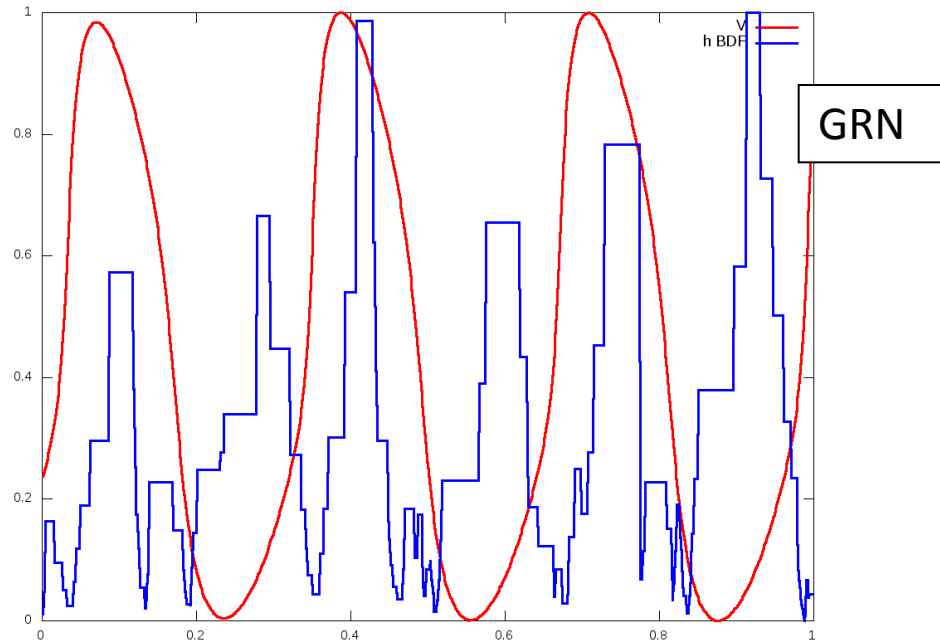
BDF from 4.5 to 23.7  
times faster than  
Euler

In average, BDF  
consumes 80%  
more memory;

AM: from 5.6 to 31.6  
times faster than  
Euler

Model		Euler	ATSH	BDF
NBL	Run-time(s)	28.0	5.0	6.2
	Memory(kB)	180	180	316
	Error(%)	0.07	0.17	0.9
TTP	Run-time(s)	317.0	48.7	40.8
	Memory(kB)	180	180	312
	Error(%)	0.02	0.5	0.8
GRN	Run-time(s)	47.4	1.5	2.0
	Memory(kB)	152	152	288
	Error(%)	0.9	0.9	0.2
BDK	Run-time(s)	165.4	10.0	11.5
	Memory(kB)	196	146	356
	Error(%)	0.003	0.6	0.6

Same memory



X axis =time (s); y axis, AP in mV, dt in s, normalized

# Summary

- AM x Euler: from 6 to 32 times faster than Euler, with same memory consumption

(Rafael Sachetto PhD thesis)

## Tissue Model: Adaptive mesh + time step + OPENMP

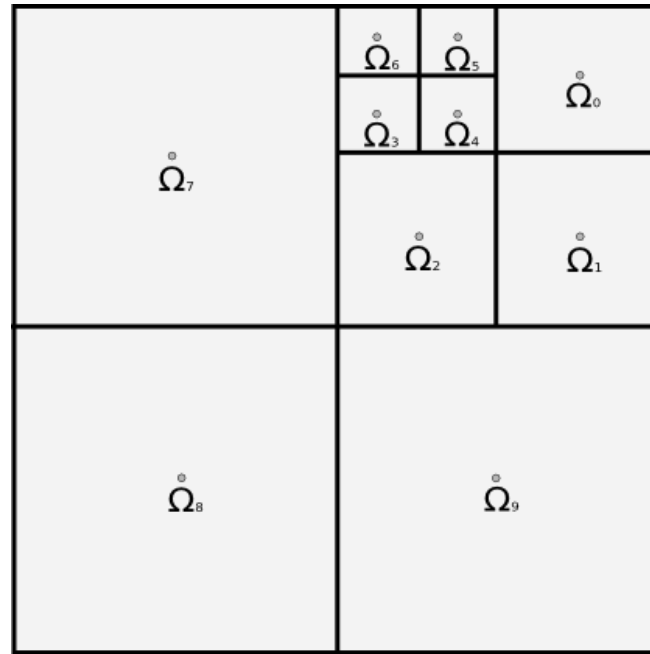
- Electrical wave propagation: only a fraction of the excitable medium is occupied by wavefronts.
- Wavefront demands fine mesh.
- It is possible to take into account the scale differences in the phenomena via reliable and efficient solutions.
- Adaptive mesh procedure:
  - *Autonomous Leaves Graph (ALG)*.

- Computer: 2 quad-core Intel(R) Xeon(R) CPU E5420 2.50GHz  
8 GB RAM
- Cell Model: Bondarenko et al. (40ms simulation)
- Non-linear system of PDE: Operator Splitting
- ODE System: Solved with the Adaptive Time Step method described before
- PDE: Discretized with Finite Volume Method, Implicit Euler
- Adaptive Mesh generation: based on ALG data structure (Graphs) and Peano-Hilbert Space Filling Curve – Generates non-conformal meshes – used both for structures and nonstructured meshes
- Linear System: CG
- Parallelization: OPEMP
- L2 relative error computed from a very fine spatial and time discretization (25x25um)

# ALG

- Graph-based Data structure that can be integrated to the linear system solver to properly represent different geometries.
- Generic data structure, which does not rely on any type of numerical method, on the geometry of the problem nor on the problem's nature.

# ALG



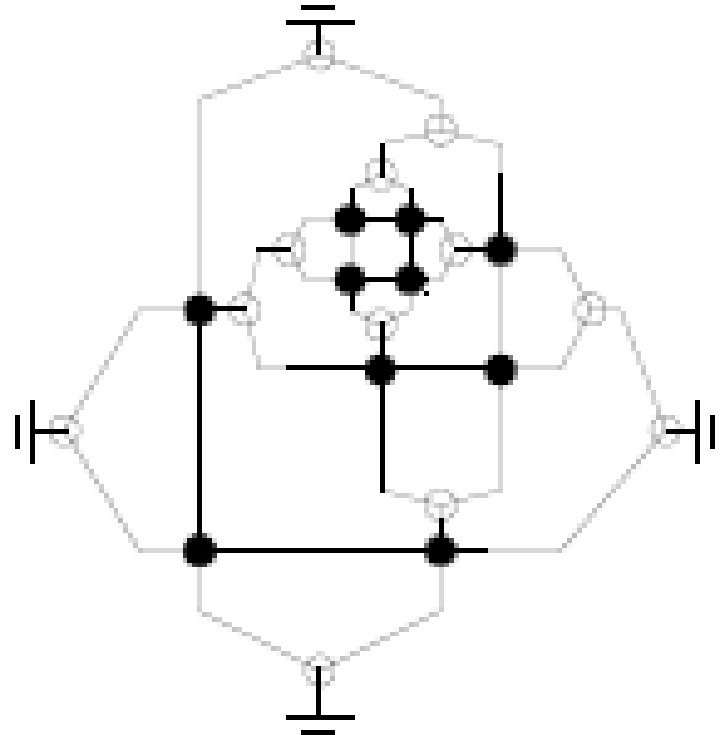
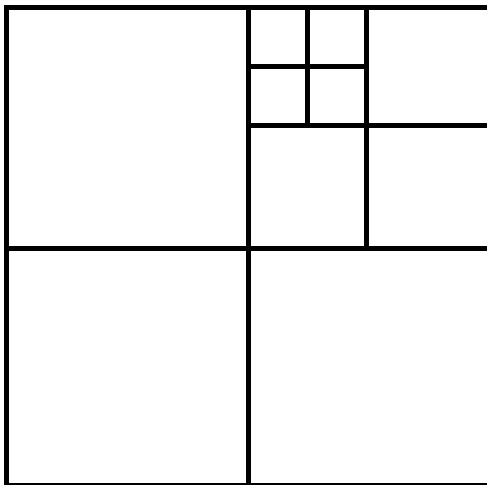
$$\begin{aligned} \alpha V_{i,j}^* - \sum_{k=1}^{m_1} \sigma_{x_{r',k}} (V_{r,k} - V_{i,j}) + \sum_{k=1}^{m_2} \sigma_{x_{l',k}} (V_{i,j} - V_{l,k}) \\ - \sum_{k=1}^{m_3} \sigma_{y_{t',k}} (V_{t,k} - V_{i,j}) + \sum_{k=1}^{m_4} \sigma_{y_{b',k}} (V_{i,j} - V_{b,k}) = V_{i,j}^n \end{aligned}$$

where  $\alpha = (\beta C_m h_{i,j}^2) / \Delta t$ .

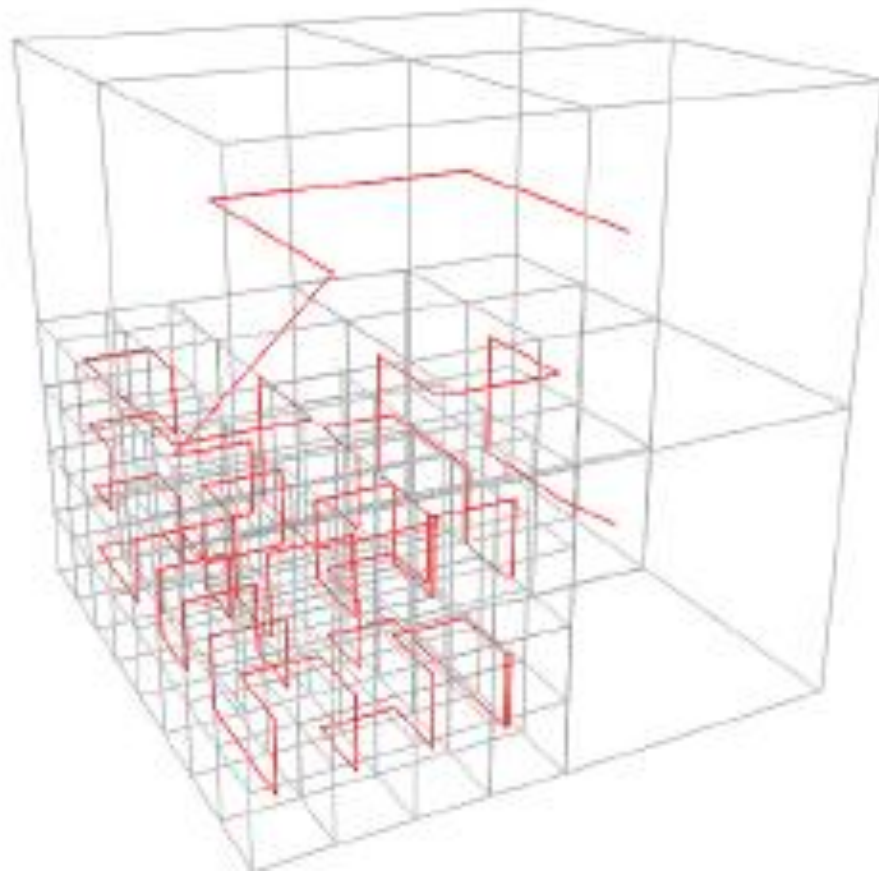


# ALG Data-Structure

- Black dot- Volume/Element node
- White dot – Interface node
- Ground – Domain Boundary
- Directions are omitted on graph for simplicity



# Sorting the mesh/data-structure via Hilbert Curve



# ALG and the monodomain problem

begin

set cell model initial conditions;

set monodomain initial conditions;

assemble the monodomain matrix (Linear system form PDE);

while ( $t < t_{\text{final}}$ )

    update\_cell\_model\_state\_vector;

    solve\_cell\_model;

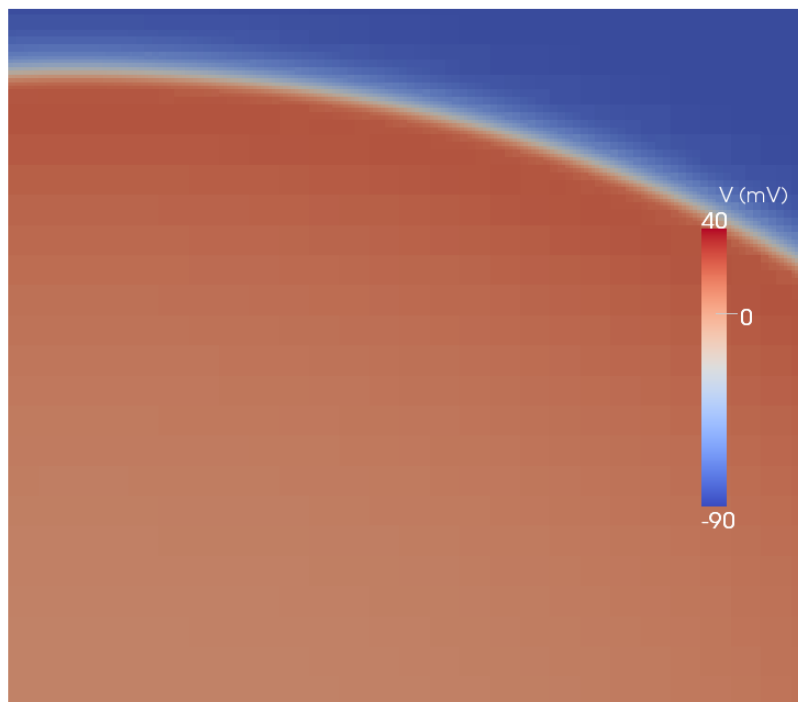
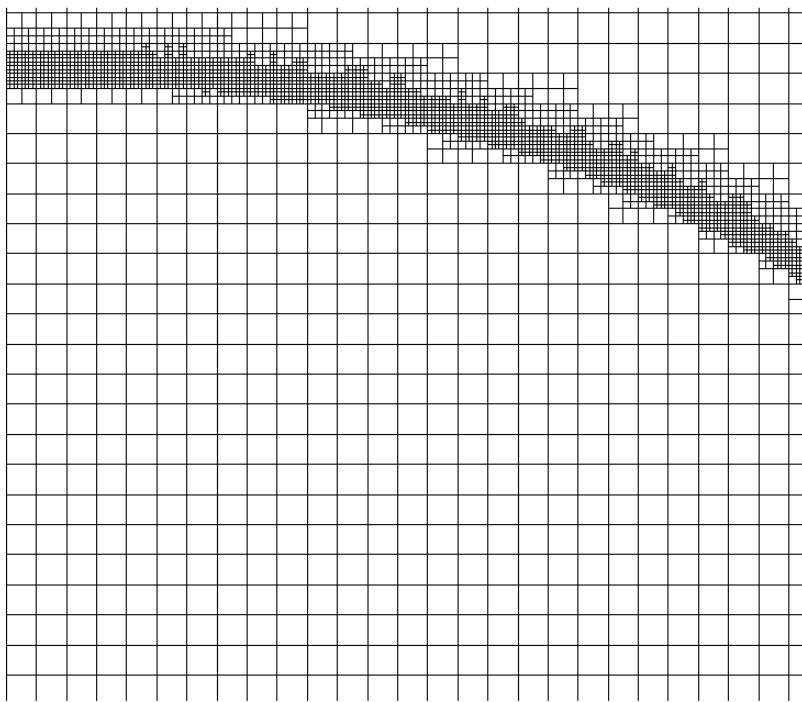
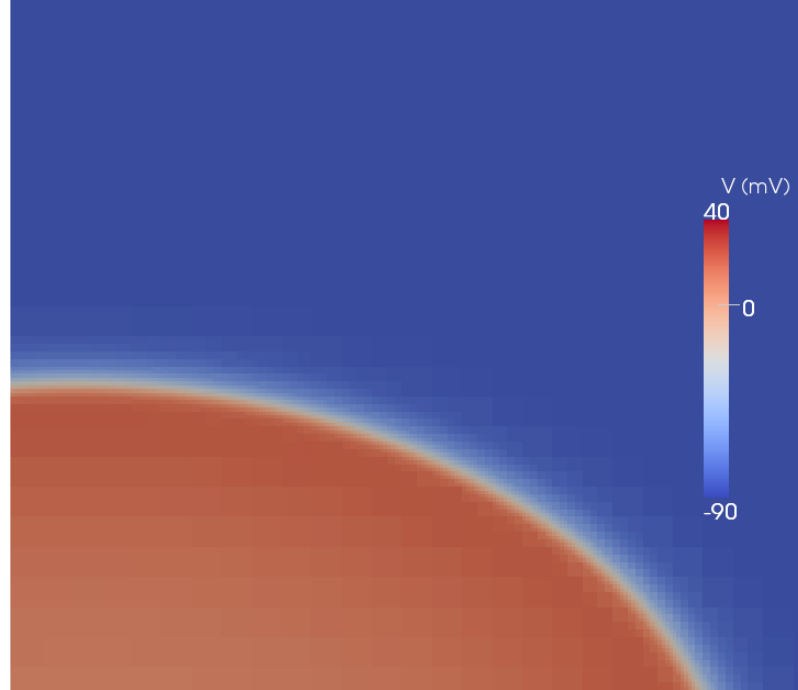
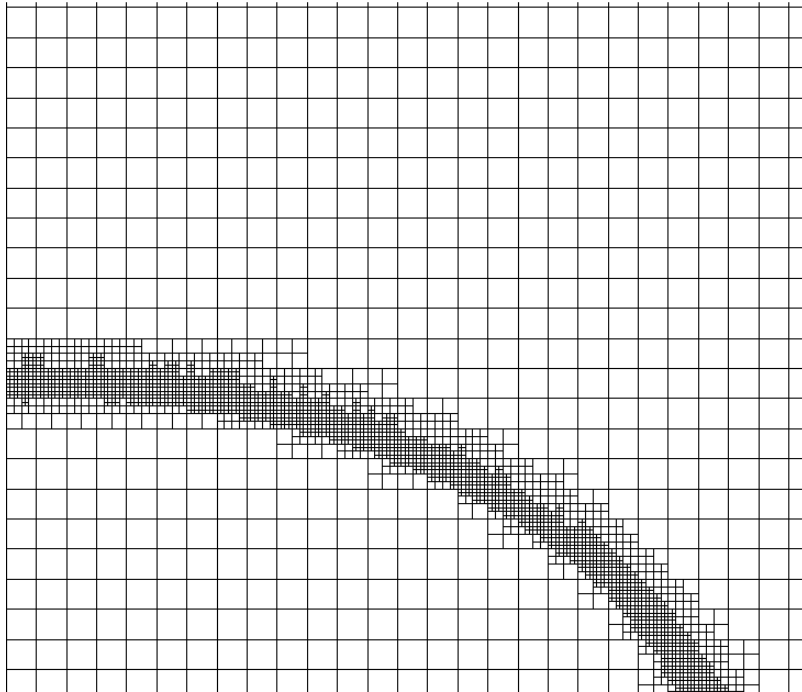
    solve Linear System (PDE) via conjugate\_gradient

    refine-unrefine

    reassemble the monodomain matrix if needed;

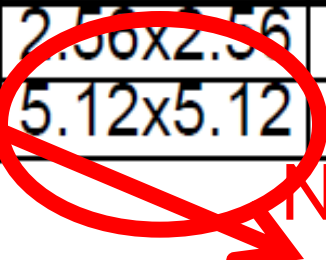
$t = t + dt$

end while



Size (cm)	DX min/max(um)	dt EDP <sub>(us)</sub>	dt EDO min/max(us)	Exec Time	Speedup	Error (%)
Fixed mesh and dt						
0.64x0.64	50/50	0.1	0.1/0.1	8.6h	1.0	1.1
Fixed mesh and two fixed dts (ODExPDE)						
0.64x0.64	50/50	10	0.1/0.1	6.8h	1.26	2.5
Fixed mesh and adapt dt						
0.64x0.64	50/50	10	0.01/0.1	1.1h	8.15	2.6
Adapt mesh and dt						
0.64x0.64	50/50	10	0.01/10	10min	48.2	2.4
Adapt mesh and dt + OPENMP(8 cores)						
0.64x0.64	50/200	10	0.01/10	1.4min	368.6	2.4
1.28x1.28	50/200	10	0.01/10	5.8min		
2.56x2.56	50/200	10	0.01/10	20min		
5.12x5.12	50/200	10	0.01/10	51min		

Size (cm)	DX min/max(um)	dt EDP(us)	dt EDO min/max(us)	Exec Time	Speedup	Error (%)
Fixed mesh and dt						
0.64x0.64	50/50	0.1	0.1/0.1	8.6h	1.0	1.1
Fixed mesh and two fixed dts (ODExPDE)						
0.64x0.64	50/50	10	0.1/0.1	6.8h	1.26	2.5
Fixed mesh and adapt dt						
0.64x0.64	50/50	10	0.01/0.1	1.1h	8.15	2.6
Adapt mesh and dt						
0.64x0.64	50/50	10	0.01/10	10min	48.2	2.4
Adapt mesh and dt + OPENMP(8 cores)						
0.64x0.64	50/200	10	0.01/10	1.4min	368.6	2.4
1.28x1.28	50/200	10	0.01/10	5.8min		
2.56x2.56	50/200	10	0.01/10	20min		
5.12x5.12	50/200	10	0.01/10	51min		


 No. Unknowns =  $1024 \times 1024 \times 41 = 43$  Millions  
 Less than a hour on a single and old (8-cores)  
 computer

# Results

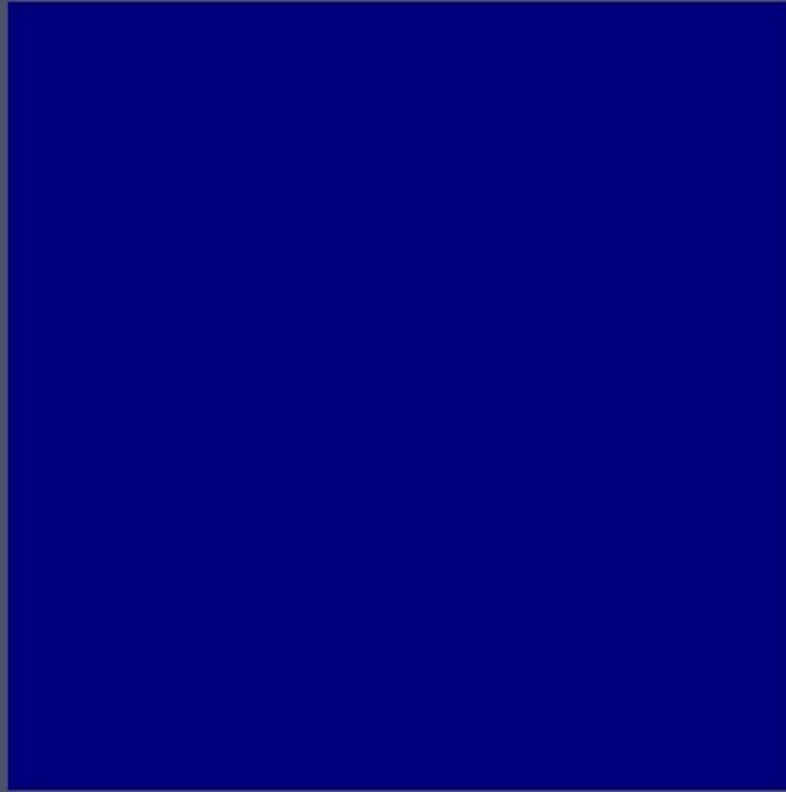
<b>0.64x0.64cm Size: Adapt time space + OPENMP</b>			
	<b>Time(s)</b>	<b>% time</b>	<b>Speedup</b>
Total	88	100,0	7,2
CG	1,3	1,5	4,5
ODE	78	88,2	8,0
Matrix	0,9	1,0	1,9
Ref/Unref	7,1	8,0	-

<b>2.56x2.56cm Size: Adapt time space + OPENMP</b>			
	<b>Time(s)</b>	<b>% time</b>	<b>Speedup</b>
Total	1203	100,00	6,00
CG	99	8,24	8,50
ODE	733	60,90	7,90
Matrix	27	2,26	6,10
Ref/Unref	369	30,65	-

# Conclusions

- **Accelerating Monodomain in:**
  - ❑ **1 computer with 1 GPU** = up to **35x** faster than 4 CPU cores
  - ❑ **1 cluster with 64 cores + 8 GPUs** = up to **420x** faster than 1 core
  - ❑ **1 computer with Adaptive time step and mesh algorithms + OPenMP (8-cores)** = up to **370x** faster than 1 core without adaptive methods
    - ❑ **ps.: Espiral simulation was more than 100x faster**





- ❑ 1 computer with Adaptive time step and mesh algorithms + OPenMP (8-cores)

- ❑ ps.: piral simulation was more than 100x faster

# Ongoing work: 3D + Adaptivity + MultiGPU

